Cognitive dysfunction in experimental cerebral malaria: Possible role of neurodegeneration and morphological alterations

Thesis submitted to the University of Hyderabad

For the degree of

Doctor of Philosophy

By

Simhadri Praveen Kumar

Reg. No.12LTPH12

Under the supervision of

Prof.P.Prakash Babu

Department of Biotechnology and Bioinformatics

School of Life Sciences

University of Hyderabad

Hyderabad

Telangana- 500046

MAY 2019

University of Hyderabad
(A Central University by an Act of Parliament)
Department of Biotechnology and Bioinformatics
School of Life Sciences
P.O. Central University, Gachibowli, Hyderabad-500046

DECLARATION

The research work presented in the thesis entitled "**Cognitive dysfunction in experimental cerebral malaria: Possible role of neurodegeneration and morphological alterations**" has been carried out by me in the Department of Biotechnology and Bioinformatics, School of Life Sciences, University of Hyderabad, Hyderabad, Telangana under the guidance of Prof. P. Prakash Babu. I hereby declare that this work is original and has not been submitted in part or full for any other degree or diploma of any other University or Institution.

Place: Hyderabad

Date:20.05.2019

Name: Simhadri Praveen Kumar

Reg.No: 12LTPH12

University of Hyderabad
(A Central University by an Act of Parliament)
Department of Biotechnology and Bioinformatics
School of Life Sciences
P.O. Central University, Gachibowli, Hyderabad-500046

Date: 20.05.2019

CERTIFICATE

This is to certify that the thesis entitled "**Cognitive dysfunction in experimental cerebral malaria: Possible role of neurodegeneration and morphological alterations**" submitted by Mr. Simhadri Praveen Kumar bearing registration number 12LTPH12 in partial fulfillment of the requirements for award of Doctor of Philosophy in the Department of Biotechnology and Bioinformatics, School of Life Sciences is a bonafide work carried out by him under my supervision and guidance.

This thesis is free from plagiarism and has not been submitted previously in part or in full to this or any other University or Institution for award of any degree or diploma.

Further, the student has the following publication (s) before submission of the thesis/monograph for adjudication and has produced evidence for the same in the form of the acceptance letter or the reprint in the relevant area of his research: (Note: at least one publication in referred journal is required the research)

Simhadri PK, Malwade R, Vanka R, Nakka VP, Kuppusamy G, Babu PP. Dysregulation of LIMK-1/cofilin-1 pathway: A possible basis for alteration of neuronal morphology in experimental cerebral malaria. Ann Neurol. 2017; 82(3):429-443. doi: 10.1002/ana.25028.

Annals of neurology (Online ISSN Number 1531-8249)

Chapter of the dissertation where this publication appears: Volume 82, issue 3.

And

A. Presented in the following conferences
   a) Attended and presented a poster on the topic "Cofilin-1 as a possible therapeutic target to prevent cognitive sequelae in cerebral malaria." in 14th meeting of Asian Pacific Society for Neurochemistry (APSN 2016) on 27th-30th August 2016 at Kuala Lumpur, Malaysia. doi: 10.3389/conf.fncel.2016.36.00127.

   b) Attended the XXIII World Congress of Neurology (WCN 2017), which was held in Kyoto, Japan on 16th-21st September 2017 and presented a poster on the topic titled "Dysregulation of LIMK-1/Cofilin-1 pathway: a possible basis for alteration of neuronal morphology in experimental cerebral malaria." https://doi.org/10.1016/j.jns.2017.08.3406

   c) Attended and presented a poster on the topic "Aberrant activity of CDK5, hyperdopamine tone alters D1R/PKA/DARPP-32/PP1 pathway; a possible basis for dysregulation of NR2B, AMPA receptors and CaMKII proteins in experimental cerebral malaria" at 29th National Congress on Parasitology and International Symposium on Malaria Biology (ISMBNCP-2018) on 1st-3rd November 2018 held at School of Life Sciences University of Hyderabad, Hyderabad, Telangana, India.

   Further, the student has passed the following courses towards fulfillment of coursework (recommended by doctoral committee) on the basis of the following courses passed during his Ph.D. degree was awarded.

	Name	Credits	Pass/Fail
1.	Research ethics and management	2	pass
2.	Biostatistics	2	pass
3.	Analytical techniques	3	pass
4.	Seminar	1	pass
5.	Lab work	4	pass

Prof.P.Prakash Babu
Department of Biotechnology and Bioinformatics

Head

Dept. of Biotechnology and Bioinformatics

Dean

School of Life Sciences

This work is dedicated to my beloved parents for their constant support and encouragement

Acknowledgements

I would like to acknowledge my supervisor Prof.P.Prakash Babu for guiding and proving me an opportunity to work in his lab related to the clinical and cognitive aspects of neuroscience.

I thank my doctoral committee members Dr.Sunanda Bhattacharya and Dr.K. P. M. S. V. Padmasree for their valuable suggestions during my research work.

I would like to thank the present and former heads of the Department of Biotechnology and Bioinformatics and present and former Deans of School of Life sciences for providing the departmental/School facilities.

I thank Dr.Venkata Prasuja and Dr.Apoorv T.S. for providing necessary inputs related to the research work design. I thank Dr.C.R.Pillai, emeritus scientist in National Institute of Malaria Research (NIMR, New Delhi) for teaching the basics of malaria parasite and training me experimental techniques related to the *in vitro* parasite culture. I also thank Dr. Anwita Madam for her constant support, motivation throughout my research work.

I am thankful to all my senior lab members Dr.Apoorv, Dr.Prabhakar, Dr.Khamusha Valli, Dr.Ramulu, Dr.Nobel, Dr.Ravindra Pandey, Dr.Deepak Babu, Mr.Karthik, Dr.Parimala and present lab members Mr.Naidu Babu, Mr.Nikhil Ranjan, Mrs.Shubhangi, Miss.Neera, Mr.Kishore, Mr.Rahul, Miss Shailaja, and former lab members Miss Ruchi, post-doctoral members Dr.Vimal Pandey, Dr.Raghu Gogada and Dr.Venkata Prasuja for creating a wonderful environment in the lab. I would like to thank my colleague, Dr.Ravisankar Vanka for sharing his knowledge and as well as proving anti-malarial drugs for my research work.

I am thankful to all the non-teaching staff of the department and school specially Mr. Rajshekhar, Mr. Shekhar, Mr.Murthy and our lab assistant Mr. Muthaym, Mrs.Revathi, Mr.Chandan for their help in doing all the office works.

I would like to thank post-graduation students Mr.Tahir Ali, Miss Sneha Kumari who had worked with me related to their dissertation especially Sneha for sharing my thoughts as a true friend. I shall be thankful to Kiran, Satyajit, Neha, Chukhu, Pritikana, Vidya, Jagadeesh and Akhila for their timely help during my research work.

Simhadri Praveen Kumar

Index

CHAPTER-1

Introduction

Malaria is still a life threatening disease in humans caused by the infection of four different species of protozoan parasite Plasmodium *called P. falciparum, P.vivax, P.ovale, P.malariae* by the bite of female *Anopheles* mosquito. In the year 2017, 219 million cases with 435 000 deaths related to malaria has been reported worldwide. Life Cycle of malaria undergoes in two phases:

a) Sexual phase in the gut of female Anopheles mosquito

b) Asexual phase in the hepatocytes and erythrocytes of human

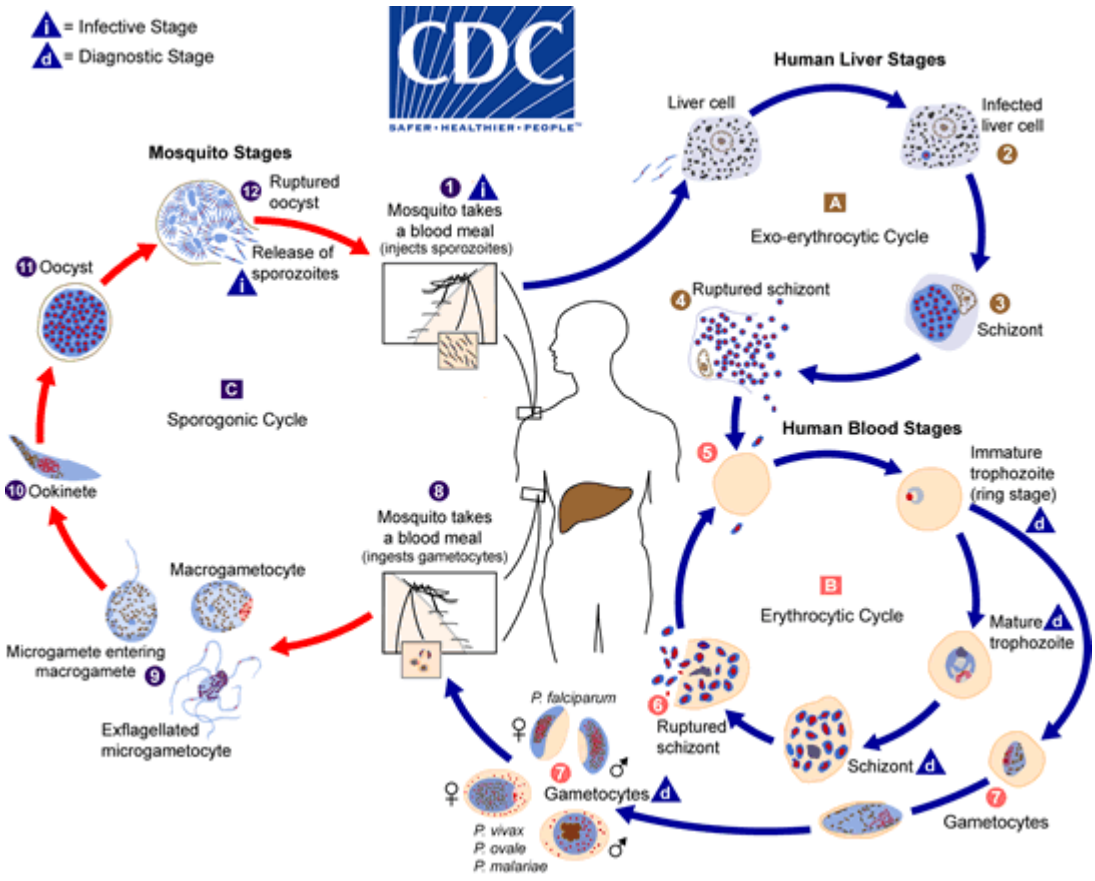

Figure 1. Representing the life cycle of malaria parasite. Source: Centre for Disease Control and Preventionhttps://www.cdc.gov/dpdx/malaria/index.html

Sporozoites invade the hepatocytes and undergo asexual reproduction to mature schizonts which rupture and release merozoites, the infectious form of the parasite. Merozoites infect the erythrozoites and mature to trophozoites further transforming to gametocytes (Figure 1.). The sexual stage of the life cycle is followed after the ingestion of male and female gametocytes by female Anopheles mosquito.

Epidemiology

According to the World malaria report 2017, 216 million cases of malaria were reported worldwide in the year 2016 [1]. Most of children of Sub-Saharan African population have been infected with malaria mainly by the *Plasmodium falciparum* (Figure 2.). Cases of severe malaria have been reported in children, adults and especially travelers in comparison to the local population in high transmission areas.

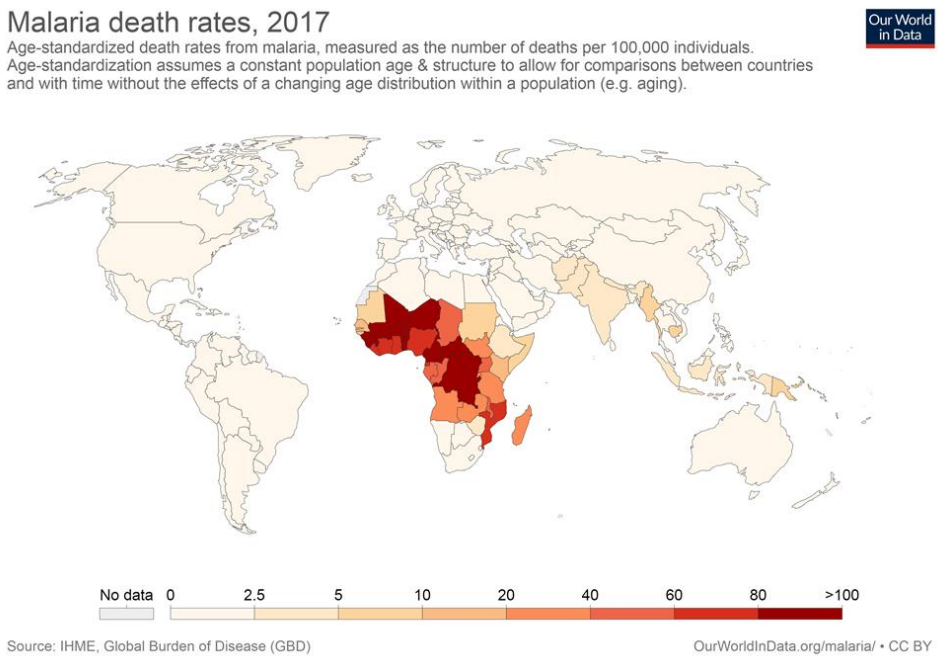

Figure 2. Representing the rate of incidence and malaria related deaths worldwide. Source: https://ourworldindata.org/malaria

Classification of malaria

Malaria is classified based on the duration of the severity of the symptoms exhibited by the individuals (Figure 3.). Severity of malaria increases with improper diagnosis, compromised immunity and delayed treatment of patients suffering from uncomplicated malaria resulting in complicated malaria. According to the World Health Organization, patients exhibiting unrousable coma at least one hour after termination of seizures is categorized as cerebral malaria (CM). Signs of CM illness include restlessness, psychotic behaviour, with abnormal posture and persistent loss of consciousness. Severe malaria infected individuals also show similar symptoms of CM with a less time interval of coma.

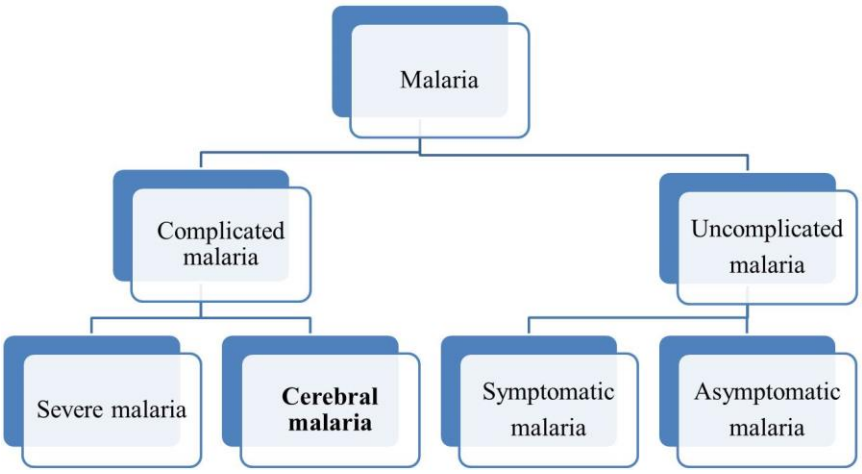

Figure 3. Representing the classification of malaria.

Uncomplicated malaria: caused by the infection of *Plasmodium falciparum* and characterized by symptoms such as fever, vomiting, headache and abdominal pain.

Complicated malaria: Increase in the density of parasitemia leading to the organ dysfunction results in the severe and cerebral malaria.

a) **Severe malaria:** Most of the complications are related to central nervous system (CNS) with recurrent seizures, organ dysfunction; relapsing fever with chills is common in both children and adults. Duration of symptoms vary from children to adults (Table 1.).

b) **Cerebral malaria (CM):** Multi-organ failure followed by severe complications of CNS with epileptic seizures, profound coma and death.

Sign or Symptom of severe malaria	**Adults**	**Children**
Duration of illness	5-7 days	1-2 days
Respiratory distress	common	common
Seizures	12%	30%
Duration of coma	2-4 days	1-2 days

Table.1. Representing the difference of signs and symptoms of severe malaria in children and adults. Derived from studies in south-east Asian adults and children, and African children [2]

Cerebral malaria (CM) is a severe neurodegenerative disease caused by the infection with *Plasmodium falciparum* and *Plasmodium vivax* [3]. It is classified under severe malaria referring to multiple organ failure ultimately leading to the death. The incidence of severe malaria is approximately two million cases with 430,000 deaths annually of which 575,000 children in Africa suffer from CM. Despite of anti-malarial therapy, 25% children and adults suffer from cognitive dysfunction [4-5]. Some of the clinical signs of CM in children start with fever followed by common cold, vomiting leading to intermittent seizures, malarial retinopathy and profound coma. Children who recover from CM suffer from neuro-cognitive sequelae with abnormalities in attention, working memory and learning capabilities. Some of the neurological

sequelae are cerebellar ataxia, hemiparesis, cortical blindness, behaviour disturbances, hypotonia and 10% of incidences with epilepsy until several weeks after illness [6]. Some of the reports suggest that behavioral disturbances can also occur in children even after surviving from malaria [7].

Pathological mechanism of CM:

The mechanisms behind the pathogenesis of CM are still not understood. Based on the observations from F.Gay *et al*. [8], some of the important stages contributing to CM are

a) Sequestration of parasite in the microvasculature of the blood.
b) Metabolic acidosis
c) Inflammatory mediators
d) Blood Brain Barrier dysfunction

a) **Sequestration of parasite in the microvasculature of the blood**: The extent of parasite burden in the blood of infected person differs which could be a leading factor for the progression of malaria to CM. Parasite infected RBC (iRBC) evades the circulation to the spleen and enters in the microvasculature and adheres to the endothelial cells through a protein called *Plasmodium falciparum* Erythrocyte Membrane Protein (PfEMP-1). Sequestration leads to the obstruction of the blood flow generating hypoxia (Figure 4.)
b) **Metabolic acidosis**: Severe hypoxic conditions alter most of the metabolic pathways leading to hyperlactatemia, with increased lactate to pyruvate ratio. Decreased oxygen content in the tissues of the organs results in increased host's anaerobic glycolysis. Based on a case study by Brand et al., 32% of children exhibited acidosis during CM [9].

c) **Inflammatory mediators**: Loss of blood flow due to adhesion of sequestered RBC to the endothelial cells leads to the secretion of pro-inflammatory cytokines such as interleukins (IL)-6, IL-1, tumour necrosis factor (TNF) resulting in the synthesis of excess reactive oxygen species (ROS) and nitric oxide (NO) and alteration of several host signaling mechanisms.

d) **Blood Brain Barrier (BBB) dysfunction**: BBB rupture is a salient feature in the pathogenesis of CM. Aberrant activation of markers on the endothelial cells such as angiopoietin-1 and 2 deregulate the endothelial integrity resulting in the BBB rupture during CM.

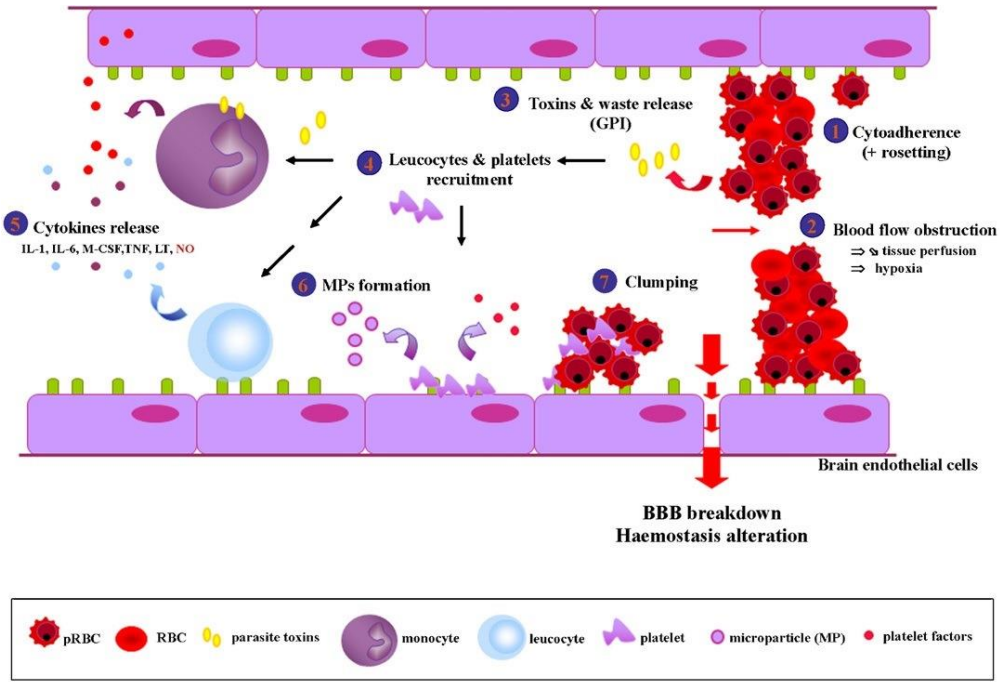

Figure 4. Schematic representation of the pathogenesis of cerebral malaria in the brain microvasculature. Source: Gay F et al. doi: 10.1016/j.neurol.2012.01.582.

Rationale of the present study

Cognitive decline in the survivors of CM, especially 25% of children below 5 years age have been reported [4-7]. Children suffering from CM show enhanced levels of pro-inflammatory cytokines and chemokines such as tumor necrosis factor-alpha (TNF-α), IL-6, IL-8 and IL-1 in the cerebrospinal fluid [10]. High levels of TNF-α in the brain is associated with cognitive impairment [10]. Prolonged seizures during CM can be associated with neurological sequelae in children. Molecular mechanisms underlying cognitive dysfunction have not been explored in CM. Multiple areas of the brain are damaged in CM, as observed in the histological sections of the postmortem samples of human. It is challenging to understand the cognitive dysfunction in the survivors of CM, therefore; the same can be studied using the experimental models of CM (ECM).

C57BL/6 mice infected with *Plasmodium berghei ANKA* mostly reiterate the symptoms of human CM (HCM) [11-12]. Symptoms exhibited by the CM infected mice such as loss of exploration, abnormal gait, loss of grooming, sociability, pilo-erection and retinopathy from day 5 to 7 post-infection. Evaluation of the symptoms of CM is determined by rapid murine coma behavior scale (RMCBS), a video based experiment performed per mouse for 3 minutes analyzed for ten behavioural parameters such as gait, balance, motor performance, body position, limb strength, pinna reflex, touch escape, toe pinch, aggression and grooming [13]. There exist some differences in the pathogenesis between HCM and ECM model such as in HCM, sequestration of leukocytes and platelets in the microvasculature of the brain whereas parasite infected red blood corpuscles (pRBC) are sequestered in ECM. Sequestration of parasite pRBC was high in the adipose tissue and lungs compared to the brain in the ECM whereas the same was not observed in case of HCM. Despite of differences in the mechanism of pathogenesis, ECM model has been

widely used to elucidate the mechanisms during the pathogenesis and efficacy of therapeutics for CM [14-16]. Mice infected with *Plasmodium yoelii* parasite exhibits the symptoms of malaria without any neurological signs of CM further considered as "asymptomatic" in our studies [17].

Study of acquisition, consolidation, storage and retrieval of memories affecting through behaviour is called "cognition". Neurons are the basic and fundamental cells responsible for the maintenance of the processes related to cognition. Neurons consist of soma (perikaryon), axon and dendrites (Figure 5.). Dendrites consist of dendritic spines which are the functional units of the neurons for the maintenance of synaptic transmission processes. Neurons confined to cortex, hippocampus, striatum are responsible for maintenance of synaptic processes responsible for the maintenance of cognition in the brain. During stress conditions involving ischemic, oxidative stress, excitotoxicity and neuro-inflammatory conditions promote neurodegeneration affecting cognitive processes in the brain. Therefore, our current research focused on the dysregulation of molecular signaling pathways responsible for the maintenance neuronal morphology during ECM.

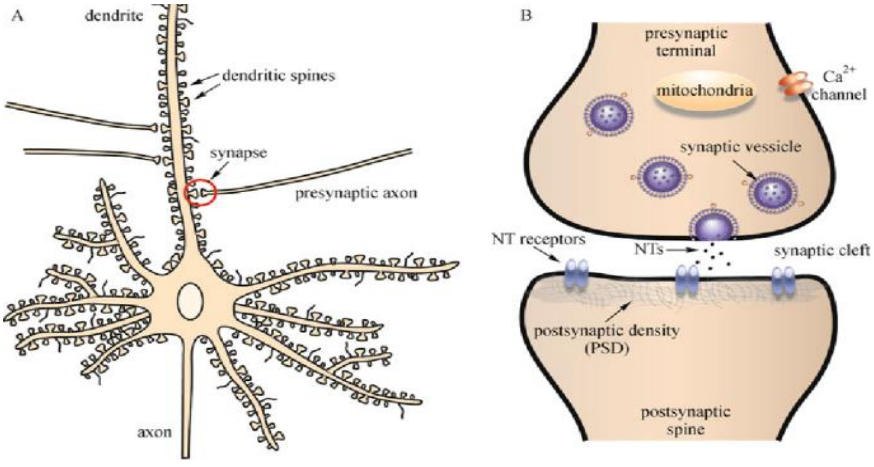

Figure 5. Representing the structure of neuron and its parts

The cytoskeletal backbone of dendrites is composed of microtubules. Dendritic spines comprise of filamentous actin (F-actin) network which maintains its stability, morphology. Assembly and disassembly of actin filaments is known as actin dynamics. Dendritic spines consist of actin stabilizing proteins, cortactin, actin related protein (ARP2/3) and actin destabilizing protein, cofilin. Cortactin promotes the polymerization of F-actin filaments through ARP2/3 protein responsible for long-term spine stabilization. Cofilin, an actin severing protein depolymerizes F-actin to globular actin (Figure 6.). Balanced functioning of the both the proteins are responsible for the stability of the F-actin in the dendritic spines. Upon the release of nootrophic factors such as brain-derived neurotrophic factor (BDNF), binds to the (tyrosine kinase receptor B (TRKB) receptor [18]. BDNF-TRKB stimulates the activation of serine/threonine protein tyrosine (PAK) kinase and RAC1 further promoting the activation of LIM kinase domain (LIMK-1) cascade. LIMK-1 phosphorylates cofilin-1 and inhibits its severing activity which promotes the enlargement and stability of the spine (Figure 7.). Dysfunction of LIMK-1 and cofilin-1 expression alters the stability of the dendritic spine during cerebral ischemia, excitotoxicity and oxidative stress involving neurodegenerative diseases [19].

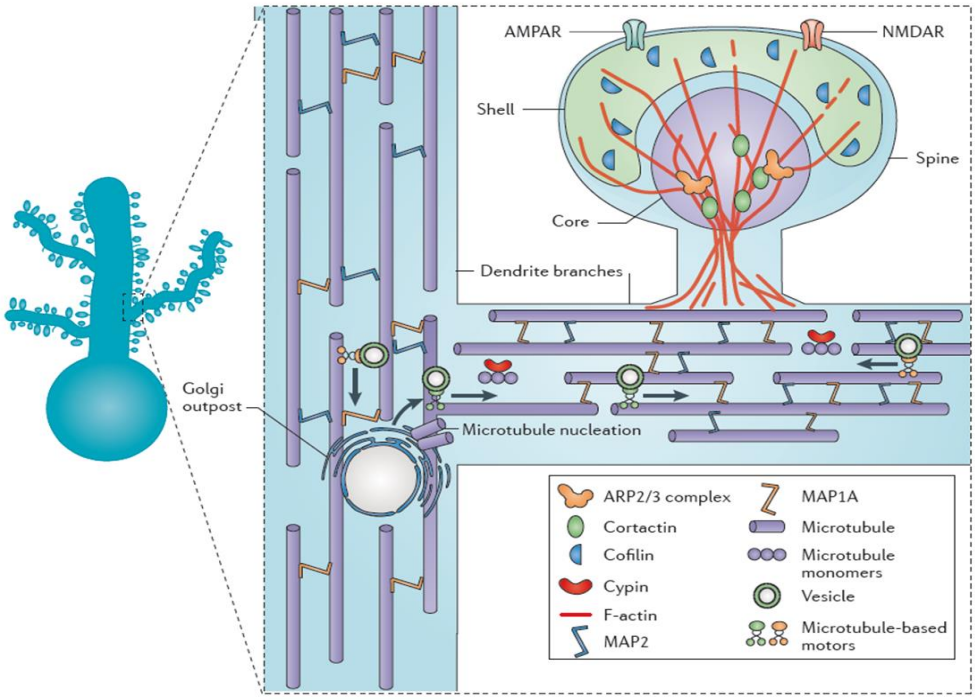

Figure 6. Representing the cytoskeletal architecture of the neuron

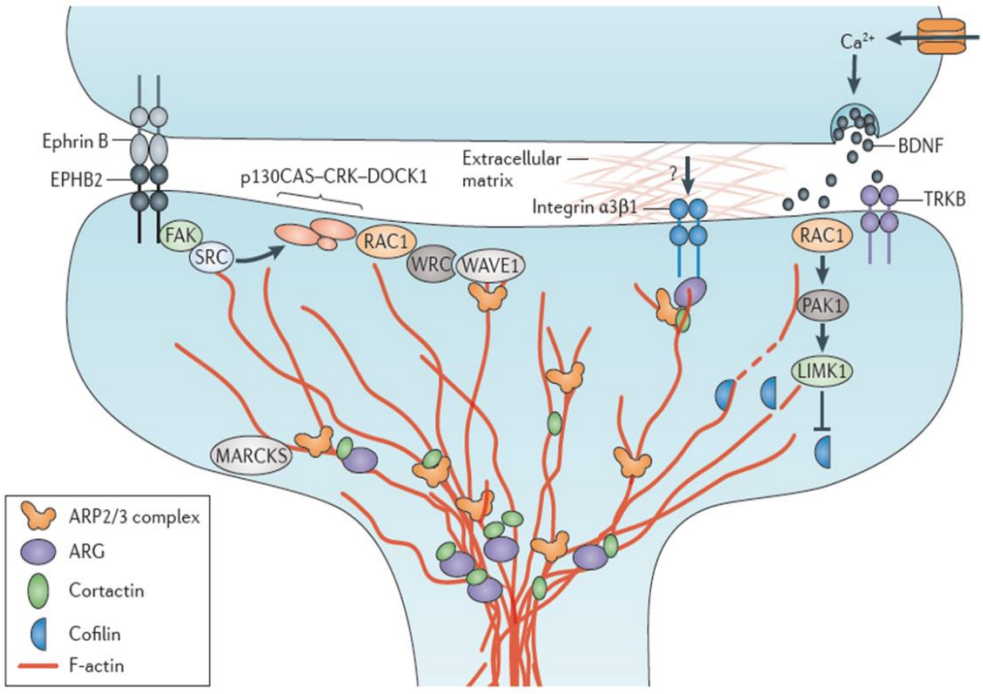

Figure 7. Representing the signaling mechanisms involved in the maintenance of the F-actin in dendritic spine. Source: Anthony J. Koleske doi:10.1038/nrn3486.

References

1) WHO. World Malaria Report; 2017, https://www.who.int/malaria/publications/world-malaria-report-2017/report/en/index.html.

2) Dondorp AM, Fanello CI, Hendriksen IC, Gomes E, Seni A (2010). Artesunate versus quinine in the treatment of severe falciparum malaria in African children (AQUAMAT): an open-label, randomised trial. Lancet. 376(9753):1647-1657.

3) Geleta G, Ketema T (2016). Severe malaria associated with Plasmodium falciparum and P. vivax among children in Pawe Hospital, Northwest Ethiopia. Malar Res Treat. 2016:1240962. doi: 10.1155/2016/1240962.

4) Boivin MJ, Bangirana P, Byarugaba J, Opoka RO et al (2007) Cognitive impairment after cerebral malaria in children: a prospective study. Pediatrics. 119(2):e360-6.

5) Bangirana P, Opoka RO, Boivin MJ, Idro R et al (2014) Severe malarial anemia is associated with long-term neurocognitive impairment. Clin Infect Dis.59(3):336-344.

6) Yusuf FH, Hafiz MY, Shoaib M, Ahmed SA (2017) Cerebral malaria: insight into pathogenesis, complications and molecular biomarkers. Infect Drug Resist.10:57-59.

7) Idro R, Kakooza-Mwesige A, Asea B, Ssebyala K et al.(2016). Cerebral malaria is associated with long-term mental health disorders: a cross sectional survey of a long-term cohort. Malar J. 15:184.

8) Gay F, Zougbédé S, N'dilimabaka N, Rebollo A et al. (2012) Cerebral malaria: what is known and what is on research. Rev Neurol (Paris).168(3):239-256.

9) Brand NR, Opoka RO, Hamre KE, John CC (2016). Differing causes of lactic acidosis and deep breathing in cerebral malaria and severe malarial anemia may explain differences in acidosis-related mortality. PLoS One. 11(9): e0163728.

10) John CC, Panoskaltsis-Mortari A, Opoka RO, Park GS et al.(2008) Cerebrospinal fluid cytokine levels and cognitive impairment in cerebral malaria. Am J Trop Med Hyg.78(2):198-205.

11) White NJ, Turner GD, Medana IM, Dondorp AM et al. (2010) The murine cerebral malaria phenomenon. Trends Parasitol.26(1):11-5.

12) Zimmerman GA, Castro-Faria-Neto H (2010) Persistent cognitive impairment after cerebral malaria: models, mechanisms and adjunctive therapies. Expert Rev Anti Infect Ther. 8(11):1209-1212.

13) Carroll RW, Wainwright MS, Kim KY, Kidambi T et al. (2010) A rapid murine coma and behavior scale for quantitative assessment of murine cerebral malaria. PLoS One.5(10): e13124.

14) Serghides L, McDonald CR, Lu Z, Friedel M et al. PPARγ agonists improve survival and neurocognitive outcomes in experimental cerebral malaria and induce neuroprotective pathways in human malaria. PLoS Pathog. 10(3):e1003980.

15) Nacer A, Movila A, Baer K, Mikolajczak SA et al. (2014) Neuroimmunological blood brain barrier opening in experimental cerebral malaria. PLoS Pathog.8(10):e1002982.

16) Higgins SJ, Purcell LA, Silver KL, Tran V. et al. (2016) Dysregulation of angiopoietin-1 plays a mechanistic role in the pathogenesis of cerebral malaria. Sci Transl Med.8(358):358ra128.

17) Kaul DK, Nagel RL, Llena JF, Shear HL.(1994) Cerebral malaria in mice: demonstration of cytoadherence of infected red blood cells and microrheologic correlates. Am J Trop Med Hyg. 50(4):512-521.

18) Koleske AJ (2013) Molecular mechanisms of dendrite stability. Nat Rev Neurosci. 14(8):536-550.

19) J.R. Bamburg, B.W. Bernstein, R.C. Davis, K.C. Flynn (2010) ADF/cofilin-actin rods in neurodegenerative diseases. Curr Alzheimer Res.7(3): 241–250.

20) Hoffmann A, Pfeil J, Alfonso J, Kurz FT et al.(2016) Experimental Cerebral Malaria Spreads along the Rostral Migratory Stream. PLoS Pathog.12(3):e1005470.

21) Miranda AS, Brant F, Rocha NP, Cisalpino D et al.(2013) Further evidence for an anti-inflammatory role of artesunate in experimental cerebral malaria. Malar J. 12:388.

22) Strangward P, Haley MJ, Shaw TN, Schwartz JM et al.(2017) A quantitative brain map of experimental cerebral malaria pathology. PLoS Pathog. 13(3):e1006267.

23) Milner DA Jr, Whitten RO, Kamiza S, Carr R et al. (2014) The systemic pathology of cerebral malaria in African children. Front Cell Infect Microbiol. 4:104.

To achieve the above hypothesis, we propose three objectives

a) **To study cortical pyramidal neuronal ultrastructure in ECM**
b) **To study dendritic spine density and morphology of cortical pyramidal neurons in ECM**
c) **To study the role of LIMK-1/cofilin-1pathway in ECM**

Based on the previous reports, prominent cortical damage was observed in HCM and ECM [20-23]. Therefore, we studied the morphological aspects of layer 5 cortical pyramidal neurons by Golgi-Cox staining method and neuronal arborization pattern by Sholl analysis method in ECM compared to asymptomatic, anemic and control group of mice.

Golgi Cox staining: This is the most widely used staining method for studying the morphological aspects of neurons. It was first discovered by Camillo Golgi, an Italian physician and scientist who published his findings related to Golgi cox staining in the year 1873. This method was further improved by Santiago Ramon Y Cajal describing novel facts about the neuronal morphology in the brain.

INTRODUCTION

Malaria is one of the life-threatening diseases till date world over. According to World Health Organization (WHO), over 429,000 people died due to malaria worldwide in the year 2015. Malaria can be fatal in the form of cerebral malaria (CM) due to lack of proper diagnosis, improper treatment and compromised immune system of the malaria-infected individuals. CM is a neurodegenerative disease characterized by symptoms of fever, epileptic seizures, coma and even death caused by *Plasmodium falciparum* infection[1]. Underlying mechanism of CM pathology include sequestration of infected Red Blood Corpuscles (RBC's) in the brain microvasculature leading to disruption of the blood brain barrier[1]. Cognitive deficits in children and adults are reported even after recovery from CM[1].

Neuronal morphology plays a critical role in maintaining the neural activity and its functions. Dendritic arborization/ramification and maintenance of spine density of a neuron determine the extent of synaptic connectivity pattern in the brain. Alteration of neuronal morphology and dendritic spine density/morphology in pyramidal neurons has been reported in several neurodegenerative diseases affecting the cognitive functions[2]. However, this particular aspect is poorly defined in the context of CM.

Loss of neurotrophic factors such as Brain Derived Neurotropic Factor (BDNF), Nerve Growth Factors; neurotrophin-3 and neurotrophin-4 appear as primary reasons for cognitive impairment during neurodegenerative diseases[3]. Predominantly, diminution of BDNF in the brain may lead to cognitive impairment during CM[4, 5, 6]. Binding of BDNF to tyrosine kinase B (TrkB) receptor leads to the transcription and translation of several proteins aiming synaptic plasticity in the brain[7]. The LIMK-1/Cofilin-1 pathway is one of the downstream pathways of BDNF–TrkB signaling, includes LIMK-1, cofilin-1 and phospho-cofilin-1 (p-cofilin-1) proteins, which

perform vital functions in the brain maintaining actin cytoskeleton, dendritic spine morphology and density for functional synapses[15]. Cofilin-1 is an actin severing protein, ubiquitously expressed in the brain regulating the actin dynamics[10]. LIMK-1 is a serine/threonine kinase protein, abundantly expressed in the brain[10]. It is a potent regulator of actin reorganization machinery via phosphorylating cofilin-1 protein (inactive form) at serine residue which eliminates the binding of cofilin-1 to the actin[8, 9, 10]. LIMK-1 specifically regulates neuronal morphology maintaining the axonal outgrowth[11].

Actin is an important cytoskeletal protein which involves in neuronal development in the brain[12]. It consists of two isoforms; β-actin and γ-actin. β-actin participates in several developmental processes such as synaptogenesis, axonal guidance[12]. It is localized in dendritic spines of the neuron, which are the major elements of the synapse[13]. Dendritic spine size, morphology and density play a major role in maintaining learning and memory functions[14]. Based on the shape of the dendritic spines they are categorized into various types; thin, short, stubby and mushroom[15]. Mushroom spines are recognized as "memory spines", which contain Post Synaptic Density (PSD) proteins[16]. Dysregulation of neuronal actin and cofilin are associated with loss of cognition and degenerative conditions[17]. Exposure to oxidative stress, glutamate induced excitotoxicity, ATP depletion and pro-inflammatory cytokines induce activation of cofilin-1 leading to the formation of actin-cofilin rods in the brain[17]. Consistent with the fact that neuronal ultrastructure, dendritic spine density and morphology are responsible for maintaining vital neural functions, we asked whether its alteration is linked to the pathophysiology during CM. This prompted us to investigate the fate of neuronal morphology at ultrastructural level and a possible relation to LIMK-1/Cofilin-1 pathway in experimental CM (ECM).

SUBJECTS/MATERIALS AND METHODS

Ethics Statement

The experiments on the animals were carried after the approval from Institutional Animal Ethics Committee (UH/IAEC/PPB2014-I/68), University of Hyderabad, India.

Animals

Male C57BL/6, 3-4 week old (15-20g) mice were purchased from National Institute of Nutrition, Hyderabad and acclimatized at 25^0C with animal feed and water *ad libitum* at animal house facility, University of Hyderabad.

Animals were grouped into a) healthy controls (CON) (n=22), b) asymptomatic malaria (ASY) (positive control); *Plasmodium yoelii 17XL* (Pyl) infected mice (n=17). Mice were infected intraperitoneally with Pyl strain which resembles human malaria without exhibiting the symptoms of CM[18] from day 5-10 c) Mice infected intraperitoneally with *Plasmodium berghei ANKA* (PbA) reiterates the symptoms of human CM (n=19) on day 5-10 and d) Mice infected with Pyl strain with loss of RBC's are considered anemic (ANEM) from day 15-16 (n=16). Out of the above animals, experimental groups: CON (n=9), CM (day-7;n=8), ASY (day-7;n=11) and ANEM (day-16;n=9) were anesthetized with the dosage of ketamine (150mg/kg) combined with xylazine (10 mg/kg) and perfused intracardially with 0.9 % saline solution followed by 4% paraformaldehyde. Brains were subjected to dehydration in 20-30% sucrose solution for 3-4 days and cryosectioned at 15-20µm thickness for performing immunofluorescence and 100-200µm for Golgi-Cox experiment using Leica cryomicrotome CM1850.

Parasite infection

Parasite vials PbA and Pyl were procured from National Institute of Malaria Research (NIMR), New Delhi, India and stored in liquid nitrogen. Initially, three mice (source mice) were infected intraperitoneally with $1x10^6$ PbA and Pyl blood stage RBC's diluted in 0.2 ml of chilled sterile 1x Phosphate Buffered Saline (PBS) (pH-7.4). The parasitemia was monitored daily by staining the caudal blood smears by Giemsa stain (GS500 Sigma-Aldrich). $1 x10^6$ PbA parasites were passaged to rest of the mice intraperitoneally after confirmation of 3-5% parasitemia in the source mice. Control mice were administered with 0.2 ml of PBS buffer intraperitoneally.

Evaluation of CM by RMCBS

Assessment of behaviour in the infected mice through RMCBS (Rapid Murine Coma Behaviour Scale) is an accurate way to predict the manifestation of CM[19]. It is a time bound experiment performed in the post infected animals. Animals infected with PbA (n=19) and Pyl (n=9) parasite were video graphed for 90 seconds to assess ten behavioural parameters i.e. gait, balance, motor performance, body position, limb strength, touch escape, pinna reflex, toe pinch, aggression and grooming from day 5-10. Each parameter was scored 0-2 points based on the performance of the infected mouse. The total score was calculated for each mouse per day (0-20).

Golgi-Cox staining

Golgi-Cox staining is still a gold standard technique to determine the detailed morphology of neurons. Golgi-Cox staining was preferred as a reliable staining to determine the neuronal morphology, dendritic spine density and its morphology in all the experimental groups due to its less background. The brains collected after craniotomy were subjected to Golgi-Cox stain for 17 days at room temperature under dark condition followed by sucrose dehydration and

cryosectioning at 100µm thickness for dendritic spine studies whereas 200µm thick brain sections were used to analyze the dendritic arborization. Development of the Golgi-impregnated brain sections was performed as per the study conducted by Zaquot and Kaindl[20].

Dendritic spine density quantitation

Dendritic spine density of all the groups was quantified manually by counting the number of spines per 10µm length of the dendrites of layer 5 cortical pyramidal neurons of the Golgi-Cox impregnated brain sections. 21 distal dendrites of 10 neurons per section (n=8 animals per experimental group) were used for dendritic spine quantification from pictures captured at 100x resolution using Carl Zeiss microscope (NLO 710). Dendritic spine morphology was represented as inset pictures magnified to 200% of their original size. Statistical analysis of the dendritic spine density was performed with the average of the total number of spines per 10µm dendrites from each group and compared by means of one-way ANOVA[21].

Sholl analysis

Neuronal branching was evaluated in the Golgi-impregnated images of layer 5 cortical pyramidal neurons of all the experimental groups through Sholl analysis. It is an algorithm that creates imaginary concentric circles from the center of the soma to the tip of the dendrites of a neuron[22]. The complexity of neuronal arborization was evaluated based on counting the maximum number of intersections of the dendrites of a neuron (Nm or critical value) with the circles, critical radius (r_c);the distance from the soma at maximum Nm and number of primary dendrites (Np) (dendrites emerging from the neuron's soma). From the above parameters, Schoenen ramification index (Nm/Np); the ratio of number of maximum branching (Nm) to the number of primary branching (Np) was calculated. Soma centered images (11 neurons per section; n=8

animals per group) captured at 40x resolution using Carl Zeiss microscope (NLO 710) were converted to 8-bit greyscale images using Adobe Photoshop CS6 software, skeletonized and subjected to threshold using the Image J software. Sholl analysis was carried out using Sholl plugin in the Image J software 1.49v, National Institute of Health, U.S.A.[23]. The linear method of Sholl plot was applied; the graph was plotted for the average number of intersections (Nm) of the neurites of each experimental group on Y-axis against the radial distance of the neurites from the soma (µm) on X-axis.

Fluoro Jade C staining

Fluoro-Jade C staining (AG325 Millipore) is ideally carried out to observe the neurons undergoing neurodegeneration in brain sections. Brains collected from all the experimental groups were subjected to sucrose dehydration steps and cryosectioned at -25^{0}C at 12 µ thick sections. Staining was performed according to the protocol reported by Ehara and Ueda[24]. The sections were examined under Olympus BX51 microscope using a filter system to observe the fluorescence under 60x objective (Excitation: 385 nm, Emission: 425 nm).

Double immunofluorescence staining

20µm thickness brain cryosections of all the experimental groups were subjected to washing using 1x PBS with 0.3M glycine for 30 minutes. The sections were permeabilized with 0.4% Triton-X 100 in 1x PBS for 20 minutes at room temperature. The sections were blocked for 2 hours with 5% normal goat serum in 1x PBS with 0.3% Triton-X 100 at room temperature followed by incubation with primary antibody at 1:100 concentration for 3-4 nights at 4^{0}C in the same buffer. Primary antibodies used for this study include anti-cofilin-1(5175S), anti-phospho-cofilin-1 (3313S), anti-LIMK-1 (3842) and anti-β-actin (3700T mouse, 4970 rabbit) from Cell

Signaling Technology and anti-neurofilament heavy polypeptide antibody (ab7795) from abcam. After the primary antibody incubation, the sections were washed with 1x PBS for 30 minutes at room temperature followed by incubation with the secondary antibody: Anti-rabbit IgG (4412S Alexa Fluor® 488 Conjugate) and Anti-mouse IgG (4409S Alexa Fluor® 555 Conjugate) from Cell Signaling Technology for 1 hour at room temperature. Sections were washed with 1x PBS and mounted with prolong gold antifade reagent with DAPI (8961S Cell Signaling Technology). All the images were captured on laser scanning confocal microscope (Carl Zeiss LSM 880) using ZEN Blue software at 40 x magnification. To study the exact location of actin-cofilin rods, we probed the anti-β-actin (3700T) and anti-cofilin-1(5175S) antibody individually with anti-neurofilament heavy polypeptide antibody in CON and CM brain sections. Evaluation of actin-cofilin rods in CM and ASY brain sections (n=7 images per group) was carried out manually by quantitative morphometry using Image J software (counting the number of rods in the images of 300dpi resolution of the brain sections immunostained with β-actin and cofilin-1). The area was set constant for all the images representing actin-cofilin rods before analyzing their content.

Estimation of ROS by DCFDA method

DCF-DA (2', 7'-Di Chloro Fluorescin Diacetate) (D6883 Sigma-Aldrich) is a reduced form of non-fluorescent stain, acts as an indicator for Reactive Oxygen Species (ROS). Upon oxidation and esterification, the acetate groups of DCF-DA are cleaved to highly fluorescent 2', 7'-Dichlorofluorescin. Whole brain tissues (n=6 per group) were weighed, (100mg) homogenized in 1x PBS using Dounce homogenizer and centrifuged at 6000 rpm for 15 minutes at 4^0C. 10µl of the supernatant was mixed with 55µl of 0.02M of HEPES dissolved in deionized water. 90µl of freshly prepared DCF-DA (20µM concentration dissolved in DMSO culture grade solution) was added to the above mixture in a 96 well plate and incubated at 37^0C for 30 minutes at dark

condition. Fluorescence intensity was determined with a plate reader at an excitation wavelength of 485 nm and the emission wavelength of 515 nm using Tecan Spectrofluorimeter infinite 200 PRO instrument.

Preparation of brain tissue lysates

Animals were euthanized, brains were collected onset of CM on (day 7;n=7), (CON;n=9), (ASY day 7;n=7), (ANEM;n=7) on day 15 and stored at -80^{0}C. Tissues (100 mg) of all the experimental groups were homogenized using Dounce homogenizer with 8 to 10 strokes at 4^{0}C in Radio-Immunoprecipitation Buffer (RIPA) (50mM Tris-HCl, 150mM NaCl, 1% NP-40, 0.5% sodium deoxycholate, and pH-8). Protease and phosphatase inhibitor (P8340, P0044 Sigma-Aldrich) (10µl per 1ml of lysate) and 1mM phenylmethylsulphonyl fluoride (PMSF) were added to the homogenate. The homogenate was centrifuged at 12,000 rpm for 15 minutes at 4^{0}C using KUBOTA 7780 refrigerated centrifuge. The supernatant was frozen upon collection at -80^{0}C.

Western blotting

Estimation of protein concentration was carried out by Bradford method (B6916 Sigma-Aldrich). 50 µg of the protein of tissue sample was resolved by 15% Sodium Dodecyl Sulphate-Poly Acrylamide Gel Electrophoresis (SDS-PAGE). The gel was transferred onto the nitrocellulose membrane (Protran Amersham GE) in Towbin buffer (Tris-HCl- 3 g, glycine-14.4 g, deionized water - 800ml, methanol -200ml pH-8.3) overnight for 16 hours at 4^{0}C. The membrane was washed with Tris-buffered saline (TBS) containing 0.05% Tween 20 for 5 minutes and blocked with 5% skimmed milk for 1 hour followed by incubation with the primary antibodies of anti-cofilin-1(5175S), anti-phospho-cofilin-1 (3313S), anti-LIMK-1 (3842), anti-β-actin (4970S) and anti-GAPDH (5174T) (1: 1000 dilution each) (Cell Signaling Technology U.S.A.) overnight for

16 hours at 4^0C. The membrane was washed with TBS and incubated with the anti-rabbit IgG (whole molecule) secondary antibody (A3687 Sigma-Aldrich) conjugated to alkaline phosphatase for 2 hours at room temperature. Chemiluminescence signal against the alkaline phosphatase conjugated secondary antibodies were analyzed by adding 120µl of BCIP (5-bromo-4-chloro-3-indolyl-phosphate) (SRL chemicals) solution in conjunction with 120µl of NBT (Nitro Blue Tetrazolium) (SRL chemicals) solution and added to 4ml of alkaline phosphatase buffer (Tris-2.422 g, NaCl- 1.68 g and $MgCl_2$- 0.203 g for 200ml of distil water), poured onto the membrane and kept on the rocker for 10 minutes under dark condition.

Densitometric analysis of all the protein expression data, normalized with the loading control (GAPDH) was performed using Image J software 1.49v Wayne Rasband, National Institute of health (NIH), U.S.A and the graphs were plotted using Sigma Plot 11.0 software.

RNA isolation and RT-PCR analysis

Total RNA was isolated from the whole brain samples of all the experimental groups (n=4) using Trizol reagent (T9424 Sigma Aldrich). cDNA was synthesized from 1µg concentration of RNA sample using PrimeScript™ 1st strand cDNA Synthesis kit (Takara Bio). Semi-quantitative PCR (Applied Biosystems Veriti 96 well Thermal cycler) was carried out in duplicates for 10µl reaction using Dreamtaq green PCR master mix from Thermo Fisher Scientific at 35 cycles for LIMK-1, cofilin-1, β-actin and GAPDH respectively. PCR conditions included denaturation step at 95^0C for 30seconds (stage-1), 95^0C for 2 minutes (stage-2), annealing at respective melting temperature (Tm) for 45 seconds and extension at 72^0C for 5 minutes. Quantitative PCR for above genes was performed (Applied Biosystems 7500 Fast Real-Time PCR System) using SYBR green PCR Premix ExTaq (Takara Bio) in triplicates and the expression pattern was

analyzed using ΔCt values for each sample in terms of relative gene expression after normalization with Glyceraldehyde -3 phosphate dehydrogenase (GAPDH). 1µl of cDNA and 1 picomolar concentration of primers were added to the SYBR green PCR mixture. GAPDH was used as an internal control in semi-quantitative and quantitative PCR. Primers were procured from Integrated DNA Technologies (IDT). Primer sequences and their Tm for quantitative and semi-quantitative PCR are listed in table.1.

Gene and NCBI Reference Sequence	**Forward primer sequence**	**Reverse Primer sequence**	**Size (bp)**	**Tm (^{0}C)**
LIMK-1 NM_001305875.1	5'-TGTCCGAGTCCAAGGAGTGG-3'	5'-CCCATGGCCCAGTGAGTCA-3'	202	59.3
Cofilin-1 NM_007687.5	5'- CTGGGCCCCCGAGAATGC-3'	5'-CTCCAGGGAAATGACGGCGC-3'	178	61.4
β-actin NM_007393.5	5'-GATCCTGACCGAGCGTGGCTA-3'	5'- ACCGCTCGTTGCCAATAGTGATG-3'	191	60.4
GAPDH NM_008084.3	5'-GTGTGAACGGATTTGGCCGTATTG-3'	5-'TTTGCCGTGAGTGGAGTCATACTG-3'	146	58.8

Table1. Primers used for quantitative and semi quantitative PCR.

Statistical Analysis

All multiple pairwise comparisons for western blots, dendritic spine density, Sholl data, semi-quantitative and quantitative PCR were analyzed by one-way ANOVA followed by student Neuman-Keuls method ($P<0.05$ was considered as significant) using Sigma plot software 11.0.

Parasitemia curve and Sholl graph was plotted using XY format of GraphPad Prism software version 5.03. Results were represented as the mean ± Standard error of the mean (SEM).

RESULTS

Neurobehavioural assessment for symptoms of ECM

Symptoms of CM appear from day 5 -10 post-infection[19]. Animals symptomatic to CM were assessed more frequently, as follows: mice were evaluated every 12 hours when the RMCBS score was 16–20 and every 4 hours when the RMCBS score was 11– 15. The mice were considered moribund and sacrificed at the total score of 10-13. The PbA parasite-infected mice showed impaired locomotion; touch response, pinna reflex and grooming behaviour with a total RMCBS score of 11 on day 7 and 10 on day 8 (Video file; CM) (Fig 1). We observed mild impairment in touch response and pinna reflex behaviour in some (n=5 out of 9) of ASY group while performing the RMCBS on day 7 (Video file; asymptomatic). Anemic mice were not subjected to RMCBS experiment. No behavioural impairment was observed in control mice (Video file; Control). Out of nineteen animals, eleven were symptomatic to CM.

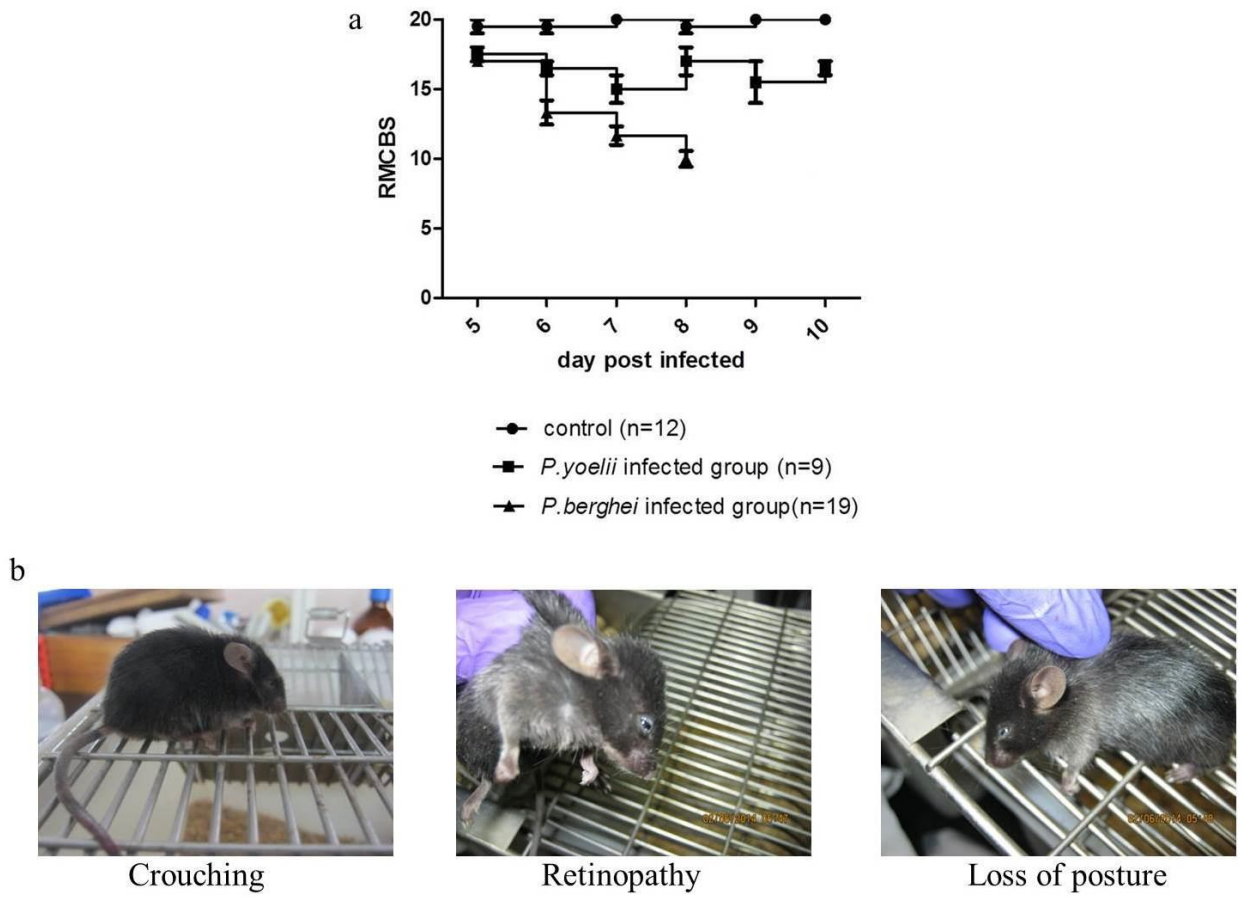

Figure 1. a) Graph representing the RMCBS scores to assess behavioural parameters from day 5-10 in *P.berghei*, *P.yoelii* infected mice and CON group. b) Abnormal behavior involving crouching, loss of posture and signs of retinopathy (retinal hemorrhages).

Alteration of neuronal morphology at ultra-structural level in ECM

Fluoro-Jade C stain selectively stains the damaged neurons which fluoresce as bright green extended dots. The intensity of the fluorescence as well as the number of dots represents the extent of neurodegeneration. We observed significant neurodegeneration in the cortical areas of CM, ASY and ANEM brain sections (Fig 2B to D). We did not observe fluorescence in the control brain regions (Fig 2A). Golgi-Cox staining is known for its metallic impregnation to the neurons specifying minute details related to the axon, dendrites and dendritic spines. We focused on the layer 5 pyramidal neurons in the cortical areas of the Golgi-impregnated brain sections of

all the experimental groups. Dendritic varicosities (swelling of dendrites) were specifically observed in Golgi-impregnated neurons of CM infected brain sections which have not been reported elsewhere in animal models of CM till date (Fig 3B to D). Dendritic varicosities were not observed in Golgi-impregnated CON (Fig 3A), ASY and ANEM brain sections (data not shown). Further, alteration in the dendritic arborization of neurons in the CM infected brain sections was observed through Sholl analysis (Fig 4G). Sholl graph illustrates that the critical radius of the cortical neurons of CM (r_c) was significantly reduced (200.0±0.64) compared to the control group (450.2±0.78) (***P<0.001). Significant reduction in the primary branching (Np) (4.23±0.71) as well as maximum intersections of the neurites (Nm/critical value) (6.46±0.34) was observed in CM brain sections compared to control group (9.01±0.12; 22.3±0.21) (***P<0.001). Based on the calculation of Schoenen ramification index, 62.5% de-ramification of neurites were observed in cortical regions in CM infected (1.59±0.07) compared to all the control group (2.54±0.16) (**P=0.001) (Table 1).We analyzed 9.2 dendritic spines per 10µm dendrite in CM infected group compared to CON (35.8 spines/10µm dendrite), ASY (16.7 spines/10µm dendrite) and ANEM (24.8/10µm dendrite) groups (Fig 4E). The dendritic spine density of layer 5 pyramidal neurons was significantly reduced in CM compared to the control group (***P<0.001). We observed altered morphology of dendritic spines as well as loss of mushroom spines in CM, ASY and ANEM groups (Fig 4B to D).

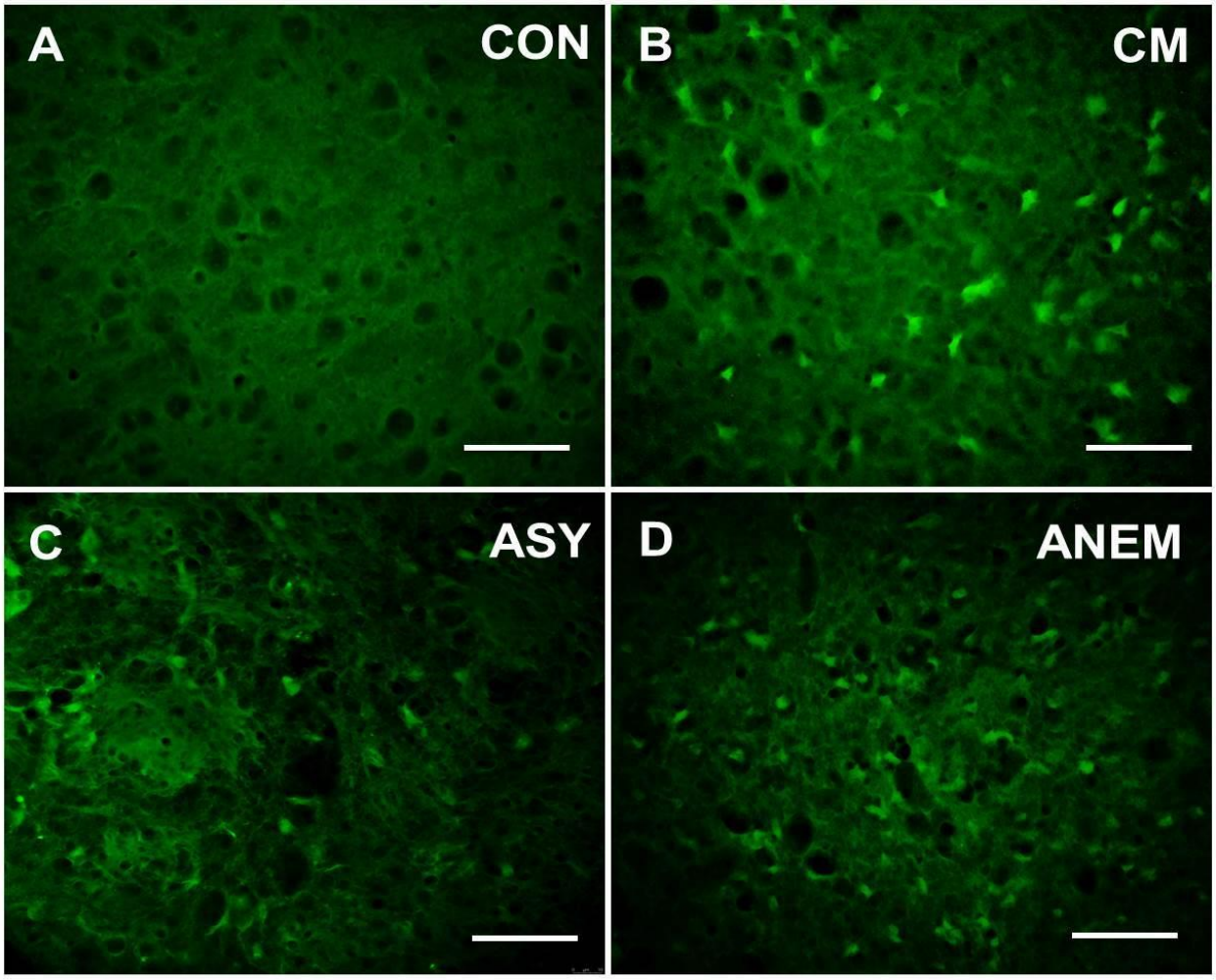

Figure 2. Illustrates the degenerated neurons stained by Fluoro Jade C stain in the cortical areas of B) CM, C) ASY and D) ANEM brain sections. Scale bars in A,B,C,D = 80µm.

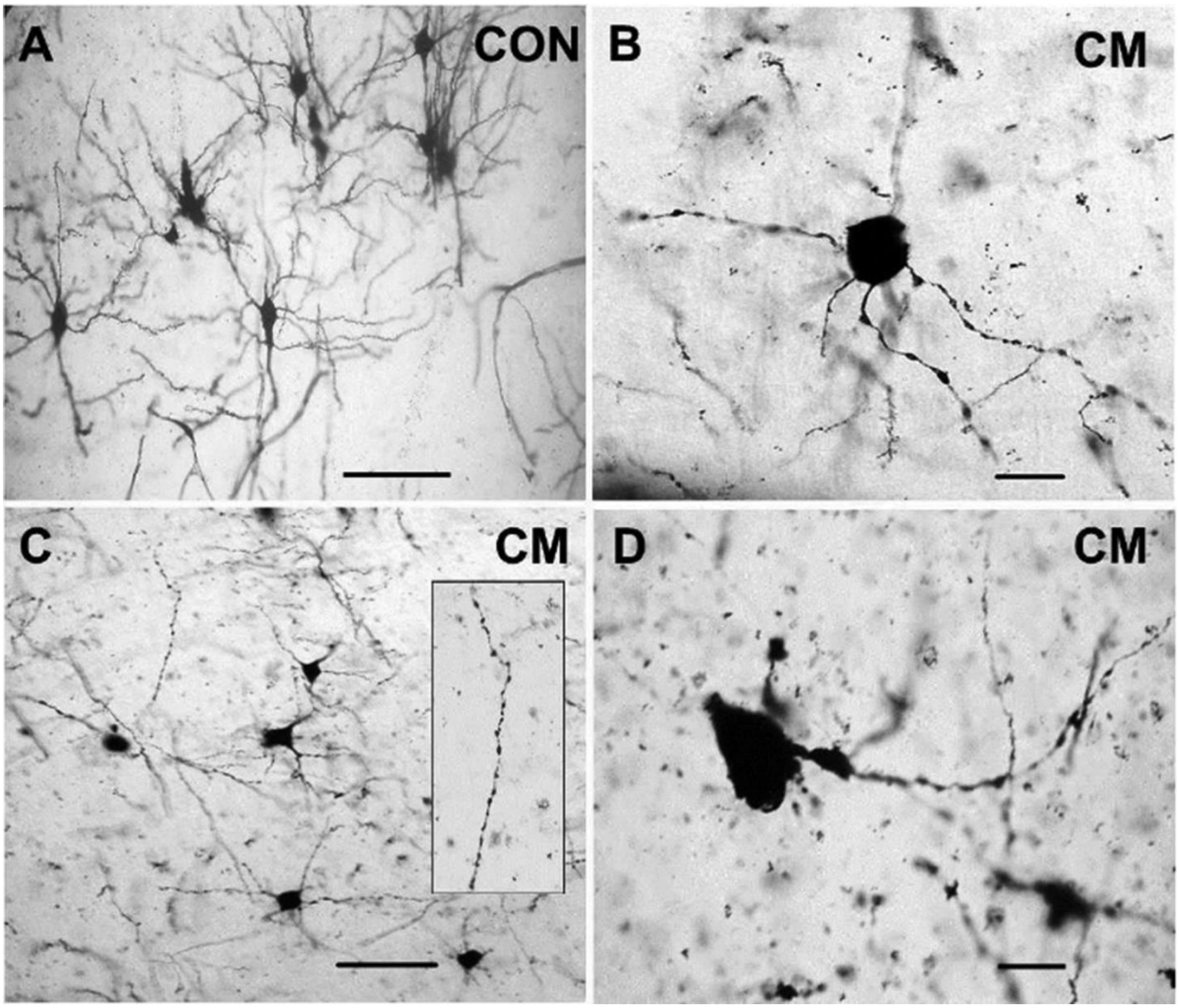

Figure 3. Representing the Golgi-Cox stained pyramidal neurons of layer 5 cortical area of A) Control neurons (CON) with extensive dendritic arborization, B,D) CM infected neuron representing the dendritic varicosities, C) CM infected neurons lacking dendritic arborization with varicosities. Scale bars in A,C = 60µm and B,D = 20 µm. (original magnification X1000).

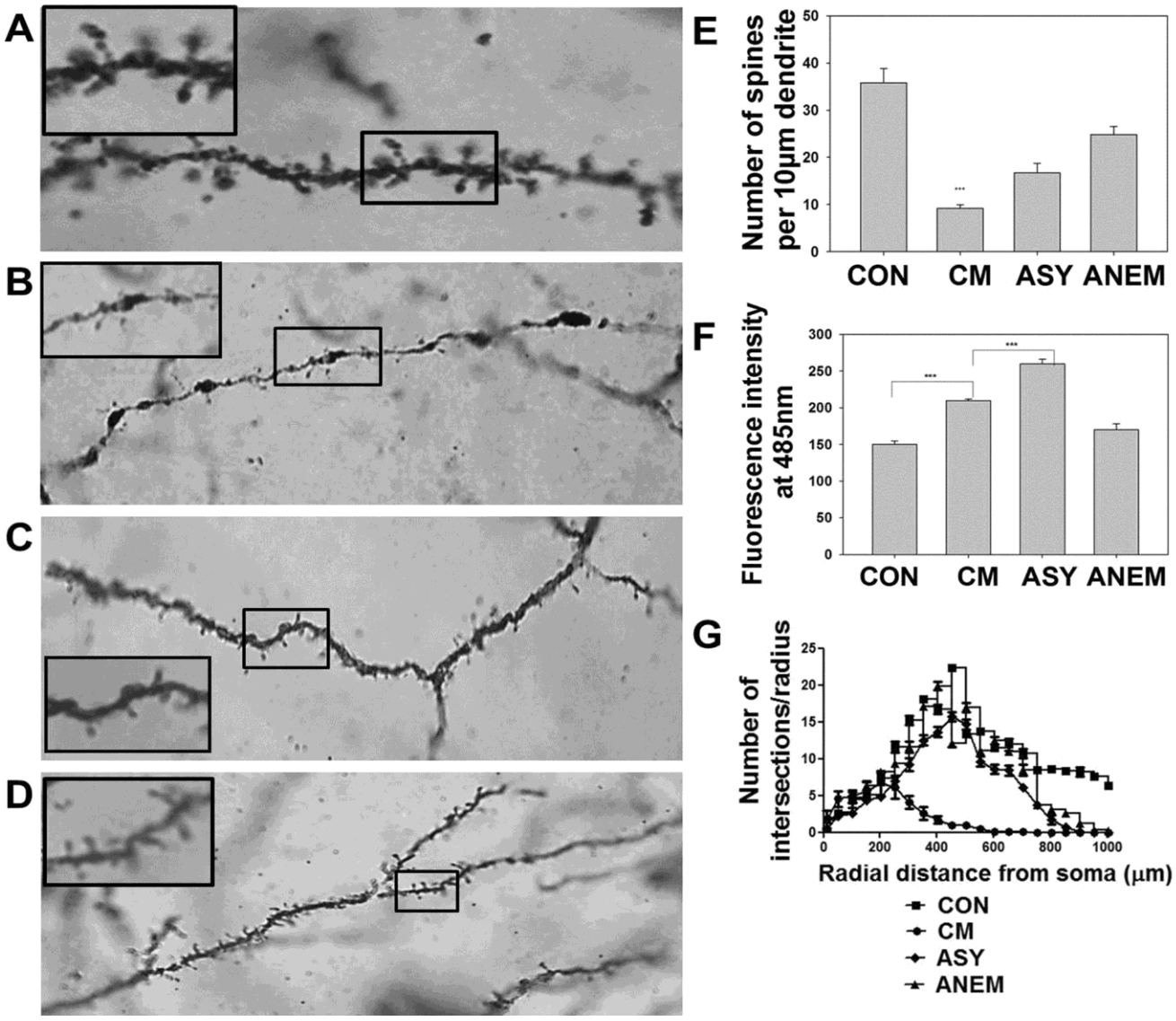

Figure 4. Illustrates Golgi-Cox stain impregnated dendritic spines of layer 5 cortical pyramidal neurons of all the experimental groups, representing magnified images of dendritic spine morphology of A) control dendrite (CON) with mushroom spines, B) CM infected dendrite with varicosities lacking spines, C) Malaria infected (ASY) dendrite with stunted spines, D) dendrite of anemic (ANEM) brain with altered spine morphology. E) Graph representing the dendritic spine densities (mean + SEM) per 10µm of dendrite (n=21 dendrites per group). Statistical significance: ***P<0.001. F) Graph representing the fluorescence intensity of ROS in the whole brain lysate of all the experimental groups using 2′,7′-Dichlorofluorescin diacetate method (n=7 brain samples per group). Statistical significance: ***P<0.001. G) Graphical representation of dendritic arborization pattern (Mean ±SEM) of all the experimental groups through Sholl analysis (n=11 neurons per group). Scale bar in A,B,C,D = 2µm for images representing dendrite spine morphology and 8 µm for images illustrating dendrite of all the experimental groups.

S No.	Number of parameters	CM	CON	ASY	ANEM
1	Maximum number of intersections to the circle (Nm)	**6.46±0.34*** **	22.3±0.21	15.5±0.23	19.89±0.67
2	Critical value rc (µm)	**200.0±0.64*** **	450.2±0.78	450.3±0.27	400.0±0.34
3	Number of primary branches (Np)	**4.23±0.71*** **	9.01±0.12	7.86±0.65	8.41±0.75
4	Schoenen ramification index (Nm/Np)	**1.59±0.07** **	2.54±0.16	2.03±0.14	2.41±0.17
	n= neurons/animals	16/5	16/7	16/5	16/6

Table 2. Parameters analyzed from the Sholl graph and the soma centered Golgi-Cox impregnated images in all the experimental groups. Statistical significance ***P<0.001, **P=0.001

We estimated the ROS levels in whole brain tissue lysates of all the experimental groups by DCFDA method. The measure of ROS was plotted as fluorescence intensity on Y-axis. We observed significant increase of fluorescence intensity (225.43) in CM compared to CON group (143.3) (***P value<0.001). Interestingly, we found elevated ROS levels in the ASY (264.67) than CM infected group. We observed mild increase in the ROS levels (166.67) in ANEM compared to CON group (Fig 4F).

ECM alters gene expression of LIMK-1, cofilin-1 and β-actin

We examined the gene expression patterns of LIMK-1, cofilin-1 and β-actin in the whole brain samples of all the experimental groups by performing semi-quantitative and quantitative PCR technique. We observed significant upregulation in the gene expression of LIMK-1 and cofilin-1 in CM compared to control (CON) group (** P-value<0.050) (Fig 5B to C). Upregulation of the β-actin gene expression was less significant in CM compared to CON group (* P-value=0.001) (Fig 5D) was observed after performing quantitative PCR. Noticeable changes were observed in

the gene expression pattern of cofilin-1, LIMK-1 and β-actin among CM, ASY and ANEM samples in the agarose gel after performing semi-quantitative PCR (Fig 5A). First, gene expression of LIMK-1 was upregulated in CM compared to CON group whereas it was downregulated in ASY compared to ANEM group. Second, cofilin-1 gene expression was upregulated in CM compared to CON group. Third, β-actin gene expression was slightly upregulated in CM compared to CON group whereas it was downregulated in ANEM compared to all the experimental groups. Taken together, the altered expression of the above genes is one of the crucial evidences to analyze the dysregulation of LIMK-1/cofilin-1 pathway in ECM.

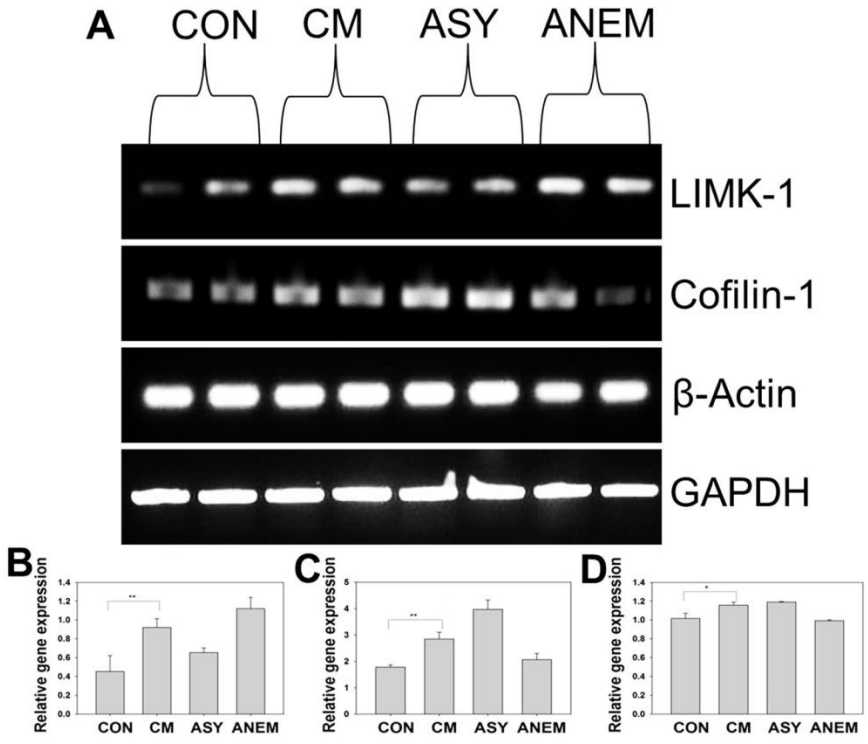

Figure 5. Representing A) gene expression pattern of LIMK-1, cofilin-1 and β-actin in all the experimental groups by semi-quantitative PCR, B) expression of LIMK-1, C) Cofilin-1, D) β-actin genes by quantitative PCR. Statistical significance **P<0.050, *P=0.001.

ECM alters protein expression of LIMK-1, Cofilin-1/p-cofilin and β-actin

After observing the gene expression pattern, our investigation shifted towards the expression of the proteins involved in the LIMK-1/Cofilin-1 pathway. Analysis of Western blots revealed the complete reduction in the expression of the LIMK-1 protein in whole brain lysate of CM compared to CON group (*** P-value<0.001) (Fig 6A, B). Reduced expression of LIMK-1 was also observed in ANEM compared to the CON group. We observed a significant decrease in the expression of cofilin-1 protein in CM compared to all the other experimental groups (**P-value=0.001) (Fig 6A, C). Interestingly, we observed a significant reduction in the expression of p-cofilin-1 in ASY and CM group (*** P-value<0.001) (Fig 6A, D) compared to CON and ANEM groups. As per the hypothesis, we observed a significant reduction in the expression of β-actin in CM compared to all the experimental groups (*** P-value<0.001) (Fig 6A, E). GAPDH was used as a loading control.

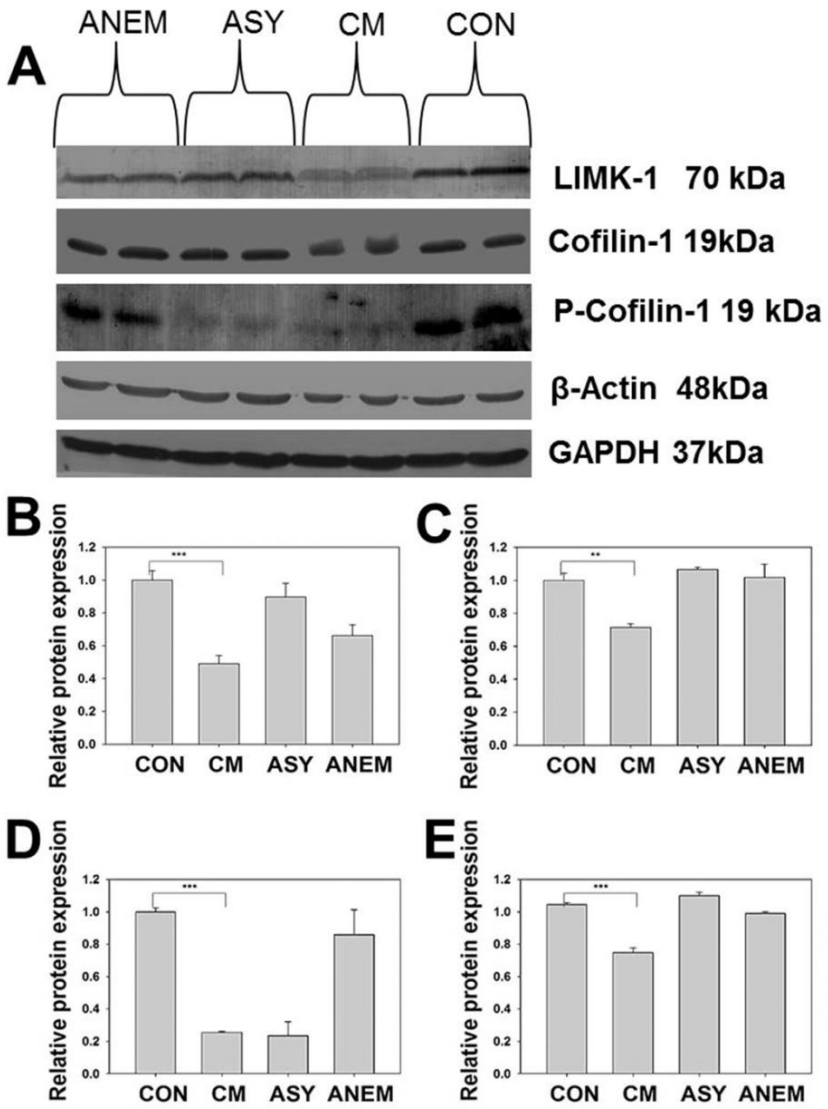

Figure 6. Representing the protein expression pattern by western blotting A) LIMK-1, Cofilin-1, p-cofilin-1, β-actin and GAPDH in the whole brain lysates of mice symptomatic to CM, ASY, CON and ANEM. Densitometric analysis for protein expression of B) LIMK-1, C) Cofilin-1, D) p-cofilin-1, E) β-actin. Statistical significance: ***P<0.001, **P=0.001

Actin-cofilin rods are detected in the neurites during ECM

Stress induced actin-cofilin rods are the pathogenic hallmark in most of the neurodegenerative diseases[25]. By performing the double immunofluorescence technique for actin and cofilin-1 proteins in the 20µm brain cryosections, we detected actin-cofilin rods in the cortical regions of CM (Fig 7C, D), ASY (Fig 7E, F) and ANEM (data not shown) brain sections through confocal

imaging. Actin filaments (red) were continuous, colocalized with cofilin-1(green), completely surrounding the nucleus and widely distributed in the control brain sections (Fig 7A, B). We identified an average of 10 actin-cofilin rods in cortical areas of CM compared to ASY group brain sections at a constant area of 8.790m^2 of all the images (*** P-value<0.001) (Fig 7G). Further, we identified that the actin and cofilin rods are localized at the distal neurites in the cortical and hippocampal region of the CM infected brain sections (Fig 8D to I) compared to CON group (Fig 8A to C).

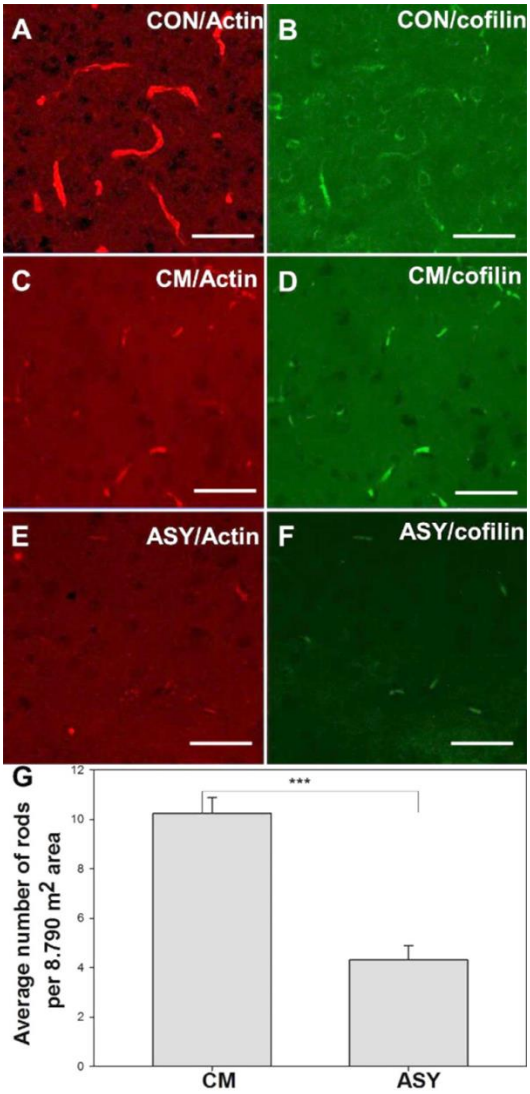

Figure 7. Illustrating double immunofluorescence staining indicating co-localization of A) β-actin (red) and B) Cofilin-1 (green) in the cortical regions of control, C) β-actin (red)

discontinuous rods, D) Cofilin-1 (green) rods in cortical regions of CM, E) β-actin (red) and F) Cofilin-1 (green) rods in cortical regions of ASY brain sections, G) Graph representing the average number of actin-cofilin rods in CM and ASY images (n=6 images) per 8.790m2 area of brain sections. Statistical significance: ***P<0.001. Scale bar in A,B,C,D = 20µm

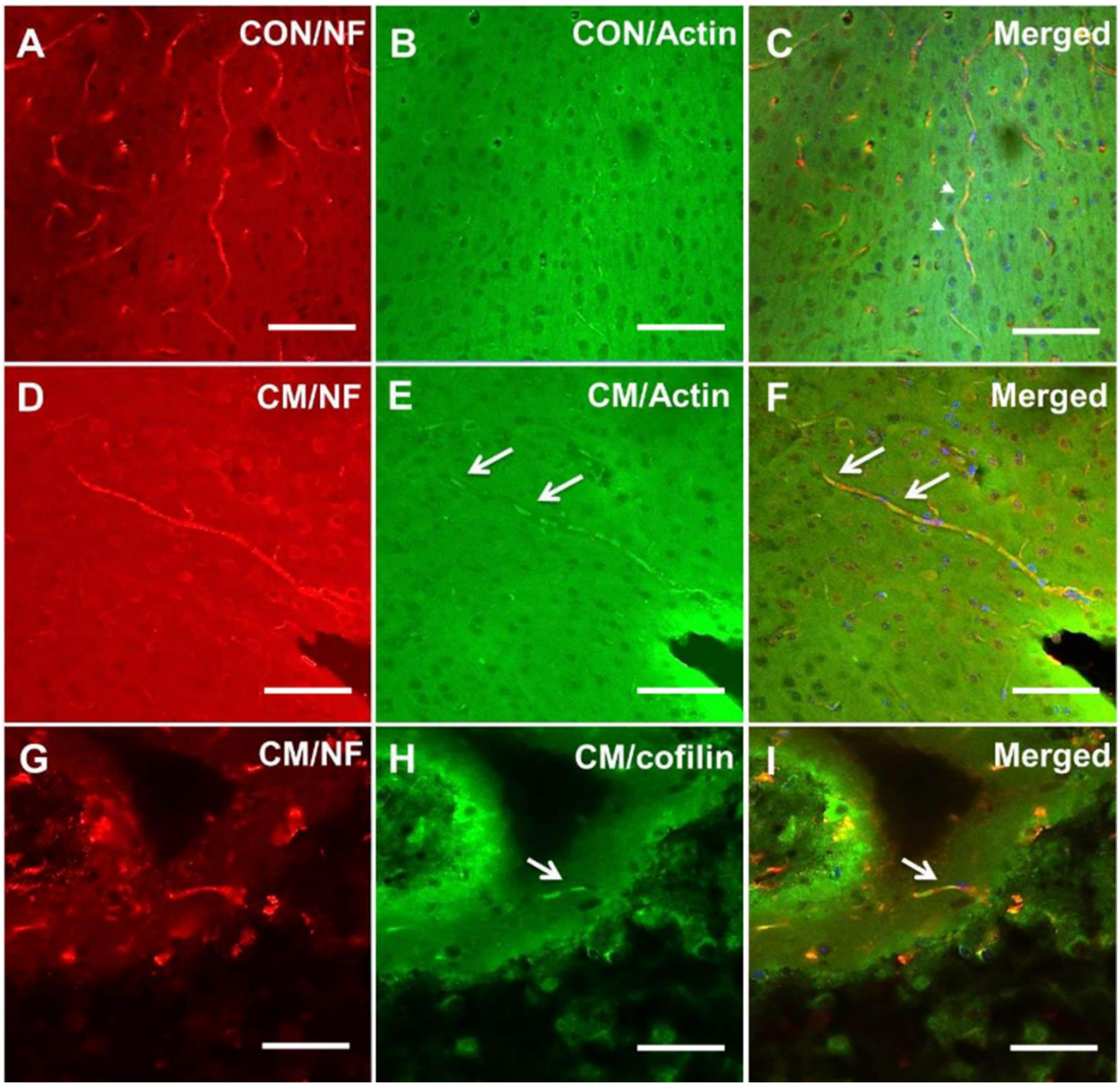

Figure 8. Illustrating the neurites stained with A) neurofilament antibody (NF) (red) colocalized with B) β-actin (green) and C) arrow heads representing the merged actin in the neurites at the cortical regions of the CON group, D-F) β-actin rods (green) colocalized within the distal neurites (red) of the cortical regions of the CM group and G-I) Cofilin rods (green) colocalized within the neurites (red) of the hippocampal region of CM brain section. Arrow marks representing the actin-cofilin rods in panel F and I. Scale bar = 20µm.

DISCUSSION

PbA infected C57BL/6 mice is the widely accepted model, which re-iterates significant symptoms of human CM. Recently, the relevance of PbA infected mouse model to human CM has been reported by complementation of its orthologous proteins with *Plasmodium falciparum* that restores sequestration and virulence[26]. A significant downfall in the RMCBS score on day 7 and 8 shows that mice infected with PbA parasites were symptomatic to CM. The hemorrhages at cortical regions in CM and ASY brain sections proved that PbA and Pyl parasites were able to invade the brain tissues on day 6-8 post infection (data not shown). Furthermore, we observed significant neurodegeneration by Fluoro Jade C staining in cortical regions of brain sections of CM, ASY and ANEM groups. Therefore, we assumed possible chances for alteration of neuronal morphology in the experimental paradigm.

In the present study, we demonstrated the ultrastructure of the neurons using Golgi-Cox stained brain sections of cortical region, layer 5 (internal pyramidal layer) consists of large pyramidal neurons, which are mostly involved in maintaining learning and memory functions in the brain[27]. We showed significant loss of mushroom spines in CM, ASY and ANEM brain sections which could be correlated to the impairment of learning and memory functions. Focal swelling of dendrites also known as dendritic varicosities is one of the pathological signs of the altered dendrites reported in stroke, dementia, Alzheimer's and Parkinson's diseases[28, 29, 30]. Dendritic varicosities are reported to be the hallmark of excitotoxicity (e.g. NMDA receptor mediated) injury in the brain[31]. Loss of dendritic spines tends to reduce synapses during neurodegeneration that impacts cognitive impairment. Most of the dendritic spines were lost at the site of dendritic varicosities in CM which could be due to the engulfment of spines by the

swollen dendritic membrane[32]. Thus, reduced dendritic spines, altered dendritic arborization and spine morphology of cortical layer 5 pyramidal neurons could impact cognitive impairment in CM. Sholl analysis is ideally suited for Golgi-Cox stained individual neurons. Based on previous studies, it appears that BDNF regulates the primary dendrite formation in cortical neurons[33]. Through Sholl analysis, we found that the number of primary dendrites (Np) was reduced in CM compared to all the experimental groups. Significant reduction of the critical radius (r_c) and Nm value/critical value determine the reduced length and ramification pattern of the dendrites in CM. We have observed reduced Shoenen ramification index which is a sign of impaired dendritic arborization in CM. Therefore, we assume impaired neural ramification/ arborization could affect the connectivity pattern during CM. ROS are considered as potent neurotoxic molecules affecting the function of enzymes and cytoskeletal proteins. Excessive amount of ROS leads to cognitive impairment in mammals[34]. Then we asked a question whether oxidative stress has any role in the post CM outcome. We observed significant increase in ROS levels in CM compared to control suggesting that oxidative stress might be crucial in the pathogenesis of CM. Our results are in agreement with previous observation that PbA infected mice induce oxidative stress contributing to the pathogenesis of CM[35]. Interestingly, we observed increased ROS in the brain lysate of ASY compared to CM group.

Loss of dendritic spines is directly proportional to the diminution of β-actin protein during the pathology. Therefore, we questioned that what could be the fate of signaling pathways which maintain reorganization of actin in the brain during CM. Several cytoskeletal signalling pathways maintain the dendritic spine stability such as binding of Ephrin-B to EPHB2 receptor which triggers the activation of GTPase Rac-1, binding of Myristoylated alanine-rich C kinase substrate (MARCKS) to actin filaments[15]. LIMK-1/Cofilin-1 pathway is activated upon binding

of neutrophic factors on the postsynaptic membrane which is involved in the maintenance of actin. Importantly, LIMK-1/Cofilin-1 pathway dependent actin remodeling is necessary for maintaining dendritic spine morphology and synaptic plasticity[36]. Indeed, knockout mice for LIMK-1 have significant impairment of long-term synaptic plasticity which drives the long-term memory functions in the brain[37]. Further, deletion of LIMK-1 gene is associated with Williams Syndrome, a neurodevelopmental disorder resulting in impairment of learning abilities and visuospatial cognition in human[37]. Altered gene expression of cofilin-1 and β-actin has been reported in ECM previously[38]. Based on the differential gene expression pattern compared to the control sample, we have identified LIMK-1 as a novel host molecule in the brain which could serve as a prognostic biomarker affected during the pathology of ECM. Interestingly, we observed diminished expression of proteins compared to the prominent gene expression patterns of LIMK-1, cofilin-1 and β-actin in ECM. We assume either suppression of the translation machinery or rapid degradation of the translation product of the above genes during the pathology. Therefore, we have found a significant negative correlation between the gene expression and protein levels of LIMK-1/cofilin-1pathway in ECM. The pathology of CM involves cerebral ischemia, oxidative stress, glutamate induced excitotoxicity, endoplasmic reticulum stress that deviate numerous signaling pathways in the brain. Stress induced actin-cofilin rods are associated with several neurodegenerative diseases such as stroke, Alzheimer's disease and cerebrovascular dementia[17]. Rods impair the synaptic plasticity and play a major role in impairment of cognition[17]. Apart from actin–cofilin rods, we have also identified LIMK-1 and p-coflin-1 proteins co-localized with actin in the rod like structures in the CM infected brain sections (data not shown). We observed actin-cofilin rods in the neurites at cortical and hippocampal regions of the CM infected brain sections which could be a striking evidence for

the disruption of neuronal morphology and its functions during the pathology of CM. Presence of actin-cofilin rods in the neurites has been reported in Alzheimer's disease[17]. To the best of our knowledge, our findings represent the first report for the presence of actin-cofilin rods in the pathology of ECM. As per the protein levels, we assume the loss of LIMK-1 might influence several activities such as activation of cofilin-1, loss of mushroom spines and downregulation of β-actin expression during CM. However, the role of LIMK-1/Cofilin-1 pathway in CM is not yet understood. Further, downregulation of cofilin-1 and p-cofilin-1 might also affect dendritic spine morphology and maintenance of β-actin during CM. In fact, low concentration of cofilin-1, promote disassembly of actin whereas high levels of cofilin promote actin nucleation and assembly[39]. We speculate that low expression of cofilin-1 may associate with the actin degradation and loss of dendritic spines in CM. High concentrations of p-cofilin-1 are directly linked to enlargement of dendritic spine regulating the learning functions by improving the long-term potentiation (LTP) [40, 41]. It appears that loss of p-cofilin-1 could affect the dendritic spine enlargement in CM and the ASY group. Nevertheless, further research is essentially needed to understand the exact mechanism underlying β-actin downregulation via LIMK-1/Cofilin-1 in the pathophysiology of CM. Earlier, our group has demonstrated the loss of PSD protein-95 in ECM, which can be correlated to the altered spine morphology and density[42].

Interestingly, we came across mild impairment in the behaviour while performing the RMCBS experiment in ASY group. According to previous studies, cognitive impairment was also observed in children recovering from malaria[43]. Apart from impaired behaviour, we have also observed elevated levels of ROS, reduced dendritic spine density, loss of mushroom spines, diminished p-cofilin-1 expression and localized actin–cofilin rods in the brain sections of ASY group. Therefore, our results agree with the cognitive impairment due to malaria in human.

Evidence regarding the impairment of cognition exists in the form of diminution of BDNF levels in ECM[4, 5, 6]. Studying the downstream functions of BDNF signaling in murine CM models could provide new insight to the neuropathology responsible for the loss of long term memory and synaptic plasticity.

Artemisinin-based combination therapy is currently recommended for the treatment of CM. Based on previous studies, it appears that artemisinin derivatives have neurotoxic effects inducing oxidative stress in the brainstem altering the behavioural pattern in rodents[44, 45]. About 25% survivors of human CM suffer from depression, memory loss, inattentiveness and aggressive behaviour[46]. Therefore, there is an urgent need to study the molecular and behavioural effects after administration of drugs, which can improve cognition in combination to the artemisinin derivatives in experimental models of CM. Nootropics (drugs that improve cognition) are often used to treat cognitive impairment in patients suffering from stroke, Alzheimer's, attention deficit hyperactivity disorders etc[47]. These drugs belong to the category of psychotropic agents which emphasize in improving learning and memory functions in the brain[48]. Several nootropic drugs have been reported to improve the levels of neurotrophic factors in the hippocampal brain region of rodents[49]. Nootropics are associated with enhancing the neural ramification process leading to improvement of brain plasticity[50]. Nevertheless, administration of nootropics having anti-oxidative properties targeting the therapeutic intervention for actin-cofilin rod formation along with standard anti-malarial derivatives may have better efficacy in restoring the cognition during the onset of CM.

Conclusion

In summary, the present results provide strong evidences of altered neuronal morphology, neuronal arborization, and impaired dendritic spine density; morphology in ECM. Further, dysregulation of LIMK-1/Cofilin-1 pathway and formation of actin-cofilin rods could be attributed to impaired morphological aspects of neurons during ECM. Hence, this study may have profound impact in establishing newer therapeutic strategies aiming at long term cognitive impairment after CM.

References

1. Idro R, Marsh K, John CC, Newton CR. Cerebral Malaria; mechanisms of brain injury and strategies for improved neuro-cognitive outcome. Pediatr Res 2010;68:267–274.

2. Luebke JI, Weaver CM, Rocher AB et al. Dendritic vulnerability in neurodegenerative disease: insights from analyses of cortical pyramidal neurons in transgenic mouse models. Brain Struct Func 2010;214:181–199.

3. Zuccato C, Cattaneo E. Brain-derived neurotrophic factor in neurodegenerative diseases. Nat Rev Neurosci 2009;DOI: 10.1038/nrneurol.2009.54.

4. Comim CM, Reis PA, Frutuoso VS, et al. Effects of experimental cerebral malaria in memory, brain-derived neurotrophic factor and acetylcholinesterase activity [correction for acitivity] in the hippocampus of survivor mice. Neurosci Lett 2014;DOI: 10.1016/j.neulet.2012.06.051.

5. Linares M, Marín-García P, Perez-Benavente S, et al. Brain-derived neurotrophic factor and the course of experimental cerebral malaria. Brain Res 2013;DOI: 10.1016/j.brainres.2012.10.040.

6. De Miranda AS, Brant F, Campos AC, et al. Evidence for the contribution of adult neurogenesis and hippocampal cell death in experimental cerebral malaria cognitive outcome. Neuroscience 2015;DOI: 10.1016/j.neuroscience.2014.10.062.

7. Yoshii A, Constantine-Paton M. Post-synaptic BDNF-TrkB Signaling in Synapse Maturation, Plasticity and Disease. Dev Neurobiol 2010;70:304–322.

8. Wang W, Mouneimne G, Sidani M, et al. The activity status of cofilin is directly related to invasion, intravasation, and metastasis of mammary tumors. J Cell Biol 2006;173:395–404.

9. Bernard O. Lim kinases, regulators of actin dynamics. Int J Biochem Cell Biol 2007;39:1071-1076.

10. Meng Y, Zhang Y, Tregoubov V, et al. Abnormal Spine Morphology and Enhanced LTP in LIMK-1 Knockout Mice. Neuron 2002;35:121–133.

11. Dong Q, Ji YS, Cai C, Chen ZY. LIM kinase 1 (LIMK1) interacts with tropomyosin-related kinase B (TrkB) and Mediates brain-derived neurotrophic factor (BDNF)-induced axonal elongation. J Biol Chem 2012;DOI: 10.1074/jbc.M112.405415.

12. Cheever TR, Ervasti JM. Actin isoforms in neuronal development and function. Int Rev Cell Mol Biol 2013;DOI: 10.1016/B978-0-12-407704-1.00004-X.

13. Matus A. Actin-based plasticity in dendritic spines. Science 2000;290:754-758.

14. Sarmiere PD, Bamburg JR. Head, Neck, and Spines: A Role for LIMK-1 in the Hippocampus. Neuron 2002;35:3-5.

15. Koleske AJ. Molecular mechanisms of dendrite stability. Nat Rev Neurosci 2013;14:536–550.

16. Bourne J, Harris KM. Do thin spines learn to be mushroom spines that remember? Curr Opin Neurobiol 2007;17:381-386.

17. Davis RC, Maloney MT, Minamide LS, et al. Mapping Cofilin-Actin Rods in Stressed Hippocampal Slices and the Role of cdc42 in Amyloid-β-Induced Rods. J Alzheimers Dis 2009;18:35-50.

18. Sarfo BY, Henry B Armah, Ikovwaiza Irune, et al. Plasmodium yoelii 17XL infection up-regulates RANTES, CCR1, CCR3 and CCR5 expression, and induces ultrastructural changes in the cerebellum. Malar J 2005;DOI:10.1186/1475-2875-4-63.

19. Carroll RW, Wainwright MS, Kim KY, et al. A rapid murine coma and behavior scale for quantitative assessment of murine cerebral malaria. PLoS One 2010;DOI: 10.1371/journal.pone.0013124.

20. Zaqout S, Kaindl AM. Golgi-Cox staining step by step. Front Neuroanat 2016; DOI:10.3389/fnana.2016.00038.

21. Alcantara-Gonzalez F, Juarez I, Solis O, et al. Enhanced dendritic spine number of neurons of the prefrontal cortex, hippocampus and nucleus accumbens in old rats after chronic donepezil administration. Synapse 2010;DOI:10.1002/syn.20787.

22. Sholl DA. Dendritic organization in the neurons of the visual and motor cortices of the cat. J Anat 1953;87:387–406.

23. Ferreira TA, Arne V Blackman, Julia Oyrer, et al. Neuronal morphometry directly from bitmap images. Nat Methods 2014;DOI:10.1038/nmeth.3125.

24. Ehara A, Ueda S. Application of Fluoro-Jade C in Acute and Chronic Neurodegeneration Models: Utilities and Staining Differences. Acta Histochem Cytochem 2009;42:171-179.

25. Bamburg JR, Bernstein BW, Davis RC, et al. ADF/Cofilin-actin rods in neurodegenerative diseases. Curr Alzheimer Res 2010;7:241-250.

26. De Niz M, Ullrich AK, Heiber A, et al.The machinery underlying malaria parasite virulence is conserved between rodent and human malaria parasites. Nat. Commun 2016;DOI: 10.1038/ncomms11659.

27. Adams JD Jr. Chemical interactions with pyramidal neurons in layer 5 of the cerebral cortex: control of pain and anxiety. Curr Med Chem 2009;16:3476-3479.

28. Wu F, Catano M, Echeverry R, et al. Urokinase-type plasminogen activator promotes dendritic spine recovery and improves neurological outcome following ischemic stroke. J Neurosci 2014;DOI: 10.1523/JNEUROSCI.5309-13.2014.

29. Herms J, Dorostkar MM. Dendritic spine pathology in neurodegenerative diseases. Annu Rev Pathol 2016;DOI: 10.1146/annurev-pathol-012615-044216.

30. Ferrer I, Guionnet N, Cruz-Sanchez F, Tunon T. Neuronal alterations in patients with dementia: a Golgi study on biopsy samples. Neurosci Lett 1990;114:11-16.

31. Ikegaya Y, Kim JA, Baba M, et al. Rapid and reversible changes in dendrite morphology and synaptic efficacy following NMDA receptor activation: implication for a cellular defense against excitotoxicity. J Cell Sci 2001;114:4083-4093.

32. Hasbani MJ, Schlief ML, Fisher DA, Goldber MP. Dendritic spines lost during glutamate receptor activation reemerge at original sites of synaptic contact. J Neurosci 2001;21:2393–2403.

33. Dijkhuizen PA, Ghosh A. BDNF regulates primary dendrite formation in cortical neurons via the PI3-kinase and MAP kinase signaling pathways. J Neurobiol 2004;62:278-288.

34. Massaad CA, Klann E. Reactive oxygen species in the regulation of synaptic plasticity and memory. Antioxid Redox Signal 2011;DOI: 10.1089/ars.2010.3208.

35. Imai T, Iwawaki T, Akai R, et al. Evaluating experimental cerebral malaria using oxidative stress indicator OKD48 mice. Int. J Parasitol 2014;DOI: 10.1016/j.ijpara.2014.06.002.

36. Liu A, Zhou Z, Dang R et al. Neuroligin 1 regulates spines and synaptic plasticity via LIMK1/cofilin-mediated actin reorganization. J Cell Biol 2016;DOI:10.1083/jcb.201509023.

37. Todorovski Z, Asrar S, Liu J, et al. LIMK1 regulates long-term memory and synaptic plasticity via the transcriptional factor CREB. Mol Cell Biol 2015;DOI:10.1128/MCB.01263-14.

38. Oakley MS, McCutchan TF, Anantharaman V, et al. Host biomarkers and biological pathways that are associated with the expression of experimental cerebral malaria in mice. Infect Immun 2008;DOI: 10.1128/IAI.00525-08.

39. Bamburg JR, Bernstein BW. Roles of ADF/cofilin in actin polymerization and beyond. F1000 Biol Rep 2010; DOI:10.3410/B2-62.

40. Rust MB. ADF/cofilin: a crucial regulator of synapse physiology and behavior. Cell Mol Life Sci 2015;DOI: 10.1007/s00018-015-1941-z.

41. Fedulov V, Rex CS, Simmons DA, et al. Evidence that long-term potentiation occurs within individual hippocampal synapses during learning. J Neurosci 2007;27:8031-8039.

42. Eeka P, Chaitanya GV, Babu PP. Proteolytic breakdown of cytoskeleton induces neurodegeneration during pathology of murine cerebral malaria. Brain Res 2011;DOI: 10.1016/j.brainres.2011.08.025.

43. Fernando SD, Rodrigo C, Rajapakse S. The 'hidden' burden of malaria: cognitive impairment following infection. Malar J 2010;DOI: 10.1186/1475-2875-9-366.

44. Akinlolu AA, Shokunbi MT. Neurotoxic effects of 25mg/kg/bodyweight of artemether on the histology of the trapezoid nuclei and behavioural functions in adult male Wistar rats. Acta Histochem 2010;112:193-198.

45. G Schmuck, Roehrdanz E, Haynes RK, Kahl R. Neurotoxic Mode of Action of Artemisinin. Antimicrob Agents Chemother 2002;46:821-827.

46. Idro R, Kakooza-Mwesige A, Asea B, et al. Cerebral malaria is associated with long-term mental health disorders: a cross sectional survey of a long-term cohort. Malar J 2016;DOI:10.1186/s12936-016-1233-6.

47. Froestl W, Muhs A, Pfeifer A. Cognitive enhancers (nootropics). Part 1: drugs interacting with receptors. J. Alzheimers Dis 2012;DOI:10.3233/JAD-140228.

48. Rao SB, Chetana M, Uma Devi P. Centella asiatica treatment during postnatal period enhances learning and memory in mice. Physiol Behav 2005;86:449-457.

49. Ostrovskaya RU, Gudasheva TA, Zaplina AP, et al. Noopept stimulates the expression of NGF and BDNF in rat hippocampus. Bull Exp Biol Med 2008;146:334-337.

50. Urban KR, Gao WJ. Performance enhancement at the cost of potential brain plasticity: neural ramifications of nootropic drugs in the healthy developing brain. Front Syst Neurosci 2014;DOI: 10.3389/fnsys.2014.00038.

CHAPTER-2

Introduction

One fourth of the survivors of CM retain long-term neurologic and cognitive impairment such as loss of memory, attention, speech, motor abilities, visual perception and executive functions.[4] Despite effective anti-malarial therapy, long-term cognitive impairment persists in a substantial number of children. The mechanism for the cognitive and behavioral changes in CM remains unclear.

Behavioral and cognitive deficits reported in several neurodegenerative and neuropsychiatric disorders are intensely correlated to the dysregulation of neurotransmitter release as well as its receptors confined to specified regions of the brain which are responsible for the maintenance of executive functions such as problem-solving, working memory and planning.[5-8] Magnetic resonance imaging (MRI) studies show 84.2% of children suffering from CM exhibited abnormalities in the basal ganglia while 21% of adults with CM have been reported for the involvement of edema in the striatum.[9,10] The striatum is the largest segment of the basal ganglia subdivided into dorsal (caudate, putamen) and ventral (nucleus accumbens) which is interconnected by the neuronal circuitry to the cortex, thalamus, hippocampus, substantia nigra and amygdala.[11,12] Acquisition of learning, behavior and motor skills are co-ordinated mostly in the basal ganglia, especially by striatum.[13]

Rationale of the study

Medium spiny neurons (MSNs) represent approximately 90-95% of the striatal neuronal population.[14] Most of these neurons express D1 (D1R), D2 type (D2R) receptors and some of them co-express as D1/D2 heteromer (MSNs expressing both D1R and D2R dopaminergic receptors)[15] in the dendritic spines.[14] D1R activates direct pathway necessary for stimulatory actions while D2R opposes the D1R signaling by inhibitory indirect signaling pathway in the central nervous system.[15] Dopamine plays a vital role in the spinogenesis necessary for the development of dendritic spines and neuronal architecture.[16] Activation of dopaminergic receptors directly regulates the striatal dendritic spine density, morphology and electrophysiological properties.[16] Under pathological conditions, extracellular dopamine accumulates in the synapses of MSNs (striatal neurons do not synthesize dopamine) leading to the prolonged activation of dopaminergic receptors affecting the morphology and density of striatal dendritic spines.[16,17] Chronic stimulation of D1, D2 or co-activation of D1R and D2R by elevated levels of extracellular dopamine mediate upregulation of p35 and its cleaved form, p25 activating cyclin-dependent kinase (cdk5) leading to striatal neurodegeneration.[17-19]

Neurons projecting from the substantia nigra to dorsal striatum are critical in regulating behavioral and learning abilities.[20, 21] Dopamine and cyclic-AMP regulated phosphoprotein of molecular weight 32kDa (DARPP-32) is a neuronal phosphoprotein, highly expressed in the MSNs, regulates the biochemical, transcriptional and behavioral effects of dopamine signaling.[22] Phosphorylation of DARPP-32 at Thr34 is regulated by dopamine by D1R via cyclic adenosine mono phosphate /protein kinase A (cAMP/PKA) which is a potent inhibitor of protein phosphatase-1 (PP-1). Activation of cdk5, Ca2+/calmodulin-dependent protein kinase II alpha (CaMKIIα) phosphorylates DARPP-32 at Thr75 which acts as an inhibitor of PKA upon

administration of cocaine.[22-24] PP-1 plays a major role in the dephosphorylation of glutamate receptors such as N-methyl-D-aspartate (NMDA) and α-amino-3-hydroxy-5-methyl-4-isoxazolepropionic acid (AMPA) receptors and kinases such as CaMKIIα.[23] PP-1α and PP-1γ1 are enriched in dendritic spines. PP-1γ1 forms a complex with spinophilin and neurabin, reorganizing the actin filament for maintaining the shape of the dendritic spine.[25] Overexpression of $G_{q\alpha}$ (G-protein coupled receptor) together with D1 and D2 receptors enhance the dopamine mediated increase in the intracellular Ca^{2+} response.[26] Increased levels of Ca^{2+} leads to the activation of CaMKIIα and calcineurin.[27] Simultaneously, D2R also activates Ca^{2+} dependent protein phosphatase, calcineurin by the activation of phospholipase C and inositol triphosphate (IP3).[28,29] D1R interacts with NMDA receptors in the presence of glutamate, activates ERK1/2[20, 30- 31] Activation of ERK1/2 by D2R is not completely understood.[20] Role of ERK1/2 is primarily involved in the formation of long term memory as it regulates the expression of plasticity-related proteins including brain-derived neurotrophic factor (BDNF), activity-regulated cytoskeleton-associated protein (Arc).[32] Striatal-enriched tyrosine phosphatase (STEP) is a potent negative regulator of ERK1/2 which contributes to the cognitive impairment in several psychiatric and neurological diseases such as Alzheimer's, fragile X syndrome, schizophrenia, Huntington's, Parkinson's disease.[33-35] The dopaminergic signaling mechanism is illustrated in the graphical format (Figure 1.). For better understanding of the molecular mechanisms as well as determining potential therapeutic targets, C57BL/6 mice infected with *Plasmodium berghei ANKA* has been widely accepted experimental cerebral malaria (ECM) model that reiterates several symptoms of human cerebral malaria (HCM) such as retinopathy, seizures, disruption of Blood-Brain Barrier (BBB) integrity and long term cognitive impairment.[2,36-37] The pathology of CM includes

oxidative stress, neuro-inflammation and glutamate mediated excitotoxic neurodegeneration[38, 39] but dopaminergic signaling pathways and its role in striatum have not been elucidated till date.

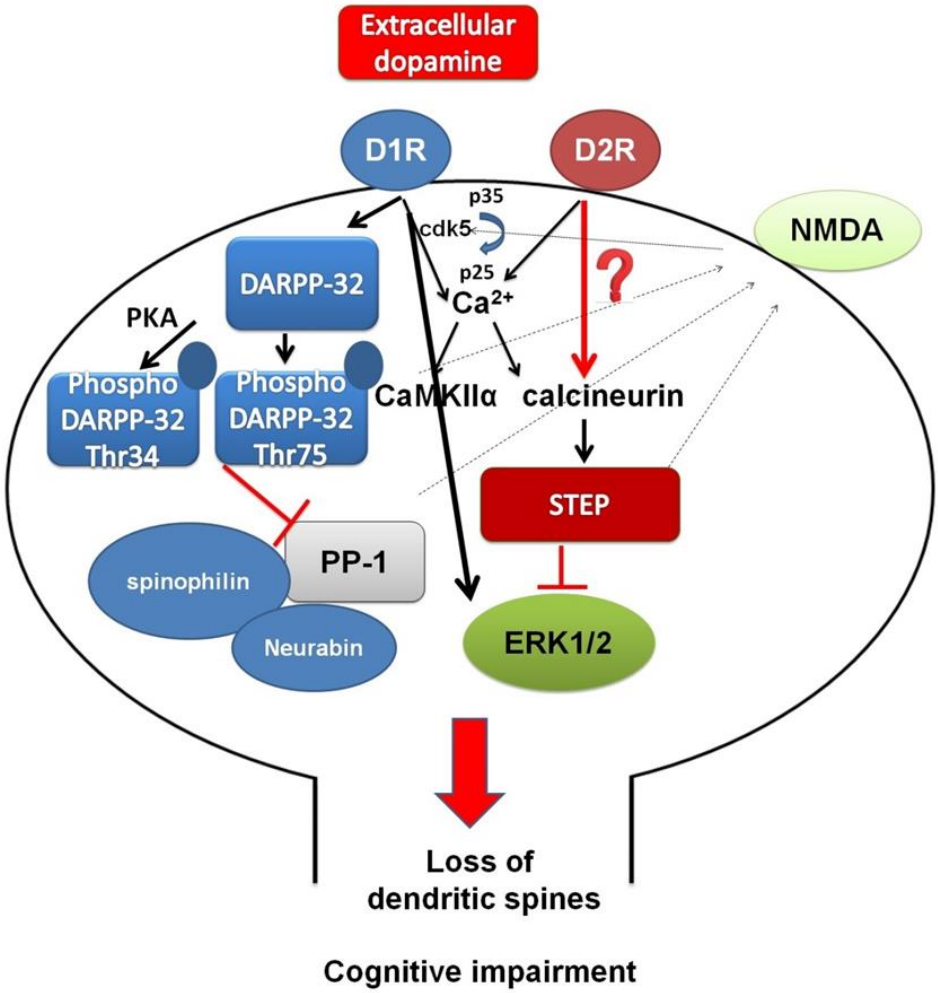

Figure 1. Hypothetical representing the downstream signaling of D1R and D2R signaling in the dendritic spines upon excess release of extracellular dopamine. Hyperdopamine tone in the striatum leads to the aberrant expression of dopaminergic D1R, D2R receptors elevating calcium response and facilitates PKA mediated phosphorylation of DARPP-32 at Thr34 inhibiting protein phosphatase-1 (PP-1). Dopamine activates cdk5 by the cleavage of p35 to p25. Cdk5 phosphorylates DARPP-32 at Thr75 which a potent inhibitor of PKA. PP-1 interacts with neurabin and spinophilin regulating the NMDA receptors and the morphology of dendritic spine. Interaction of D2 and D1 activates calmodulin-dependent protein kinase II (CaMKIIα) and calcineurin. It is unknown whether activation of D2R mediates the activation of striatal-enriched tyrosine phosphatase (STEP), a potent inhibitor of ERK1/2 resulting in the loss of dendritic spines in experimental cerebral malaria.

To achieve the above hypothesis, we proposed three objectives

a) To study expression of D1R and D2R in the striatal brain sections of ECM

b) To study dendritic spine density and morphology of medium spiny neurons in ECM

c) To study the downstream signaling of the dopaminergic signaling in ECM

Methodology

Animals

C57BL/6 male and female mice (15-20g) of three-four weeks old were purchased from National Institute of Nutrition, (ICMR-NIN) Hyderabad, India and acclimatized at appropriate conditions with animal feed and water *ad libitum* at animal house facility, University of Hyderabad, Hyderabad, India.

Parasite infection

Parasite vials of *Plasmodium berghei ANKA* (PbA) and *Plasmodium yoelii 17XL* (Pyl) were procured from the National Institute of Malaria Research, New Delhi, India and stored in liquid nitrogen. Initially, three control mice (source) per group were infected with red blood cells of PbA and Pyl parasites each at a concentration of 10^6 (pRBCs) diluted in 0.2 ml of chilled sterile 1x phosphate buffered saline (PBS) (pH-7.4) intraperitoneally. Parasitemia was monitored by Giemsa staining (Sigma Aldrich) of the caudal blood smears on the day 3-7. pRBCs from PbA and Pyl infected source mice were passaged to the rest of the mice intraperitoneally after confirmation of 3-5% parasitemia. All the animals were deeply anesthetized with ketamine (150mg/kg) combined with xylazine (10mg/kg) and perfused intracardially with 0.9 % saline solution.

Evaluation of the neurological signs of CM by RMCBS

Rapid Murine Coma Behavior Scale (RMCBS) is a quantitative behavioral tool to assess the symptoms of CM in the animal model accurately. All the mice were assessed for 2 minutes from day 5 to 10 based on ten behavioral parameters such as gait, balance, motor performance, body position, limb strength, touch escape, pinna reflex, toe pinch, aggression and grooming. Based on the performance in the above parameters, mice were scored from 0-20. The frequency of the interval of behavioral assessment was increased based on the deterioration of the behavior with a decline in the score i.e. mice were assessed every 12 hours, if the RMCBS score was 16–20; mice were assessed every 4 hours, if the RMCBS score was 11–15; mice were assessed every 2 hours, if the RMCBS score was 6–10, the mice were considered moribund and were sacrificed if the RMCBS score was ≤5.

Histological experiments

Animals sacrificed on the basis of RMCBS scores (categorized under CON, CM and ASY experimental groups) were subjected to craniotomy; brains were collected after intracardial perfusion with 0.9% saline and immediately followed by chilled 4% paraformaldehyde solution. Brain samples were subjected to dehydration in 20-30% sucrose solution for 3-4 days, coronal cryosections of striatum were cut at 20µm thickness for performing Fluoro-Jade C, double immunofluorescence and 100-200µm thickness for Golgi-Cox staining using Leica cryomicrotome CM1850.

Fluoro-Jade C staining: Fluoro-Jade C (AG325 Millipore) is an anionic fluorescent dye used as a marker for degenerating neurons. Brain sections were immersed in xylene for 45 minutes and subjected to dehydration in a solution containing 100 % ethyl alcohol containing 5 % sodium

hydroxide. Sections were washed in PBS buffer for 2 minutes and then incubated in 0.06% potassium permanganate solution for 10 minutes with gentle rotation of tissue sections at 5-10 revolutions per minute on an orbital shaker. Sections were rinsed with distilled water for 2 minutes and transferred to the solution containing 500 µl Fluoro-Jade C (1mg/ml) added to the solution (50 µl of 100% acetic acid in 49.45 ml of distilled water) and stored in the dark for 20 minutes with gentle rotation for 5-10 revolutions per minute. Finally, sections were washed in distilled water for 2 minutes, air dried at 50°C in the dark for 1 hour and mounted with DPX mounting medium. To quantify fluorescence intensity, a minimum of seven images of dimensions 722.49x 722.49 mm (height x width) of 600x magnification confined to the dorsal striatal region of all the experimental groups (n=4 animals per group) were subjected to the Image J software. The images were captured using Leica trinocular DM6B microscope with Leica Application Suite X (LAS X) software.

Double immunofluorescence experiment: Brain sections were immersed in 1x PBS with 0.3M glycine (quenching solution) for 20 minutes. The sections were permeabilized in ice-cold 100 % methanol for 10 minutes at -20°C and washed for 2 minutes in PBS buffer. Sections were blocked in the blocking buffer (1%BSA, 5% normal goat serum dissolved in 1x PBS with 0.3M glycine) for 2 hours at room temperature in a humid chamber followed by incubation with the primary antibody at 1:100 dilution for 2 days at 4°C. The sections were washed in PBS buffer for 10 minutes and incubated with the anti-rabbit IgG (4412S Alexa Fluor® 488 Conjugate) and Anti-mouse IgG (4409S Alexa Fluor® 555 Conjugate) (Cell Signaling Technology) in the dark at room temperature for 45 minutes. Sections were washed with 1x PBS buffer and mounted with Prolong® Gold antifade reagent with DAPI (8961S Cell Signaling Technology). Images were

captured using laser scanning confocal microscope Carl Zeiss LSM 880 using ZEN Blue software.

Golgi-Cox staining: It is the most extensively used method to study the morphological details of the neuronal ultrastructure. Perfused whole brain samples from all the experimental groups were subjected to Golgi-Cox stain with a change of fresh stain for every two days up to 17 days at room temperature under the dark condition, followed by sucrose dehydration at 25-40% and cryosectioned at 100µm thickness for dendritic spine studies whereas 200µm thick brain sections were used to analyze the neuronal arborization pattern in the striatal regions. Brain sections were developed as per the protocol carried out by Zubeyde Bayram-Weston et al. Images were captured using laser scanning confocal microscope Carl Zeiss LSM 880 using ZEN Blue software.

Dendritic spine density quantification

Dendritic spine density of Golgi-Cox impregnated MSNs were quantified manually by counting the number of spines per 10µm of the dendrite. 18 distal dendrites of 10 neurons per section (n=10 animals per experimental group) were considered for quantifying spine density from the images captured using Olympus BX51 microscope. Morphology of the dendritic spines of the MSNs was observed by magnifying 1000X images to 10 times of its original size.

Striatal neurodegeneration was studied by Fluoro-Jade C staining, an anionic dye which stains the neuronal cell bodies, dendrites, axons and its terminals upon neurotoxic insult followed by Golgi-Cox staining of the striatal brain sections to study the morphological details of the MSNs and dendritic spines in all the experimental groups. We performed Western blotting to observe the protein expression of D1R, D2R, phospho-DARPP-32-Thr34 and phospho DARPP-Thr75,

p35/25, cdk5, PP-1γ1, neurabin and spinophilin followed by double immunofluorescence colocalizing NeuN (neuronal marker) with D1R and D2R (NeUN-D1R, NeUN-D2R), dopamine with D1R, STEP with phospho form of ERK1/2, Thr202/Tyr204 in the striatal sections of all the experimental groups. All the statistical analysis were performed using ANOVA and $p<0.05$ was considered as significant.

Results

Neurobehavioral alteration in PbA infected mice

Videos were recorded of the parasite- infected animals from day 5-10 for 2 minutes and 1 minute in case of the CON group. We observed altered behavior in PbA infected mice from day 6 to 8. Abnormal gait, loss of grooming, touch escape, body position and pinna reflex was observed in PbA infected mice on day 6 with a total RMCBS score of 11. Mild impairment in the touch response behavioral parameter was noticed in some of the Pyl infected mice with a total RMCBS score of 16-18. No behavioral alterations were observed in the control mice. RMCBS scores of the animals from day 5-10 post-infection were represented in Figure 2

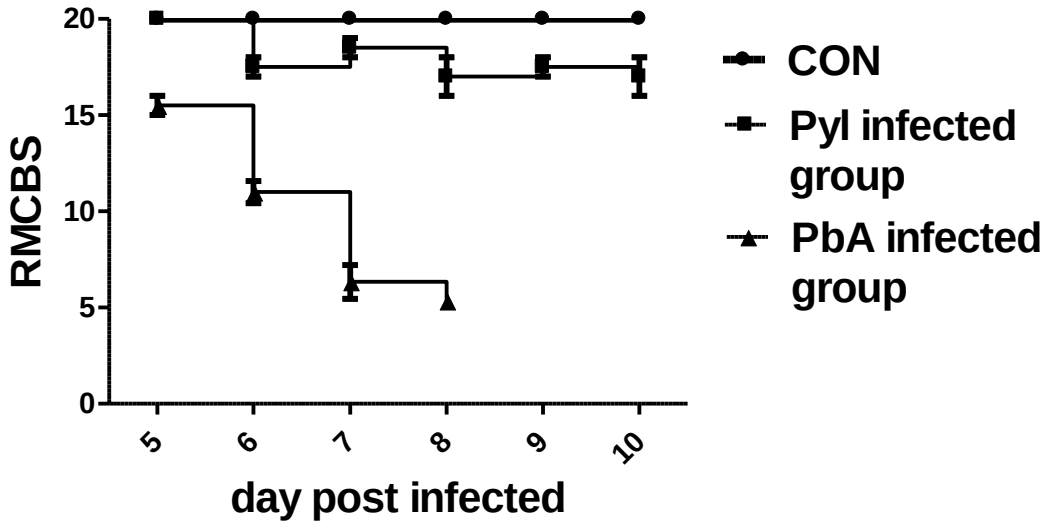

Figure 2. Alteration of neurobehavioural parameters in the PbA infected C57BL/6 mice. Graph representing the total cumulative score of rapid murine coma behaviour scale (RMCBS) in the mice infected with PbA, Pyl and CON group, based on the alteration in the behavioural parameters from day 5-10. RMCBS score in PbA infected mice was significantly reduced compared to Pyl group.

Striatal neurodegeneration in ECM

We performed Fluoro-Jade C staining of striatal brain cryosections of 20µm thickness (coronal section) in all the experimental groups. Extensive neurodegeneration was observed in the dorsal striatum of CM infected brain sections relative to the ASY and CON (Figure 3).

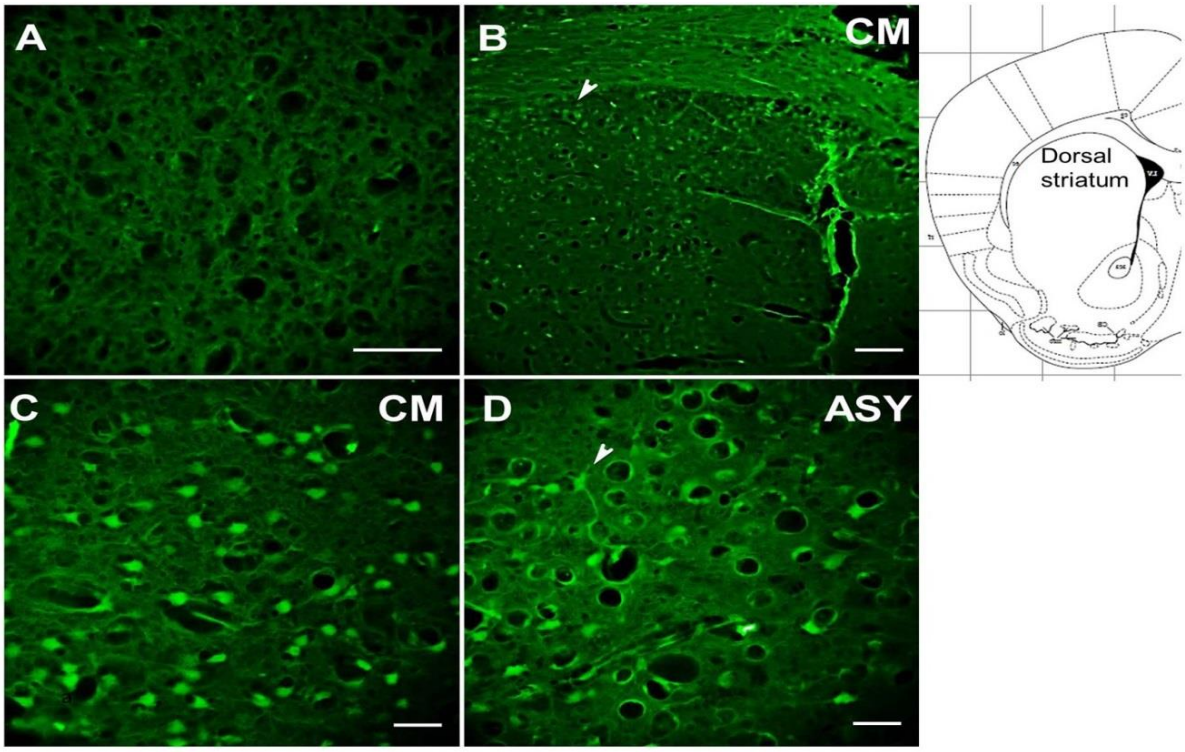

Figure 1. Representing the striatal neurodegeneration by Fluoro Jade C staining**,** reveals fluorescent spots as (arrowheads) soma of the neurons with neurites that have undergone degeneration in the dorsal striatum. A, illustrates no trace of neuronal damage in CON. B, illustrating the dorsal striatal area with fluorescent spots as degenerated striatal neurons in CM.

C, magnified image of the dorsal striatal area representing the neurodegeneration in CM. C, arrowhead representing the damaged extended neurite in ASY. (Scale bar- 20 µm in panel A, C, D and 60 µm in panel B). Cartoon diagram representing the dorsal striatum is reproduced from the mouse brain atlas by "The mouse brain in stereotaxic coordinates" by George Paxinos and Keith B. J. Franklin.

Altered morphology and dendritic spines of MSNs in CM

Golgi impregnated striatal brain sections of 100-200 µm thickness of all the experimental groups, were developed and imaging was performed using Olympus BX51 microscope. Severe regression of dendritic arbors (branching of dendrites) with somatic swellings were observed in the MSNs of the CM compared to ASY group (Figure 2C). Dendritic varicosities, focal swellings were observed along the dystrophic dendrites of the MSNs (Figure 2B, C). The total dendritic spine density in MSNs of the CM was decreased by 77.7% compared to the CON group. Dendritic spine loss with significant impairment of the dendritic spine morphology in MSNs was observed in CM and ASY compared to the CON group (Figure 2E-G).

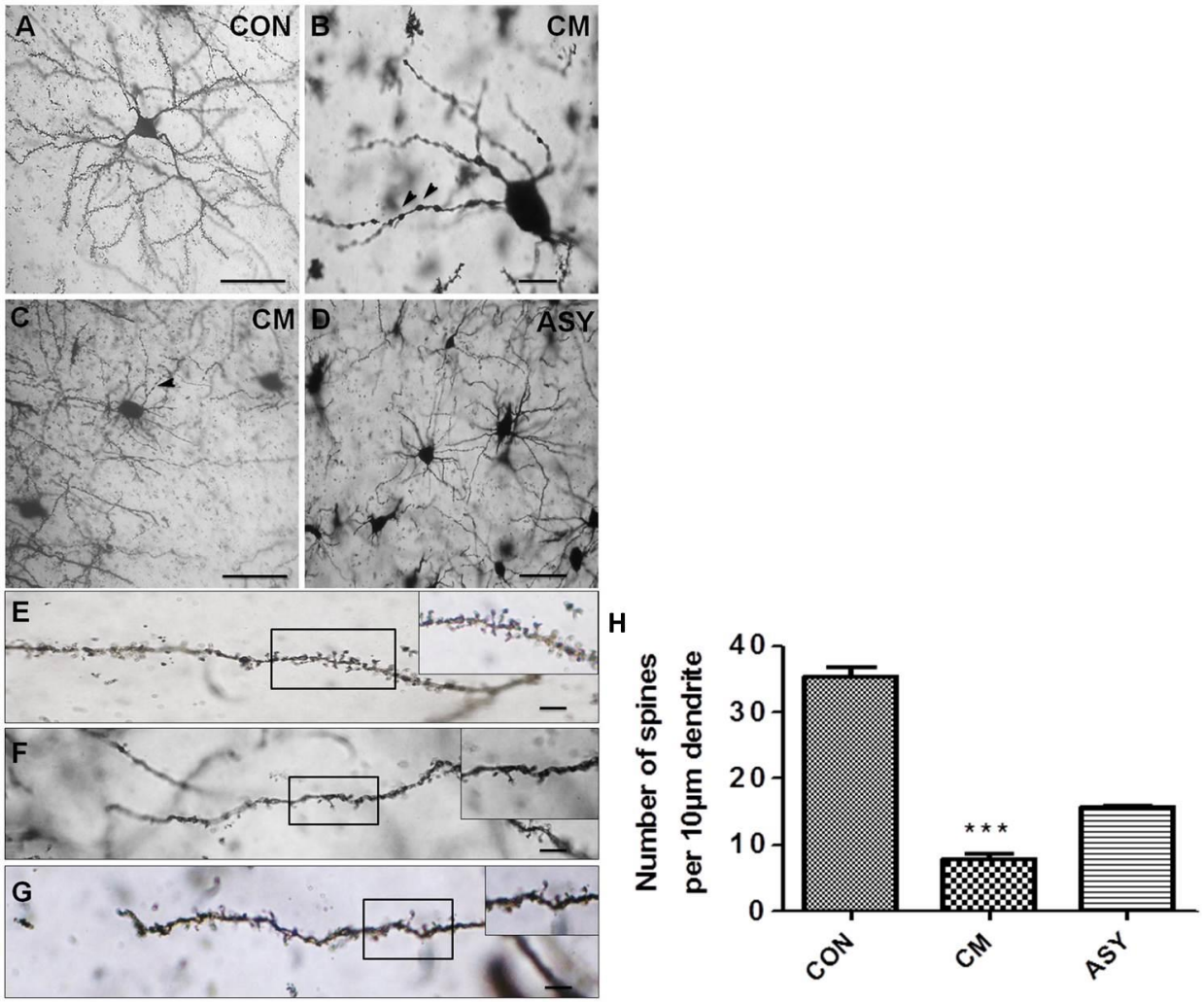

Figure 2. Altered neuronal and dendritic spine morphology of striatal neurons in ECM

A, Golgi-Cox staining reveals enriched dendritic ramification of MSNs in CON. B, C distorted ultrastructure of medium spiny neurons with reduced length of dendrites, bulged soma, dendritic varicosities (arrowheads) in the striatal regions of CM. D, loss of neuronal arborization in ASY. E, illustrating the dendrite with increased dendritic spine density with typical spine morphology. F, distorted dendrite with loss of dendritic spines and altered dendritic spine morphology. G, dendrite with reduced spine density with distinct spine morphology. (Scale bar- 20 µm in panel B and 60 µm in panel A, C and D. 10 µm in panel E, F, and G). H,

Aberrant dopaminergic signaling in CM

Expression of the protein levels involved in the dopaminergic pathway (list of primary antibodies Table 1) in the striatal lysates of all the experimental groups were quantified by Western blot. In the top row of figure 3A, the results revealed a significant increase in D1R, D2R levels followed by upregulation of phospho DARPP-32 at Thr34 in CM compared to ASY and CON. We observed a significant increase in the p35, p25 and cdk5 levels in CM and ASY (Figure 3A). Phospho DARPP at Thr75 levels were upregulated in CM and ASY. PP-1γ1 levels were downregulated in CM relative to ASY and CON (Figure 3A). Spinophilin levels were significantly upregulated in ASY and CM relative to CON while complete downregulation of neurabin was observed in CM (Figure 3A). As shown in the top row of Figure 3B, there was a significant increase in the CaMKIIα levels, its autophosphorylated form, CaMKIIα Thr286 and calcineurin in CM compared to ASY and CON. In the bottom row of figure 3B, the results reveal significant downregulation of the phosphorylated form of ERK1/2 at Thr202/Tyr204, neurabin in CM relative to ASY and CON. Densitometric analysis of the relative protein expression was quantified after normalizing with Glyceraldehyde 3- phosphate dehydrogenase (GAPDH) (Figure 3C)

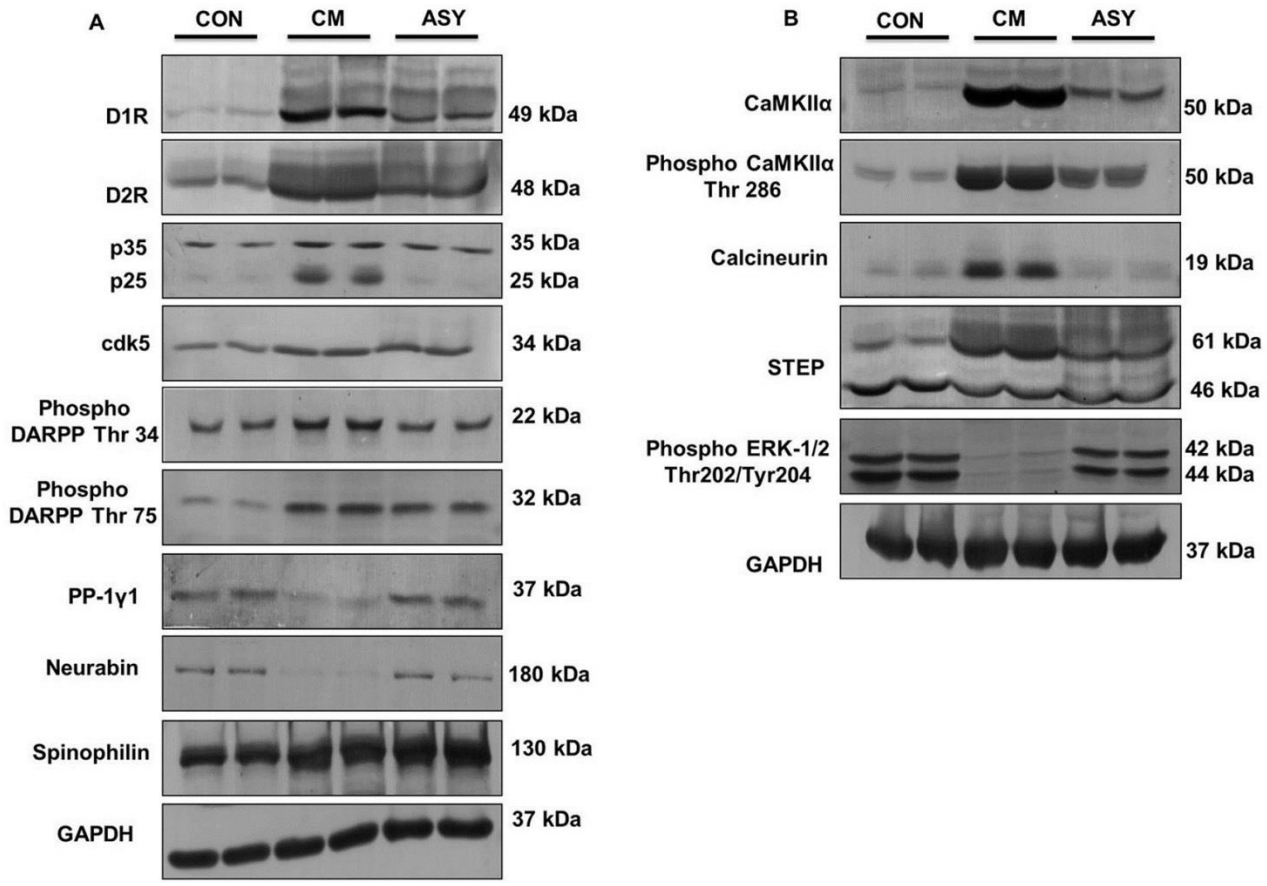

Figure 3A, B. Protein expression of dopaminergic signaling pathway was analyzed by Western blotting. A, shows the upregulation of D1R, D2R levels, cleavage of p35 to p25, phospho DARPP-32 at Thr34, cdk5 and spinophilin in CM and downregulation of PP-1γ1, neurabin in CM. B, blots representing the upregulation of CaMKIIα and phospho CaMKIIα at Thr286, calcineurin, STEP61 and downregulation of phospho ERK1/2 at Thr202/Tyr204 in CM relative to ASY and CON

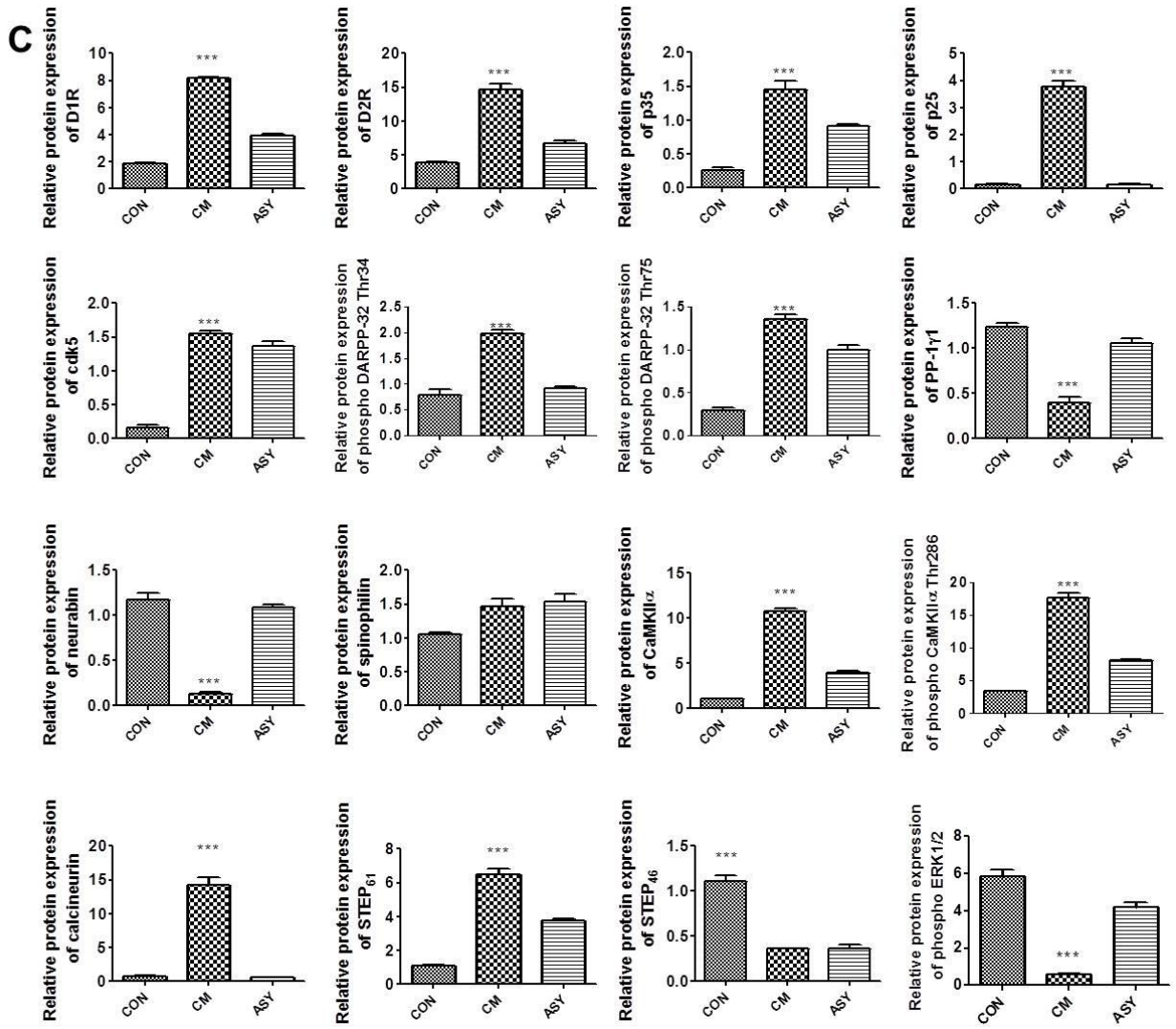

Figure 3C. Relative expression of each protein quantified after normalizing with the GAPDH as internal loading control. Graph representing significant upregulation of D1R and D2R (D1R; 8.69±0.19, D2R; 15.92±0.09), (p35; 1.567±0.023), (p25; 3.78±0.034), (cdk5; 1.556±0.100), (phospho DARPP-32 at Thr34; 1.97±0.25), (phospho DARPP-32 at Thr75;1.462±0.21), (CaMKIIα; 12.10±0.001), (phospho CaMKIIα; 18.34±0.002), (calcineurin; 15.2± 0.04), (STEP61; 6.49±0.25), (spinophilin; 1.61±0.67) and downregulation of (PP-1γ1; 0.41±0.29), (phospho ERK1/2; 0.58±0.11), (neurabin; 0.12±0.17) in CM compared to ASY and CON. STEP46 was significantly upregulated in CON (STEP46; 1.109±0.34 ***p<0.001, **p=0.004.

Immunofluorescence studies

The fluorescence intensity of D2R, D1R (source: mouse secondary antibody) colocalized with NeuN (source: rabbit primary antibody) was upregulated within the dorsolateral striatal region of CM relative to CON (Figure 4) which is in parallel to the Western blot analysis and qualitatively showed the characteristic increase in cell coma stained by NeuN in CM (Figure 4B). Double labeling of STEP and phospho ERK1/2 revealed that fluorescence intensity of STEP was increased with a reduction of phospho ERK1/2 in CM (Figure 5).

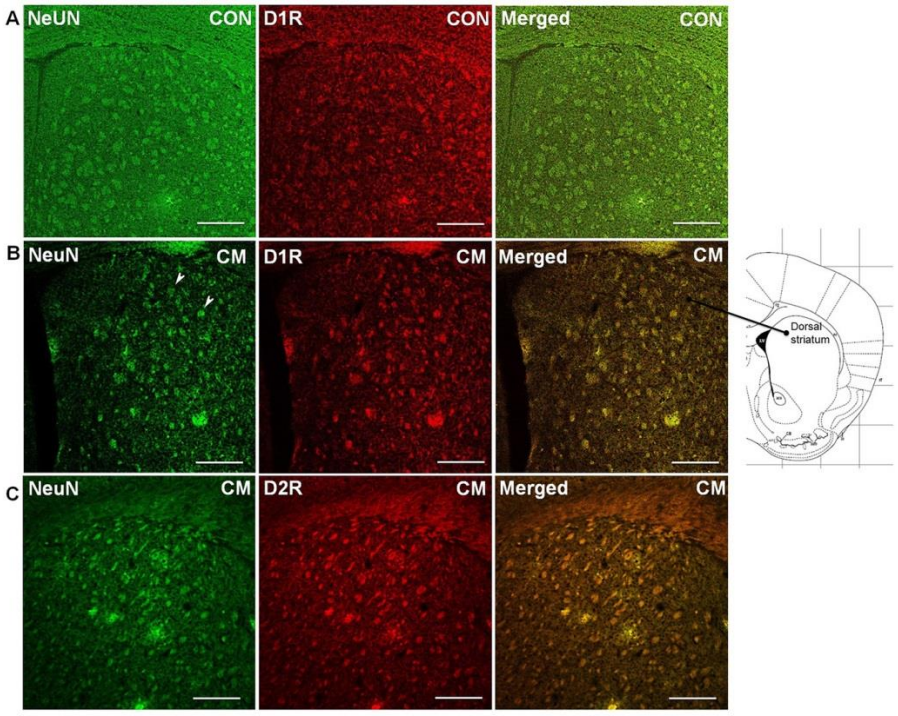

Figure 4. Aberrant upregulation of D1R and D2R colocalized with NeuN in the dorsal striatum in ECM. Representative double immunofluorescence photomicrographs of NeuN colocalized with D1R and D2R in the dorsal striatal regions of all the experimental groups. A, illustrates the colocalization of D1R with NeuN in CON with a balanced fluorescence intensity in the merged image. B, shows the increased fluorescence intensity of D1R colocalized with the NeuN in the dorsal striatum, arrowhead representing enlarged soma stained with NeuN in CM. C, representing the enhanced fluorescence intensity of D2R colocalized with NeuN at the dorsal striatum in CM. (Scale Bar-60 µm)

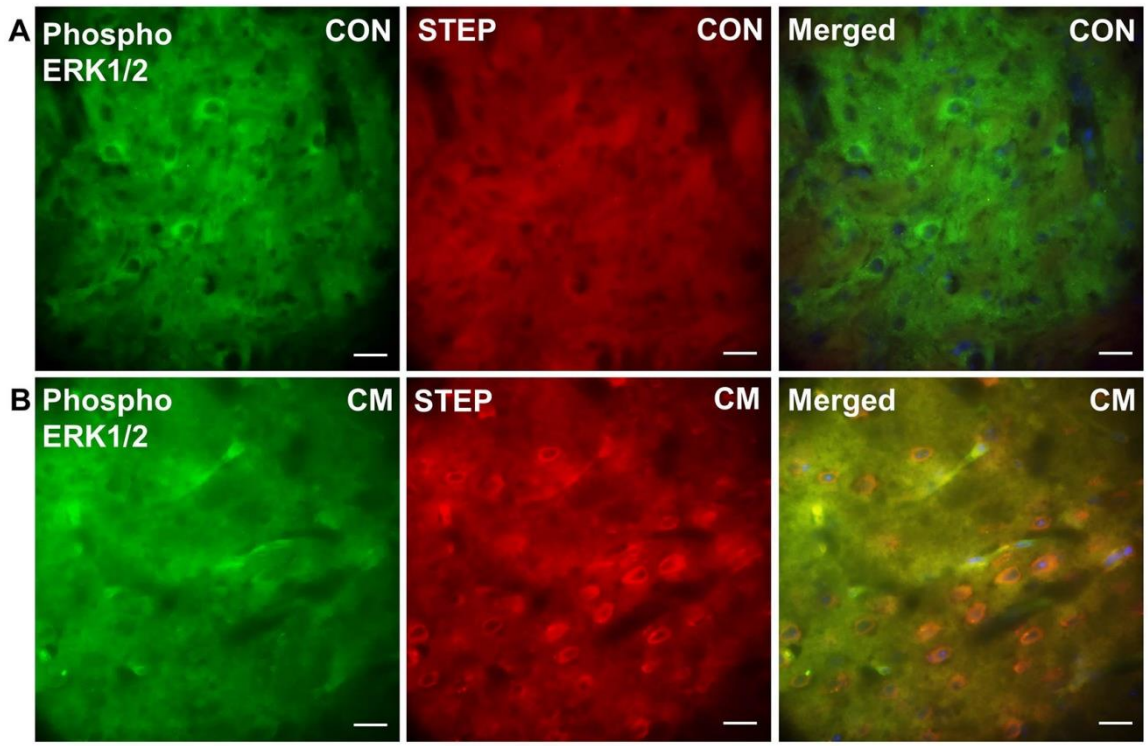

Figure 5. Colocalization of phospho ERK1/2 with STEP in the striatal sections in ECM. Double immunofluorescence photomicrographs illustrating the colocalization of STEP with phospho-ERK1/2 at Thr202 and Tyr204. A, illustrates increased fluorescence intensities of ERK1/2 with weak intensity of STEP in CON. B, illustrates low fluorescence intensity of phospho ERK1/2 with high intensity of STEP in CM. (Scale bar- 20 µm)

Name of the primary antibody	Host	Supplier	Application and dilution
Anti-dopamine	Rabbit	Abcam ab6427	Immunofluorescence 1:100
Anti-dopamine 1 receptor	Mouse	Novus Biologicals NB110-60017	Western blotting 1:1000
Anti-dopamine 2 receptor	Mouse	Santa Cruz Biotechnology sc-5303	Western blotting 1:1000
Anti-phospho-DARPP-32 (pThr34)	Rabbit	Sigma-Aldrich SAB4504378	Western blotting 1:1000
Anti-PP1γ1	Rabbit	Sigma-Aldrich P7609	Western blotting 1:1000
Anti-p35/25	Rabbit	Cell Signaling Technology #2680	Western blotting 1:1000
Anti-Cdk5	Rabbit	Abcam ab40773	Western Blotting 1:1000
Anti- phospho-DARPP-32 (Thr75)	Rabbit	Cell Signaling Technology #2301	Western blotting 1:1000
Anti-CaMKIIα	Mouse	Cell Signaling Technology #50049	Western blotting 1:1000
Anti-phospho CaMKIIα at Thr286	Mouse	Santa Cruz Biotechnology sc-32289	Western blotting 1:1000
Anti-spinophilin	Rabbit	Cell Signaling Technology #14136	Western blotting 1:1000
Anti-neurabin-1	Mouse	Santa Cruz Biotechnology sc-377407	Western blotting 1:1000
Anti-STEP	Mouse	Cell Signaling Technology #4396	Western blotting 1:1000, Immunofluorescence 1:100
Anti-calcineurin	Rabbit	R&D SystemsMAB1348	Western Blotting 1:1000
Anti-phospho ERK1/2 at Thr202/Tyr204	Rabbit	Cell Signaling Technology #4377	Western blotting 1:1000, Immunofluorescence 1:100
Anti-NeuN	Rabbit	Abcam ab177487	Immunofluorescence 1:100

Table 1. List of antibodies, their respective applications and dilution used in the study.

Discussion

Alteration of dopaminergic pathways in striatum has been extensively studied in several neurodegenerative, neuropsychiatric disorders.[16-20] Accumulation of extracellular dopamine leads to the prolonged stimulation of D1R resulting in the striatal neurodegeneration and behavioral abnormalities.[18] Double immunofluorescence findings show concurrent upregulation of D1R and D2R colocalized with NeuN, representing selective involvement of MSNs containing D1R and D2R in the dysregulation of dopaminergic signaling in CM. Multiple bands above 50 kDa in the Western blot results of D1R and D2R could be due to its glycosylation variants or isoforms of corresponding receptors expressed during pathological conditions of CM and ASY group. DARPP-32 is abundantly expressed in striatum, differentially regulates dopaminergic signaling based on the stimulation of D1 and D2R–MSN pathways.[40] Repeated administration of cocaine increases extracellular dopamine levels, shows increased phosphorylation of DARPP-32 at Thr34, Thr75 by PKA and cdk5 activation.[24] However, upregulation of phospho DARPP-32 at Thr34 and Thr75 levels can be interpreted as hyperdopaminergic condition in CM. Elevated levels of dopamine along with chronic stimulation of D1R mediate cleavage of p35 to form p25 followed by upregulation of cdk5 leading to striatal neurodegeneration.[41] Our data show positive colocalization between D1R and dopamine in the striatum of CM. Overexpression of p25 and cdk5 involves excitotoxic neuronal damage including alteration of neuronal morphology, loss of dendritic spines, impairment of the motor coordination and behavioral functions in several neurodegenerative diseases.[41, 42] In line to the above statement, Western blot results show cleavage of p35 to p25, upregulation of cdk5 in CM and ASY with reduction of dendritic spine density, abnormal MSN morphology and dendritic varicosities (mostly observed during excitotoxic neuronal damage)[43] which can be correlated to the overexpression of p25 resulting in striatal neurodegeneration in CM. Western blot results

show significant downregulation of PP-1γ1 and increased phospho DARPP-32 levels at Thr34 which could be due to the activation of D1R direct pathway in CM. PP-1 plays a critical role in the maintenance of synaptic plasticity regulating synaptic NMDA, AMPA receptors, activation of CaMKIIα, turn-over of filamentous-actin dynamics involving neurabin and spinophilin facilitating memory retention.[44] Spinophilin and neurabin are associated with PP-1γ1 for the maintenance of filamentous actin for maturation of the dendritic spine [45,46.] Overexpression of spinophilin and neurabin are associated with altered neuronal morphology.[45, 46] Abnormal expression of neurabin and spinophilin which could be associated with altered morphology of the dendritic spines of MSNs in CM. Reduction of PP-1γ1 levels enhances the phosphorylation of CaMKII at Thr286 in response to excess Ca^{2+} levels.[47] Similarly, we confirm downregulation of PP-1γ1 and significant upregulation of both CaMKIIα and CaMKIIα at Thr286 in CM which is in resemblance to the pathological condition of Angelman syndrome.[47] Selective or synergistic upregulation of D1R and D2R could promote elevation in Ca^{2+} levels in the striatal lysates of CM.[27] Dysregulation of Ca^{2+} homeostasis and hyperactivation of Ca^{2+}dependent kinases and phosphatases is one of the pathological events in the early stages of neurodegenerative diseases.[48] Our results show elevated levels of Ca^{2+} especially in the striatum compared to the whole brain lysates supported by the activation of CaMKIIα and increased levels of calcineurin in CM. CaMKIIα is majorly involved in the maintenance of dendritic spine stability while its altered expression leads to spinopathy[49] (loss of dendritic spines due to protein aggregation) and overexpression results in memory destabilization.[50] Increased total and activated form of CaMKIIα levels could be associated with the loss of dendritic spines in CM. Hyperactivation of calcineurin has been widely known for triggering neuronal apoptosis and synaptic dysfunction.[48] PP-1 and calcineurin activates $STEP_{61}$ which opposes the strengthening of synaptic receptors

promoting internalization of NMDA-2B subunit in the synapses.[34] Inactivation of ERK1/2 by STEP impairs learning and memory functions in the brain. Inhibition of STEP enhances motor and cognitive functions by restoring BDNF, ERK levels in several animal models of neurodegenerative and neuropsychiatric diseases.[52-54] Western blot show upregulation of $STEP_{61}$ in parallel to the immunofluorescence result with significant downregulation of phospho ERK1/2 at Thr202, Tyr204 in CM. Stimulation of D1R direct pathway activates ERK1/2 by the blockade of $STEP_{61}$ while D2R activates $STEP_{61}$ by indirect pathway opposing the D1R mediated direct pathway.[55-57] Besides D2R indirect signaling pathway, excitotoxic NR2B-NMDA stimulation also leads to the activation of STEP.[58]

Conclusion

It is unclear whether D2R or its downstream targets activate STEP resulting in the inhibition of ERK1/2 in CM. Further research is necessary to understand the role of direct and indirect pathways of dopaminergic signaling affecting synaptic transmission in the animal models of CM. Overall, our findings provide strong evidence for the dysregulation of dopamine signaling as well as loss of ultrastructure of MSNs and dendritic spines in the dorsal striatal regions of ECM. We strongly presume that accumulation of extracellular dopamine is an early event aiming striatal neurodegeneration in CM.

References

1.Burton A. Gaining ground against cerebral malaria. Lancet Neurol. 2017;16(5):345-346.

2.Odhiambo OC, Wamakima HN, Magoma GN et al. Efficacy and safety evaluation of a novel trioxaquine in the management of cerebral malaria in a mouse model. Malar J. 2017;16(1):268.

3.Yusuf FH, Hafiz MY, Shoaib M, Ahmed SA. Cerebral malaria: insight into pathogenesis, complications and molecular biomarkers. Infect Drug Resist. 2017;10:57-59.

4.Idro R, Kakooza-Mwesige A, Asea B, et al. Cerebral malaria is associated with long-term mental health disorders: a cross sectional survey of a long-term cohort. Malar J. 2016; 5:184.

5.Sarter M, Bruno JP, Parikh V. Abnormal neurotransmitter release underlying behavioral and cognitive disorders: toward concepts of dynamic and function-specific dysregulation. Neuropsychopharmacology. 2007;32(7):1452-1461.

6.Xu Y, Yan J, Zhou P et al. Neurotransmitter receptors and cognitive dysfunction in Alzheimer's disease and Parkinson's disease. Prog Neurobiol. 2012; 97(1):1-13.

7.Reddy PH. A critical assessment of research on neurotransmitters in Alzheimer's disease. J Alzheimers Dis. 2017;57(4):969-974.

8.Murley AG, Rowe JB. Neurotransmitter deficits from frontotemporal lobar degeneration. Brain. 2018;141(5):1263-1285.

9.Potchen MJ, Kampondeni SD, Seydel KB et al. Acute brain MRI findings in 120 Malawian children with cerebral malaria: new insights into an ancient disease. AJNR Am J Neuroradiol. 2012;33(9):1740-1746.

10.Maude RJ, Barkhof F, Hassan MU et al. Magnetic resonance imaging of the brain in adults with severe falciparum malaria. Malar J. 2014;13:177.

11.Simpson EH, Kellendonk C, Kandel E. A possible role for the striatum in the pathogenesis of the cognitive symptoms of schizophrenia. Neuron. 2010;65(5):585-596.

12.Baez-Mendoza R, Schultz W. The role of the striatum in social behavior. Front Neurosci. 2013;7:233.

13.Gagnon D, Petryszyn S, Sanchez MG et al. Striatal neurons expressing D1 and D2 receptors are morphologically distinct and differently affected by dopamine denervation in mice. Sci Rep. 2017;7:41432.

14.Graybiel AM, Grafton ST. The striatum: where skills and habits meet. Cold Spring Harb Perspect Biol. 2015;7(8): a021691.

15.Biezonski DK, Trifilieff P, Meszaros J, Javitch JA, Kellendonk C. Evidence for limited D1 and D2 receptor coexpression and colocalization within the dorsal striatum of the neonatal mouse. J Comp Neurol. 2015; 523(8):1175-1189.

16.Money KM, Stanwood GD. Developmental origins of brain disorders: roles for dopamine. Front Cell Neurosci. 2013; 7:260.

17.Chen J, Wersinger C, Sidhu A. Chronic stimulation of D1 dopamine receptors in human SK-N-MC neuroblastoma cells induces nitric-oxide synthase activation and cytotoxicity. J Biol Chem. 2003;278(30):28089-28100.

18.Cyr M, Beaulieu JM, Laakso A et al. Sustained elevation of extracellular dopamine causes motor dysfunction and selective degeneration of striatal GABAergic neurons. Proc Natl Acad Sci U S A. 2003;100(19):11035-11040.

19.Rangel-Barajas C, Coronel I, Floran B. Dopamine Receptors and Neurodegeneration. Aging Dis. 2015;6(5):349-368.

20.Klein MO, Battagello DS, Cardoso AR, Hauser DN, Bittencourt JC, Correa RG. Dopamine: functions, signaling, and association with neurological diseases. Cell Mol Neurobiol. 2019;39(1):31-59.

21.Darvas M, Palmiter RD. Restricting dopaminergic signaling to either dorsolateral or medial striatum facilitates cognition. J Neurosci. 2010; 30(3):1158-1165.

22.Svenningsson P, Nishi A, Fisone G, Girault JA, Nairn AC, Greengard P. DARPP-32: an integrator of neurotransmission. Annu Rev Pharmacol Toxicol. 2004;44:269-296.

23.Fernandez E, Schiappa R, Girault JA, Le Novere N. DARPP-32 is a robust integrator of dopamine and glutamate signals. PLoS Comput Biol. 2006;2(12):e176.

24. Kim J, Ryu IS, Seo SY, Choe ES. Activation of protein kinases and phosphatases coupled to glutamate receptors regulates the phosphorylation state of DARPP32 at Threonine 75 after repeated exposure to cocaine in the rat dorsal striatum in a Ca2+-dependent manner. Int J Neuropsychopharmacol. 2015;pyv075.

25.Edler MC, Salek AB, Watkins DS et al. Mechanisms regulating the association of protein phosphatase 1 with spinophilin and neurabin. ACS Chem Neurosci.2018;9(11):2701-2712.

26.Chun LS, Free RB, Doyle TB, Huang XP, Rankin ML, Sibley DR. D1-D2 dopamine receptor synergy promotes calcium signaling via multiple mechanisms. Mol Pharmacol. 2013;84(2):190-200.

27.Beaulieu JM, Espinoza S, Gainetdinov RR. Dopamine receptors - IUPHAR Review 13. Br J Pharmacol. 2015;172(1):1-23.

28.Hernandez-Lopez S, Tkatch T, Perez-Garci E et al. D2 dopamine receptors in striatal medium spiny neurons reduce L-type Ca2+ currents and excitability via a novel PLC[beta]1-IP3-calcineurin-signaling cascade. J Neurosci. 2000;20(24):8987-8995.

29.Jijon-Lorenzo R, Caballero-Floran IH, Recillas-Morales S et al. Presynaptic dopamine D2 receptors modulate [3H]GABA release at striatopallidal terminals via activation of PLC → IP3 → calcineurin and inhibition of AC → cAMP → PKA signaling cascades. Neuroscience. 2018;372:74-86.

30.Chen J, Rusnak M, Lombroso PJ, Sidhu A. Dopamine promotes striatal neuronal apoptotic death via ERK signaling cascades. Eur J Neurosci. 2009;29(2):287-306.

31.Xue B, Mao LM, Jin DZ, Wang JQ. Regulation of synaptic MAPK/ERK phosphorylation in the rat striatum and medial prefrontal cortex by dopamine and muscarinic acetylcholine receptors. J Neurosci Res. 2015;93(10):1592-1599

32.Medina JH, Viola H. ERK1/2: A key cellular component for the formation, retrieval, reconsolidation and persistence of memory. Front Mol Neurosci. 2018;11:361.

33.Kurup PK, Xu J, Videira RA et al. STEP61 is a substrate of the E3 ligase parkin and is upregulated in Parkinson's disease. Proc Natl Acad Sci U S A. 2015;112(4):1202-1207.

34.Karasawa T, Lombroso PJ. Disruption of striatal-enriched protein tyrosine phosphatase (STEP) function in neuropsychiatric disorders. Neurosci Res. 2014;89:1-9.

35.Lombroso PJ, Ogren M, Kurup P, Nairn AC. Molecular underpinnings of neurodegenerative disorders: striatal-enriched protein tyrosine phosphatase signaling and synaptic plasticity. F1000Res. 2016;5:2932

36.White NJ, Turner GD, Medana IM, Dondorp AM, Day NP. The murine cerebral malaria phenomenon. Trends Parasitol. 2010;26(1):11-15.

37.Nacer A, Movila A, Baer K, Mikolajczak SA, Kappe SH, Frevert U. Neuroimmunological blood brain barrier opening in experimental cerebral malaria. PLoS Pathog.2012;8(10):e1002982.

38.Reis PA, Comim CM, Hermani F et al. Cognitive dysfunction is sustained after rescue therapy in experimental cerebral malaria, and is reduced by additive antioxidant therapy. PLoS Pathog. 2010;6(6):e1000963.

39.Idro R, Marsh K, John CC, Newton CR. Cerebral malaria; mechanisms of brain injury and strategies for improved neuro-cognitive outcome. Pediatr Res. 2010; 68(4):267-274.

40.Nishi A, Shuto T. Potential for targeting dopamine/DARPP-32 signaling in neuropsychiatric and neurodegenerative disorders. Expert Opin Ther Targets. 2017;21(3):259-272.

41.Meyer DA, Richer E, Benkovic SA et al. Striatal dysregulation of Cdk5 alters locomotor responses to cocaine, motor learning, and dendritic morphology. Proc Natl Acad Sci U S A. 2008;105(47):18561-18566.

42.Lai TW, Zhang S, Wang YT. Excitotoxicity and stroke: identifying novel targets for neuroprotection. Prog Neurobiol. 2014;115:157-188.

43.Ikegaya Y, Kim JA, Baba M, Iwatsubo T, Nishiyama N, Matsuki N. Rapid and reversible changes in dendrite morphology and synaptic efficacy following NMDA receptor activation: implication for a cellular defense against excitotoxicity. J Cell Sci. 2001;114(Pt 22):4083-4093.

44.Munton RP, Vizi S, Mansuy IM. The role of protein phosphatase-1 in the modulation of synaptic and structural plasticity. FEBS Lett. 2004;567(1):121-128.

45.Brown AM, Baucum AJ, Bass MA, Colbran RJ. Association of protein phosphatase 1 gamma 1 with spinophilin suppresses phosphatase activity in a Parkinson disease model. J Biol Chem. 2008;283(21):14286-14294.

46.Terry-Lorenzo RT, Roadcap DW, Otsuka T et al. Neurabin/protein phosphatase-1 complex regulates dendritic spine morphogenesis and maturation. Mol Biol Cell. 2005;16(5):2349-2362.

47.Shioda N, Fukunaga K. Physiological and pathological roles of CaMKII-PP1 signaling in the brain. Int J Mol Sci. 2018;19(1):20

48.Shah SZ, Hussain T, Zhao D, Yang L. A central role for calcineurin in protein misfolding neurodegenerative diseases. Cell Mol Life Sci. 2017;74(6):1061-1074.

49.Robison AJ. Emerging role of CaMKII in neuropsychiatric disease. Trends Neurosci. 2014;37(11):653-662.

50.Vigil FA, Giese KP. Calcium/calmodulin-dependent kinase II and memory destabilization: a new role in memory maintenance. J Neurochem. 2018;147(1):12-23

51.Li R, Xie DD, Dong JH et al. Molecular mechanism of ERK dephosphorylation by striatal-enriched protein tyrosine phosphatase. J Neurochem. 2014;128(2):315-329.

52.García-Forn M, Martínez-Torres S, García-Díaz Barriga G et al. Pharmacogenetic modulation of STEP improves motor and cognitive function in a mouse model of Huntington's disease. Neurobiol Dis. 2018;120:88-97.

53.Xu J, Chatterjee M, Baguley TD et al. Inhibitor of the tyrosine phosphatase STEP reverses cognitive deficits in a mouse model of Alzheimer's disease. PLoS Biol. 2014;12(8):e1001923.

54.Xu J, Kurup P, Baguley TD et al. Inhibition of the tyrosine phosphatase STEP61 restores BDNF expression and reverses motor and cognitive deficits in phencyclidine-treated mice. Cell Mol Life Sci. 2016;73(7):1503-1514.

55.Paul S, Snyder GL, Yokakura H, Picciotto MR, Nairn AC, Lombroso PJ. The Dopamine/D1 receptor mediates the phosphorylation and inactivation of the protein tyrosine phosphatase STEP via a PKA-dependent pathway. J Neurosci. 2000;20(15):5630-5638.

56.Fitzpatrick CJ, Lombroso PJ. The role of striatal-enriched protein tyrosine phosphatase (STEP) in cognition. Front Neuroanat. 2011;5:47.

57.Kamceva M, Benedict J, Nairn AC, Lombroso PJ. Role of striatal-enriched tyrosine phosphatase in neuronal function. Neural Plast. 2016;2016:8136925.

58.Poddar R, Deb I, Mukherjee S, Paul S. NR2B-NMDA receptor mediated modulation of the tyrosine phosphatase STEP regulates glutamate induced neuronal cell death. J Neurochem. 2010;115(6):1350-1362.

CHAPTER-3

Introduction

Cognition is the study of acquisition, consolidation, storage and retrieval of memories affecting through behavior. Individuals suffering with cognitive impairment, show loss of dignity, sociability and responsibilities in the society. Artemisinin derivates such as artemether, artemether and artesunate are current leading anti-malarials for the treatment of human CM.[5] Despite effective anti-malarial therapy, one-fourth of the survivors suffer from cognitive decline. Based on previous studies, artemisinin derivates exhibit neurotoxic properties additionally inducing reactive oxygen species (ROS) and promoting oxidative stress in neuronal cells.[6] Adjunctive therapeutics (nootropic drugs administered along with antimalarials) target oxidative stress, inflammatory and excitotoxic damage which are the initial mediators of neurotoxicity. Nootropic drugs are neuroprotective, used to treat patients with cognitive deficits targeting the alleviation of oxidative stress, neuroinflammation and repair of the damaged neurons which can restore cognition after neurodegenerative diseases.[7] Apocynin or acetovanillone is biologically active compound present in the roots of the *Picorhiza kurroa,* a perennial plant growing in the alpine Himalaya.[8, 9] It is a selective inhibitor of nicotinamide adenine dinucleotide phosphate oxidase (NADPH oxidase), a superoxide producing enzyme, comprises of membrane-associated cytochrome b_{558} composed of one p22 phox and one gp91 phox subunit and several regulatory cytosolic subunits (p47 phox, p40 phox, p67 phox and the GTPase Rac1 or Rac2) that translocate to the membrane and associate with the cytochrome b558 and thus activating the oxidase and generating a large amount of $O2^-$ (superoxide) in the process. NADPH oxidase (NOX) consists of 7 isoforms such as (NOX1-NOX5, Diox1 and Duox2). NOX2 is principally expressed in the microglial cells. Upon neurotoxic insult, aberrant upregulation of NOX2 result is the secretion of

superoxides, free radicals and lipid hydroperoxides which directly damage the neurons through extracellular pathways.[10]

Neurons are the functional cells in the brain responsible for the maintenance of the cognitive properties and behavior.[11] Neurons consist of soma (nucleus), axon, dendrites and dendritic spines. Spines are the functional unit of neurons which are essential for synaptic transmission. Loss of neuronal morphology is an evident feature during neurotoxic conditions in neurodegenerative diseases. Reduction of the dendritic spine density is a salient feature observed in several neurodegenerative diseases with cognitive decline.[12]

Rationale

25% survivors of CM suffer from neurocognitive sequelae such as long-term memory loss and behavioral dysfunction. Behavioral alterations such as aggression, inattention, gross motor function, loss of vision, hearing deficits are observed in children under the age group of 5-14 years. The exact cause of the cognitive decline is still unknown in case of human CM.

Studying the molecular mechanisms of cognitive dysfunction is impossible in the survived individuals of CM. Therefore, animal models are the best choice to elucidate the causes for the sequelae by performing cognitive tests respective to reference (long-term memory), working (short-term memory), motor co-ordination and novelty.

Objectives:

- **Morphological assessment of neurons in mono and combination rescue treated mice**
- **Evaluation of BBB integrity by Evan's blue staining**
- **Cognitive assessment of the rescue treated mice**

Acclimatization of mice:

C57BL/6 mice of 3-4 week old/(n=30) were maintained at appropriate environmental conditions with animal feed and sterile water *ad libitum* followed by 12 hours light and 12 hours dark cycle in the animal house facility at the University of Hyderabad. All the experiments were carried out at the School of Life Sciences, University of Hyderabad. Animals included male and female C57BL/6 mice of three to four weeks old with an average weight of 15-20 g.

Infection of parasite:

pRBC vials of PbA and *P.yoelii* were procured from National Institute of Malaria Research, New Delhi and stored in liquid nitrogen. *P.yoelii* (pyl) infected mice was considered as positive control for CM infected mice as pyl infected mice does not exhibit any neurological signs despite of similar parasitic count. Cryovials were thawed and diluted in parasite buffer (1x autoclaved Phosphate buffered saline) and administered intraperitoneally by an insulin syringe to the mice. Initially three animals (source animals) were infected with PbA and after confirmation of parasitemia by Giemsa staining; we passaged the infected blood containing pRBCs to the rest of the mice.

Observation of parasitemia:

Caudal blood smears of the infected mice were collected on the microscopic slides, fixed with methanol and stained with Giemsa stain. Images of parasite were captured using Olympus BX51 microscope at 1000x original magnification. Based on the parasite count observed per 10 microscopic fields per smear, percentage parasitemia was calculated as

$$\%.of\ parasitemia\ = \frac{Number\ of\ infected\ RBCs}{Number\ of\ total\ RBCs}\ X\ 100$$

Parasitemia curve was plotted by the values of percentage of parasitemia on Y-axis and days post infected on X-axis.

Observation of symptoms:

Mice symptomatic to CM exhibit crouching, lack of grooming and epileptic seizures with abnormal behavior and death from day 7 to 9. No symptoms were observed in the mice infected with *Plasmodium yoelii* on day 7-10. Symptoms were studied using Rapid Murine Coma Behavior Score (RMCBS) method. All the mice subjected were videographed for 3 minutes on day 5-10 in a clean cage avoiding visual and olfactory cues according to ten parameters: gait, balance, motor performance, body position, limb strength, touch escape, pinna reflex, toe pinch, aggression, and grooming.

Rescue therapy

Mice treated onset of the symptoms of CM is called as rescue therapy. Our study involves targeting the drug against the mechanisms activated during CM, especially oxidative stress and neuroinflammation. Therefore, successful rescue therapy could improve the survivability but questions the restoration of cognition in the CM infected mice. We designed the experimental

dosage regimen as follows

1) 2 mg of artemether was dissolved in the arachis oil and administered intraperitoneally (i.p.) once a day for 7 days at a concentration of 25 mg/kg to the mice onset of symptoms of CM. Mice (n=7) administered with artemether alone were considered as monotherapy. Dosage of artemether was in accordance with the previous studies conducted in rodents infected with PbA.[13]
2) Apocynin was dissolved in 10% dimethyl sulphoxide (DMSO) solution and administered i.p. once a day for 7 days at concentration of 5 mg/kg together with artemether at 25 mg/kg i.p. Dosage of apocynin was in the range of the dosage used in the rodent models of neurodegeneration.[8,9,14] Mice (n=7) administered with artemether and apocynin were considered as combination therapy.

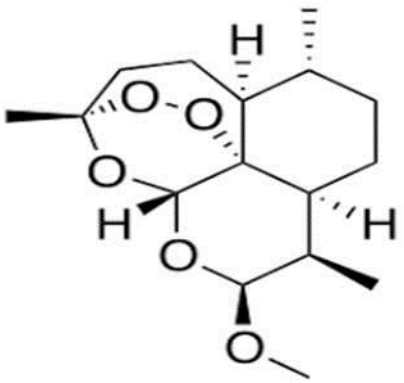

Artemether

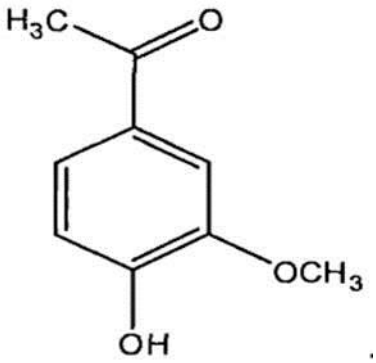

Apocynin

Cognitive assessment in the rescue treated mice

Mice were subjected to survivability for 30 days. Survivability was assessed by Kaplan-Meier survival analysis. After thirty days, cognitive tests were performed related to working, reference memory by T-maze and Barnes maze. Motor co-ordination was assessed by the beam balance

apparatus. All the test mice were acclimatized for 30 minutes in the test room before performing cognitive tests. The camera (model no. 60516, Digital USB 2.0 CMOS Camera) with lens (model No.60528, vari-focal, 2.8-1.2mm) was placed centrally at 40 cm over the mazes and connected to the laptop running ANYmaze video-tracking software version 6.0.

T- Maze test:

This cognitive test is performed to assess working memory of the animal. Alternation is the motivation of the animal to explore the environment and locate its resources such as food, water, shelter and mates.[15] Working memory can be assessed by

a) Spontaneous alternation
b) Rewarded spontaneous

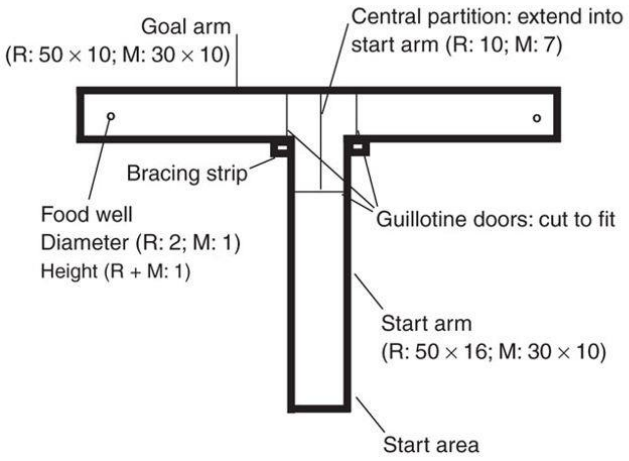

Figure 1. Representing the plan of T-maze with suitable dimensions for R: rat and M: mouse.
T maze consists of a start arm and left/ right arm as goal arm. Source: Deacon RM. Nat Protoc. 2006;1(1):7-12.

In trial 1, the animal was placed in the start arm after blocking one of the arms of the T-maze and left for exploration. The second trial (trial 2) was performed in quick succession, after

unblocking the arm, where the animal tends to choose the arm not visited previously. This kind of alternation is called spontaneous alternation. Similar to the spontaneous alternation, if the animal was made hungry and rewarded with preferred food is called rewarded alternation.

Methodology: We had selected spontaneous alternation task as both exploratory and working memory can be evaluated in the test mice. For any cognitive test, training the mouse for a limited period of time is considered as acquisition of visual and spatial memory of the environment in the maze. We habituated the mice for 3 minutes in the open arm T-maze with visual cues places at the side arms of the maze. After, habituation, the maze was cleaned using 70% alcohol solution. Mice were placed in the start arm with one of the arms blocked in the T-maze for 2 minute duration and placed them back to their home cage. After 5 minute duration, the mice were placed in the open arm T-maze and observed for its alternation pattern. Each mouse was subjected to 10 alternations. Based on the choice of its alternation, percentage of correct and wrong alternations for each mouse was calculated.

Barnes maze:

It was first described by Carol Barnes in the year 1979. This is a dry land based cognitive paradigm to determine working, reference spatial memory and cognitive flexibility of the animal. Barnes maze consists of an elevated circular with 20 evenly spaced holes at its perimeter.[16]

Figure 2. Illustrating the Barnes maze apparatus with escape platform and training phase of the test mouse.

An escape platform is placed under one of the hole leaving rest of the 19 holes empty. The position of the hole with the escape platform is maintained at a constant location. Animals were trained for multiple times each day until 4 days, placing each of them at the center of the maze and guided if they were not able to locate the escape platform. Parameters assessed during the trials are

a) Primary latency: The time taken to locate the escape platform
b) Primary errors: number of incorrect holes checked prior to locating the escaping platform

Probe trial

On day 5, the escape platform was removed and reference memory was assessed by the above parameters using ANY maze tracking software in the test mice compared to control mice.

Novel object recognition test

It is a behavioral test to assess the learning and memory functions of the animals. This test can also be used to study the long-term and short-term memory in the animals by the shift of the time

interval between the acquisition phase and the test phase. It was originally described by Ennaceur and Delacour in 1988 and used primarily in rats and mice. It is fairly a simple test which can be completed by three days. This test includes habituation, training and testing. On the day of habituation, the mouse was subjected to the open arena for 5 minutes for exploration of the environment. On day 2 or on the day 1 (test day), after an interval of 30 minutes, the mice were placed at the center along with two identical objects for 5 minutes. In this, time spent with both the objects were analyzed and after 45 minute or 1 hour time period the mice were subjected to the open arena with an identical object and a new object with a different colour, shape. Time spent with the new object compared to the identical object was assessed by video captured during the test.[17]

Beam balance test

Motor co-ordination in the brain is regulated by basal ganglia especially striatum.[18] Neurodegeneration in the striatum, especially in the dorsal striatum leads to the slipping of the paw of the animals. Beam balance test consists of one meter beam of 25 mm width placed at a height of 60 cm from the ground level. The mouse was trained by placing it on one of the end and subjected it to walk towards the other end. The time taken to traverse the beam is calculated along with the scoring paw slips of the test mice.

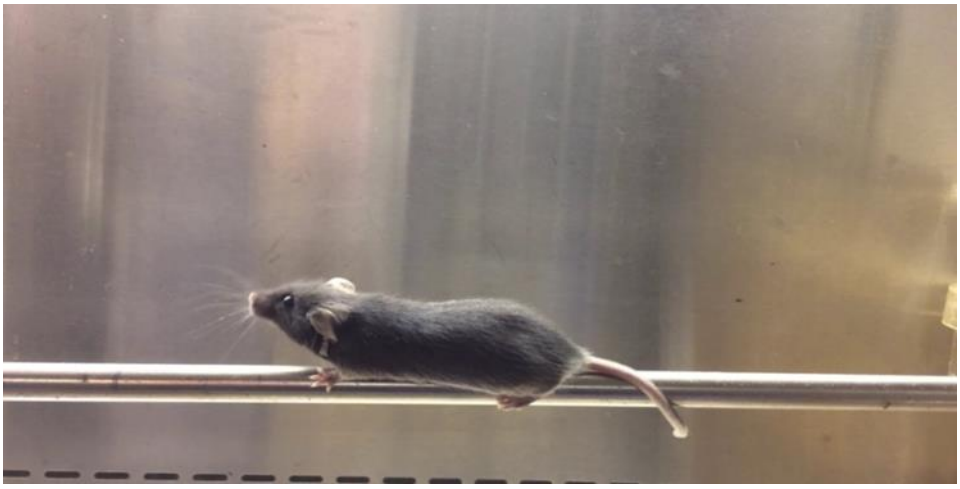

Figure 3. Illustrating the beam balance apparatus

Score	**Ability to traverse the beam**
1	Inability to cross the beam
2	Mouse exhibiting one foot slip
3	Mouse exhibiting two slips

Morphological assessment of neurons

After performing cognitive tests, the animals were deeply anethesized by deeply anesthetized with ketamine (150mg/kg) combined with xylazine (10mg/kg) and perfused intracardially with 0.9 % saline solution. Brains were collected from all the experimental mice of all the groups and subjected to histological staining

a) Golgi Cox Staining

b) Fluoro jade C staining

c) Hematoxylin and eosin staining

Golgi-Cox staining

This is the most widely used staining method for studying the morphological aspects of neurons. It was first discovered by Camillo Golgi, an Italian physician and scientist who published his findings related to Golgi cox staining in the year 1873. This method was further improved by Santiago Ramon Y Cajal describing novel facts about the neuronal morphology in the brain. The brains were subjected to Golgi-Cox staining for 17 days changing the stain for every two days.

Mice were deeply anesthetized, and brains were removed from the experimental animals (n=3) and placed them in the Golgi-Cox solution for 17 days. After the 17 day time period, brains were dehydrated at varying concentrations of sucrose (25-40%) of sucrose solution followed by cryosectioning at 200 µm for observing the neuronal morphology. Brain sections were developed as per the protocol carried out by Zubeyde Bayram-Weston et al.[20]

Fluoro-Jade C staining

This method (AG325 Millipore) is ideally carried out to observe the neurons undergoing neurodegeneration in brain sections. It is an anionic fluorescent dye used as a marker for degenerating neurons.[3] Brain sections were immersed in xylene for 45 minutes and subjected to dehydration in a solution containing 100 % ethyl alcohol containing 5 % sodium hydroxide. Sections were washed in PBS buffer for 2 minutes and then incubated in 0.06% potassium permanganate solution for 10 minutes with gentle rotation of tissue sections at 5-10 revolutions per minute on an orbital shaker. Sections were rinsed with distilled water for 2 minutes and transferred to the solution containing 500 µl Fluoro-Jade C (1mg/ml) added to the solution (50 µl of 100% acetic acid in 49.45 ml of distilled water) and stored in the dark for 20 minutes with gentle rotation for 5-10 revolutions per minute. Finally, sections were washed in distilled water

for 2 minutes, air dried at 50°C in the dark for 1 hour and mounted with DPX mounting medium. To quantify fluorescence intensity, a minimum of seven images of dimensions 722.49x 722.49 mm (height x width) of 600x magnification confined to the dorsal striatal region of all the experimental groups (n=4 animals per group) were subjected to the Image J software. The images were captured using Leica trinocular DM6B microscope with Leica Application Suite X (LAS X) software.

Hematoxylin and eosin (H&E) staining

20 µm thick sections were stained with Mayer's hematoxylin stain to observe the changes in the brain tissue morphology which features, nuclear, cytoplasmic and extracellular matrix of all the experimental groups. Changes in the nuclear morphology such as bulged nucleus hallmark for neurodegeneration during the pathology in the brain. As BBB breakage is evident in case of CM, the extent of hemorrhages can also be studied using H&E staining. The tissues sections were hydrated in distilled water and stained with Mayer's hematoxylin stain for 30 seconds, rinsed in distill water for 1 minute and stained with eosin (stains cytoplasm) as a counter stain 10-30 sec. 200 µl of glacial acetic acid was added while counter staining. The sections were dehydrated using two changes of 95%, 100% alcohol for 5 minutes and excess alcohol content was removed using 100% xylene for 3 minutes. Finally the tissue sections were mounted using DPX mounting medium.

ROS estimation by DCFDA

Total ROS levels from the brain lysates of all the experimental groups were determined using DCFDA method as described previously (chapter 1 methodology).

Evan's blue staining

Evan's blue is an azo dye which has high affinity to the serum albumin, which cannot pass through the BBB and the neural tissue is unstained. Disruption of the BBB leads to the entry of Evan's blue bound to albumin staining the whole brain to blue colour. 200 µl of 0.5% sterile injection was infected invenous to the mouse tail vein and place in the home cage. After 30 minutes, the mouse was sacrificed and the brains were weighed and collected in a 1.5 ml tube. 500 µl of formamide was added to the tube and transferred to a water bath at 55^0C and incubated for 24-48 hours to extract the Evan's blue stain from the brain. The tube with the Evan's blue /formamide mixture was centrifuged and the supernatant was estimated at an absorbance of 610nm with 500 ul formamide as blank.

Results:

Increased parasitemia in CM and ASY infected mice

We observed significant increase in the parasite count in the caudal blood smears of PbA (CM) and Pyl (ASY) infected mice. Smears were stained using Giemsa stain and parasitemia was observed from day 4 post-infection. Loss of RBC was evident in case of anemic mice (ANEM).

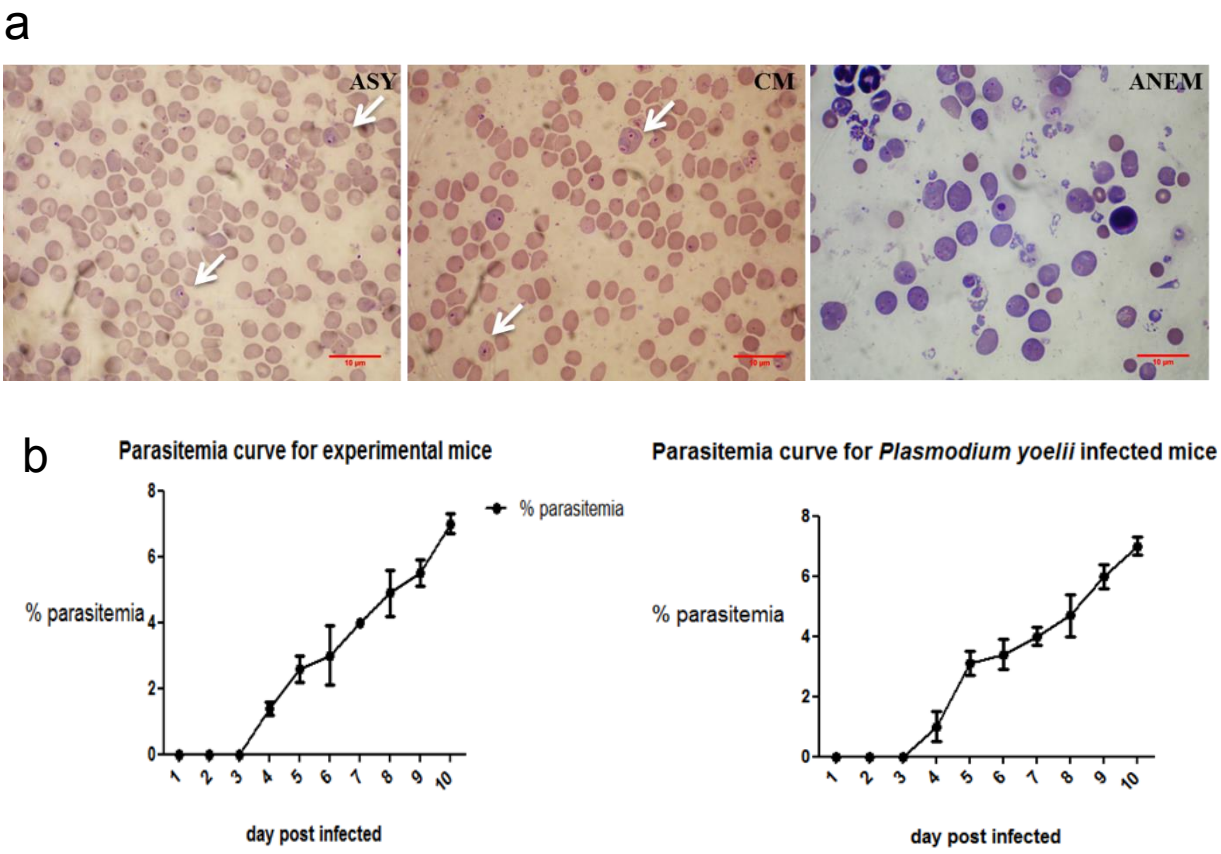

Figure 4. a) Representing the Giemsa stained parasite infected RBCs in CM and ASY experimental groups. Loss of RBC was observed in caudal smears of anemic group. b) Graph representing the % parasitemia with significant increase in the parasitemia count from day 3 in ASY and CM infected mice.

Evaluation of symptoms of CM

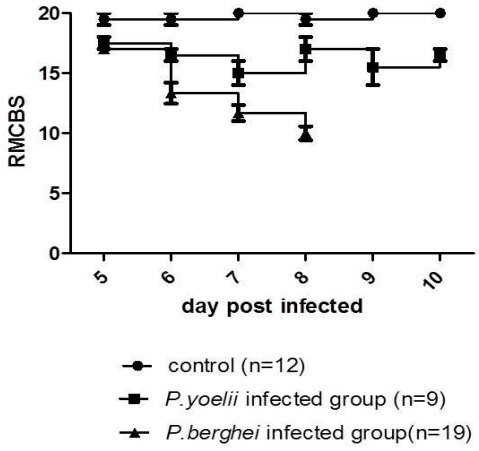

Figure 5. Illustrating the PbA infected mice onset of CM and ASY. Symptoms such as crouching, piloerection and loss of posture were observed in CM symptomatic mice. Graph representing the RMCBS score which were declined in case of CM group compared to ASY.

Survivability of the mice administered with rescue therapy

Mice administered with mono and combination therapy for 7 days were observed for survivability. Mice rescue treated with artemether alone and in combination with apocynin i.p. cleared the parasite within 48 hours and no recrudescence (re-appearance of the parasite in the blood) was observed after 7 day treatment protocol. Most of the mice died on day 8 and 9 after mono and combination therapy. We observed similar survival pattern in the mice treated with

both mono (43.7%) and combination therapy (46.6%) which is in parallel to the study by Clemmer et al.[13]

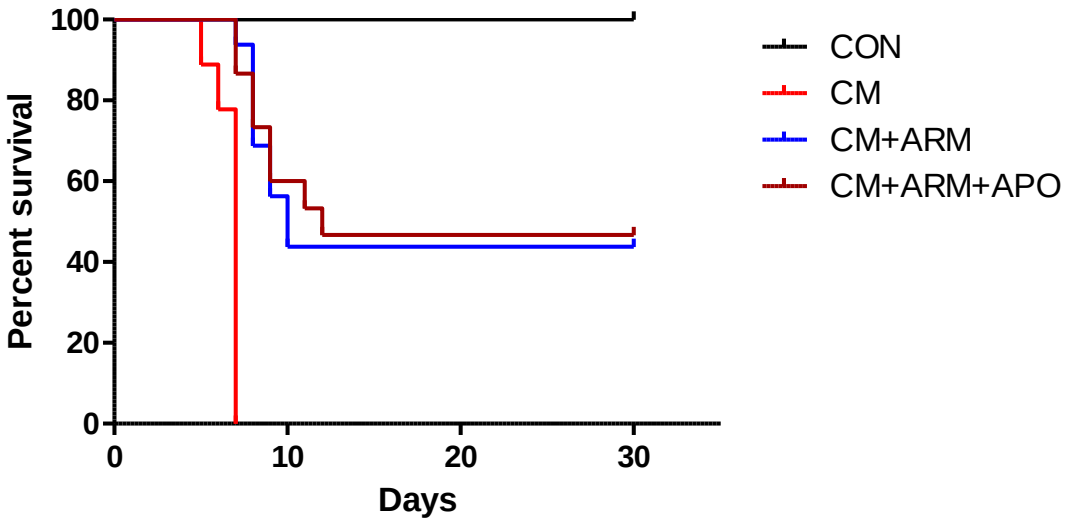

Figure 6. Similar survival percentage of the mice treated with CM+ARM (43.7%) and CM+ARM+APO (46.6%). Mice symptomatic to CM were died on day 7.

Cognitive assessment of the rescue treated mice

T-maze test

We observed significant side preference i.e if an animal has strong preference towards one of the arm in the T-maze which indicates a possibility of hippocampal lesions in the brain treated with monotherapy compared to the combination therapy and control Figure 8a. Figure 7 shows an example of an alternation and corresponding trackplots generated by the ANY-maze software 6.0 as well as the detection of the head, center of the body and tail of the animal in the maze. Our findings show that mice with combination therapy show 60 % correct alternation compared to

the monotherapy (43.3%) (Figure 7b). Therefore, mice administered with combination therapy show improved working memory compared to the monotherapy.

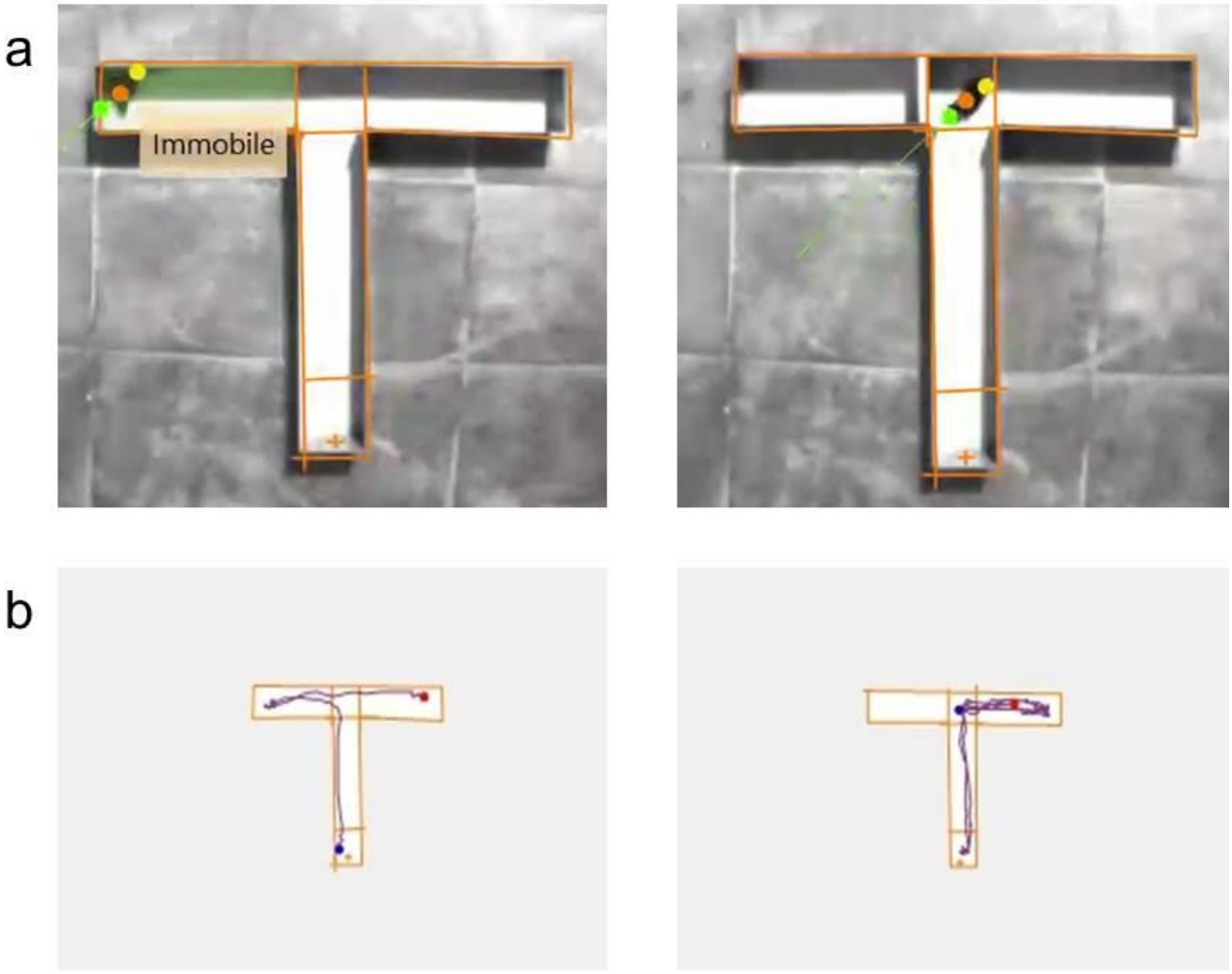

Figure 7. a, b Illustration of a correct alternation in the T-maze with corresponding trackplots of the animals subjected to the alternation by ANY-maze behaviour tracking software. The blue dot indicates the start point and red dot indicates the end point of the animal.

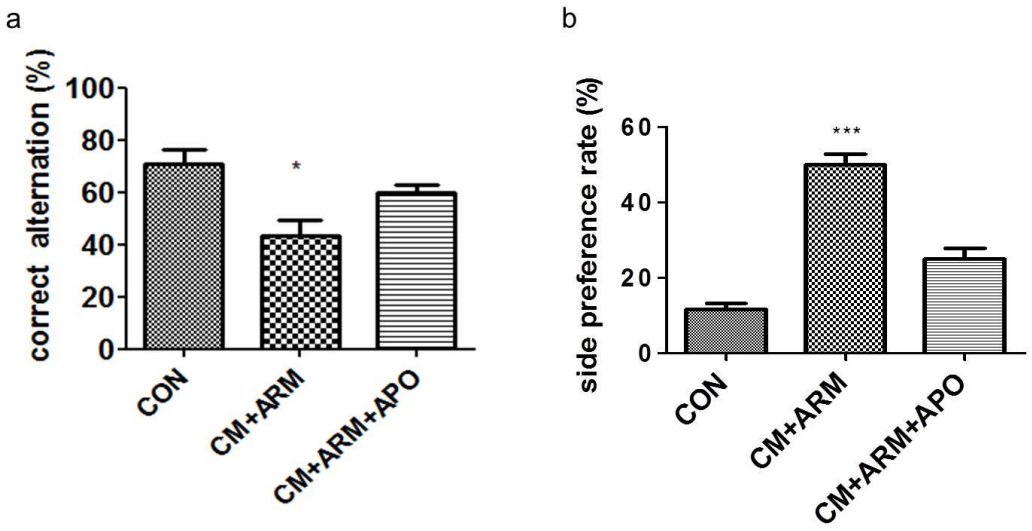

Figure 8 a) graph representing the percentage of correct alternation in all the experimental groups ie. Significant decrease in the percentage (43.3%) of the correct alternation was confirmed in the monotherapy (CM+ARM) group compared to combination therapy (60%) and CON (70.6%) b) Significant side preference in the CM+ARM administered mice was observed compared to CM+ARM+APO and CON group.*$p<0.05$, ***$p<0.001$.

Barnes maze test

We observed that there was no significant difference in the primary latency pattern between both mono and combination therapy on day 5. Interestingly, our findings show that there was significant increase in the primary errors in monotherapy administered mice (CM+ARM) compared to the combination therapy (CM+ARM+APO). Figure 9c shows representative trackplot of an animal from each group exhibiting primary latency with error. Our findings show that mice administered with combination therapy show similar spatial reference memory with less primary errors compared to the monotherapy.

a

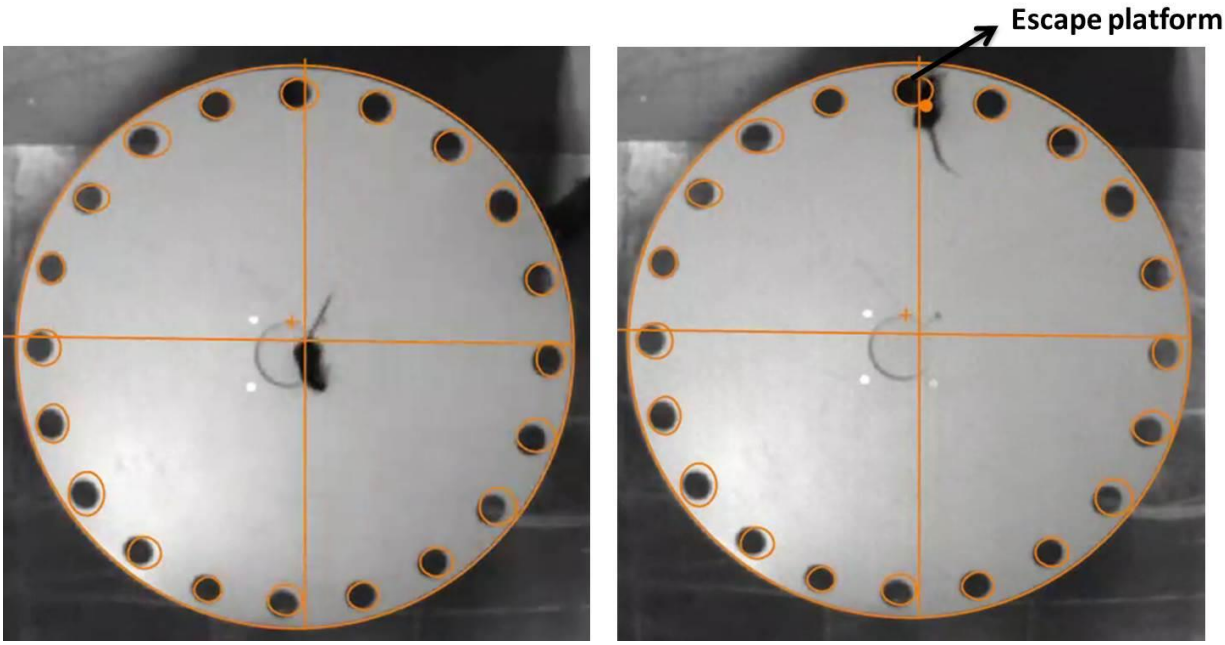
Escape platform

b

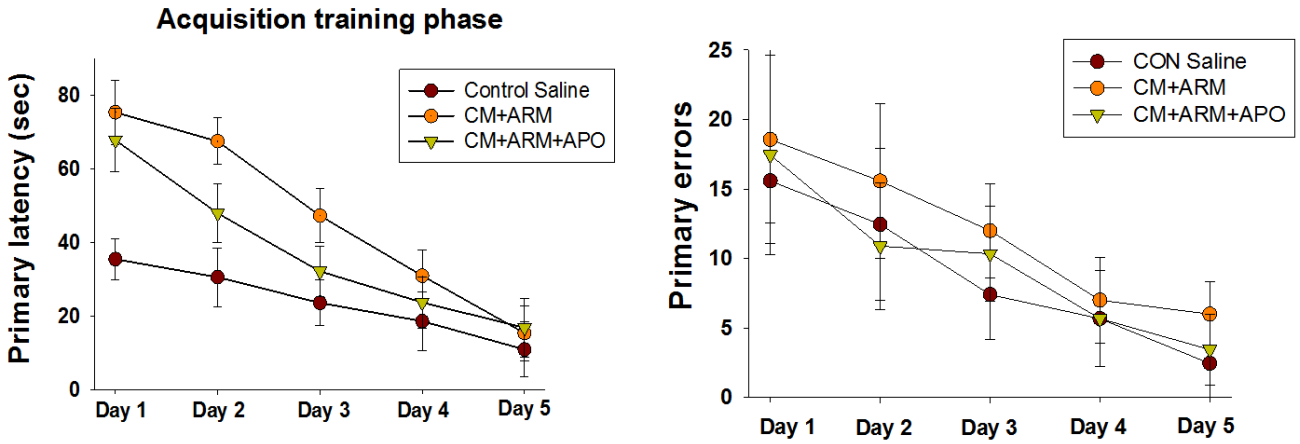
Acquisition training phase
Primary latency (sec)
0
20
40
60
80
Day 1
Day 2
Day 3
Day 4
Day 5
Control Saline
CM+ARM
CM+ARM+APO
Primary errors
0
5
10
15
20
25
CON Saline
CM+ARM
CM+ARM+APO

c

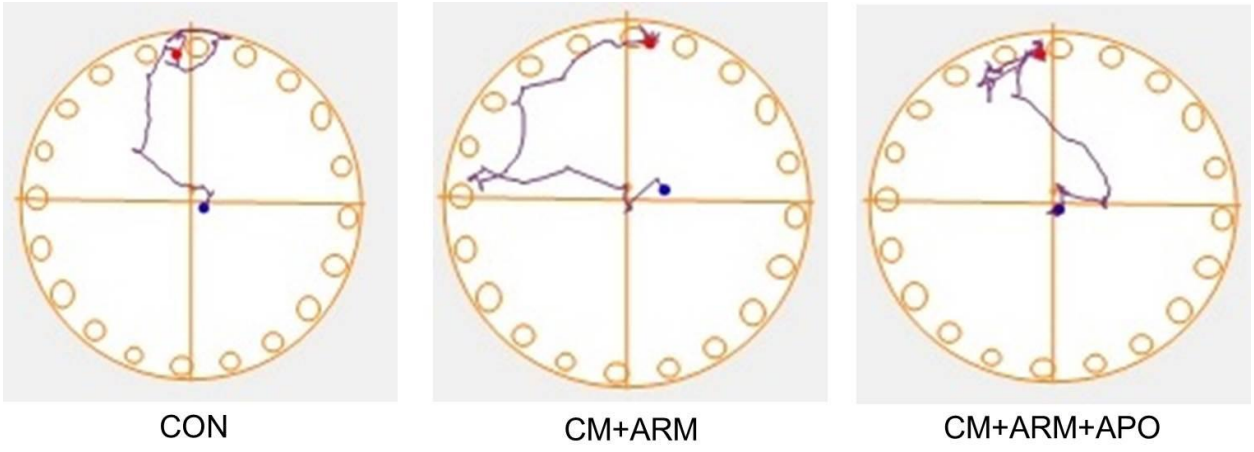
CON
CM+ARM
CM+ARM+APO

Figure 9. a) Illustrating the Barnes experiment during training session (left) and the position of the escape platform b) Graph representing the total time (sec) taken to locate the escape platform (left) by CM+ARM (15.32 sec), CM+ARM+APO (16.78 sec) and control (10.87 sec). Graph representing the number of incorrect holes visited prior to locating the escape platform (right) show that both CM+ARM+APO and control saline exhibit similar pattern of spatial learning compared to CM+ARM group. c) Representative trackplot of an animal from each group locating he escape platform and exhibiting the primary error.

Novel object recognition test

Our findings show increased novelty of the mice administered with the combination therapy compared to the monotherapy. No preference towards the objects was observed in all the test mice on the test day during (acquisition phase) i.e. mice subjected to the identical objects for 5 minutes. We observed that increased preference towards the novel object was observed in the mice administered with combination therapy compared to the monotherapy.

We observed significant increase in the exploratory time of the mice administered with the combination therapy compared to the monotherapy during the retrieval phase of the test (Figure 11). Therefore, apocynin administered along with the artemether exhibit improved learning and memory functions compared to the monotherapy.

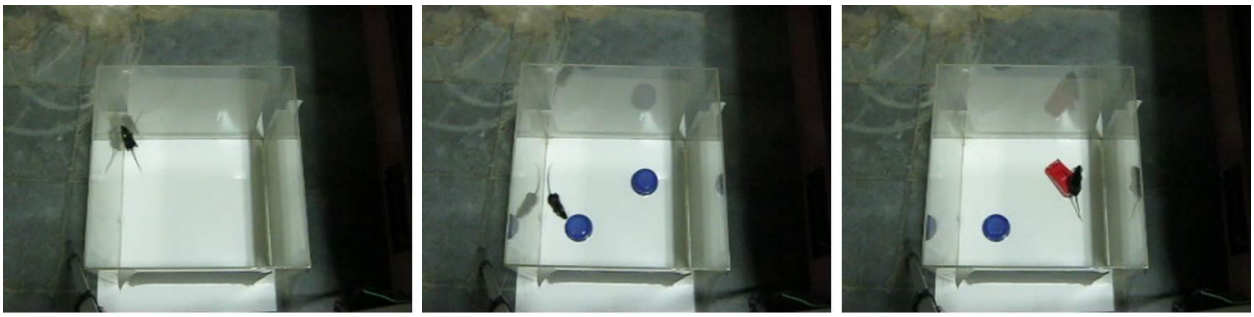

Figure 10. Illustrating the mouse subjected to the novel object recognition test.

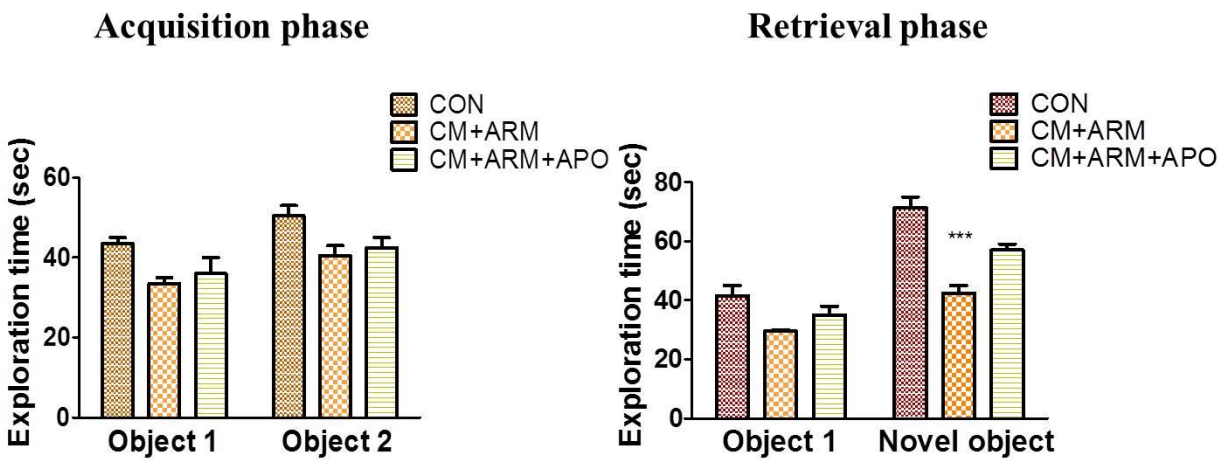

Figure 11. Graph representing that no significant difference observed in the exploration time of the mice subjected to the identical objects during acquisition phase whereas significant difference was observed in the total exploration of the mice subjected to the novel object during the retrieval phase.***$p<0.001$

Beam balance test

The average time taken to cross the beam was calculated per mouse in all the experimental groups. Paw slip score was also counted for all the test mice while traversing the beam. Our findings show that mice administered with combination therapy exhibited significant less time interval compared to the mice administered with the monotherapy. We observed that mice administered with monotherapy exhibited significant increase of the paw slips compared to the combination therapy.

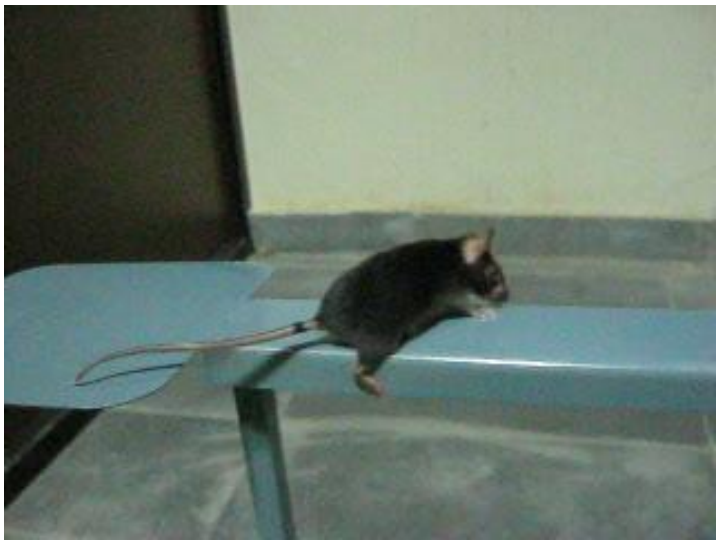

Figure 12. Illustrates mouse with paw slips while traversing the beam

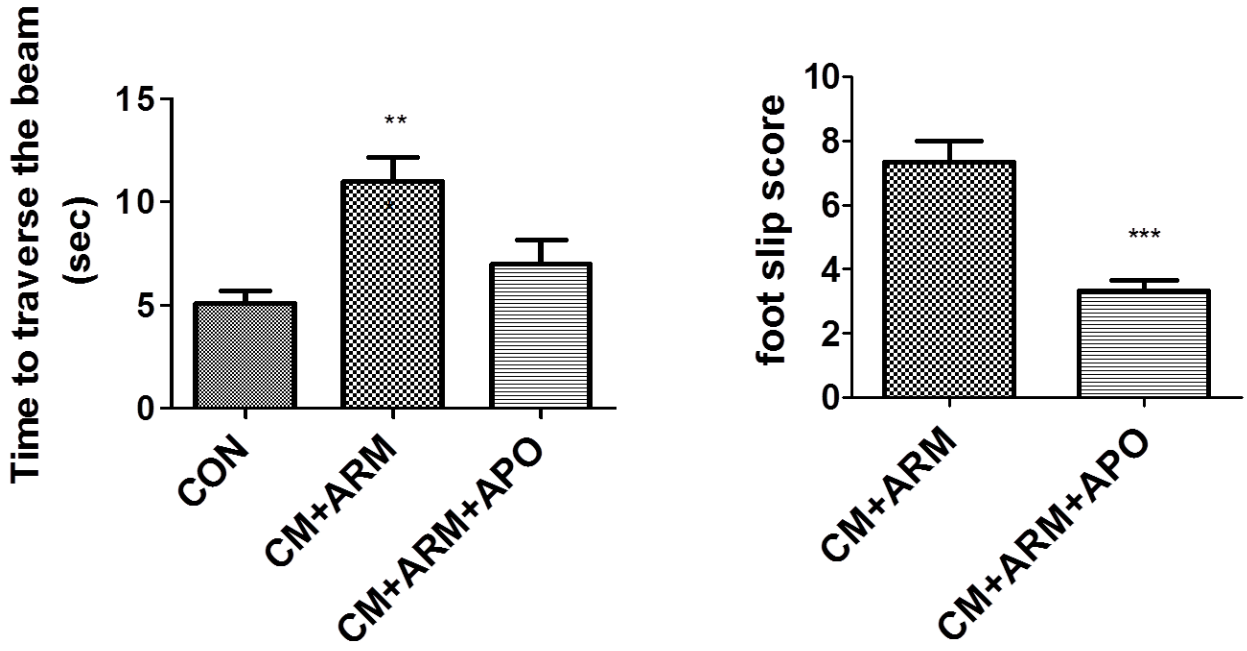

Figure 13. Graph representing (left) the average time to traverse the beam which shows that significant increase in the time taken to traverse the beam was observed in the CM+ARM mice (12 ± 1.2 sec) compared to the CM+ARM+APO (7±1.5 sec). Significant rise in the foot slip score was observed in monotherapy administered mice compared to the combination therapy.**p<0.01, ***p<0.001

Histology report

Hematoxylin & eosin staining

Our findings show that rescue therapy by both mono and combination drug dosage prevented the hemorrhages in the brain. Loss of hemorrhages in the cortical brain regions is n positive indicator for the breakage of BBB for the alleviation of the critical damage during CM (Figure 14.). Previously, apocynin has been reported to prevent the leakage of the BBB by the inhibition of NADPH oxidase during ischemic conditions in the brain. Similarly, no hemorrhages were detected in the brain sections of the mice administered with monotherapy.

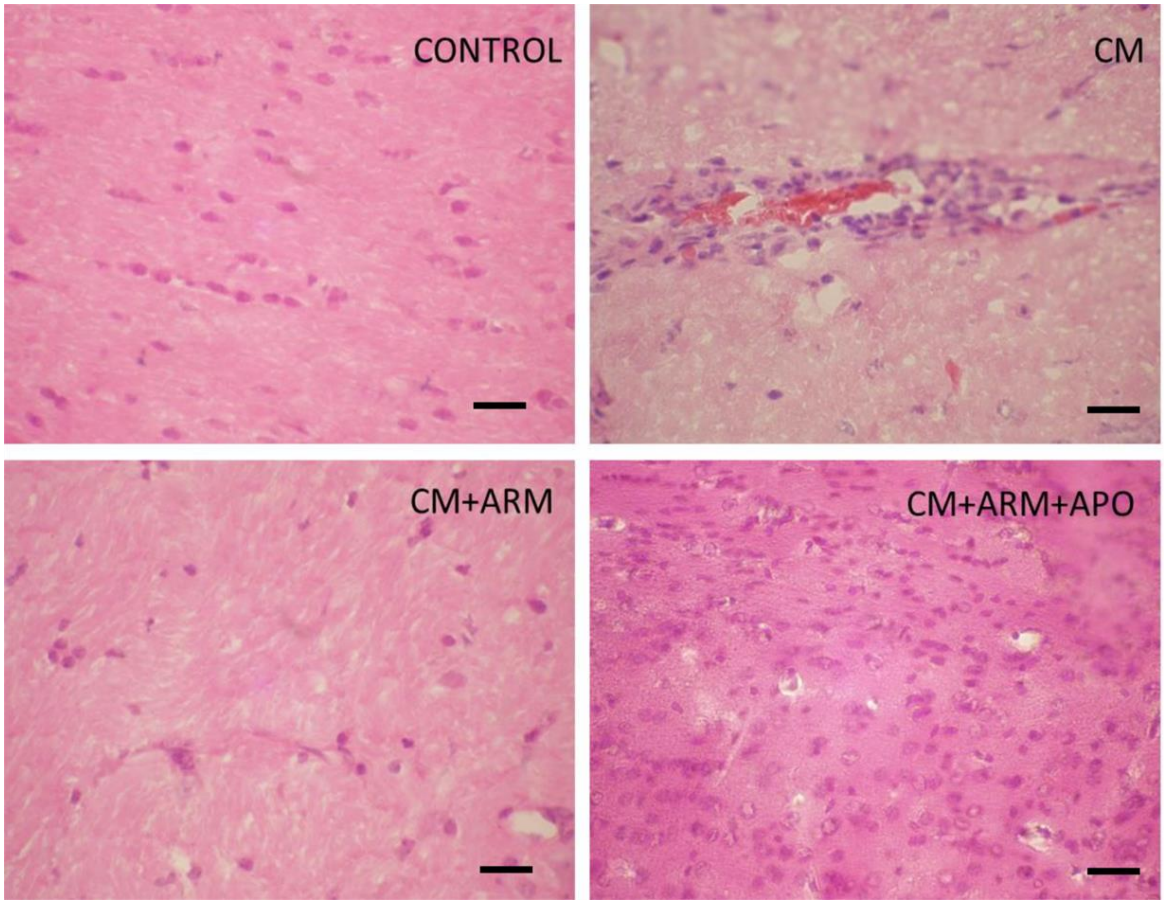

Figure 12. Petechial hemorrhages were commonly observed during CM. Mice administered with CM+ARM and CM+ARM+APO show no hemorrhages in the cortical regions of the brain sections stained by hematoxylin and eosin stain.

Fluoro Jade C staining

Our findings show significant increase in the fluorescent staining of the neurons in the cortical regions of the brain. Interestingly, neurodegeneration was observed in the cortical regions of the brain sections of the mice administered with the monotherapy compared to the combination therapy which may be due to the neurotoxicity of ARM drug.

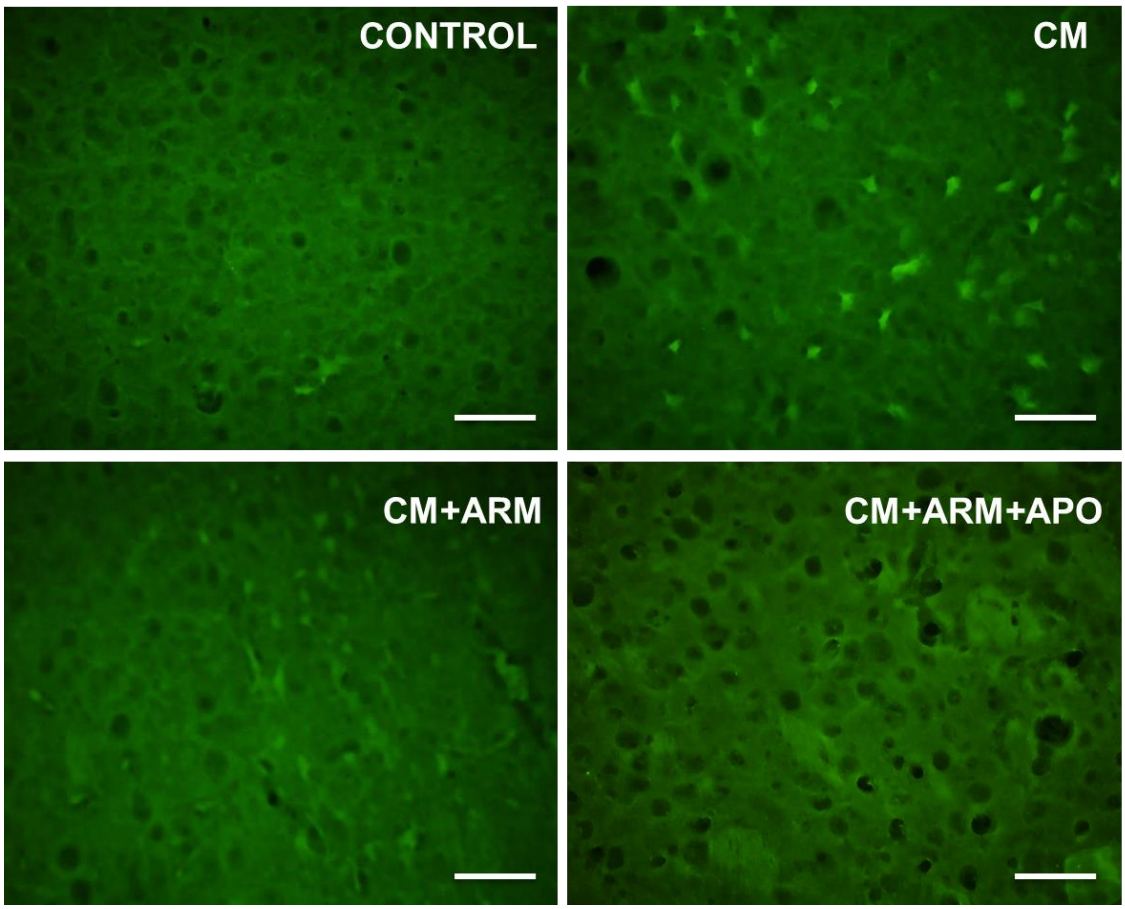

Figure 13. Illustrates the neurodegeneration in the cortical regions of the brain sections of CM, CM+ARM compared to the CM+ARM+APO group stained with the Fluoro-Jade C stain.

Golgi-Cox staining

Our findings show that the cortical neuronal arborization was improved in the mice treated with the combination therapy compared to the monotherapy. Previously, neuronal survivability was improved in the rodents with Parkinson's disease administered with apocynin.[21] Similarly, our

results show improved neuronal branching can be correlated to the restoration of the memory in the mice administered with combination therapy.

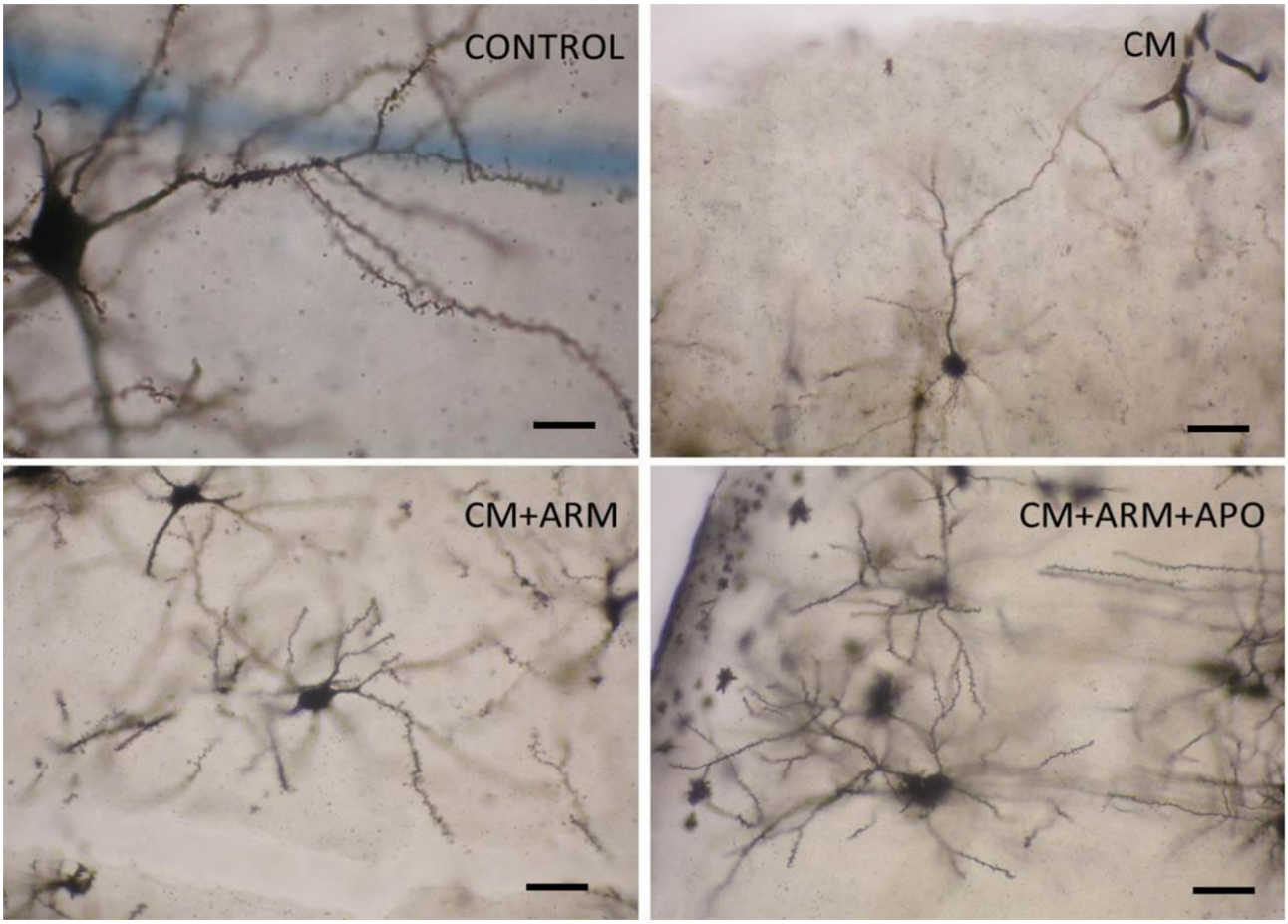

Figure 14. Representing the improved neuronal arborization in the cortical regions of the Golgi-impregnated brain sections in the mice administered with the combination therapy compared to the monotherapy.

Estimation of ROS by DCFDA

Our findings show that ROS levels were significantly decreased in the whole brain lysates of combination therapy administered mice compared to the monotherapy. Fluorescence intensity which corresponds to the ROS levels were significantly high in the whole brain lysates of CM (191.67±1.4) whereas significant reduction of the same was observed in brain lysates of combination therapy (112.86) compared to the monotherapy (148±0.7) mice.

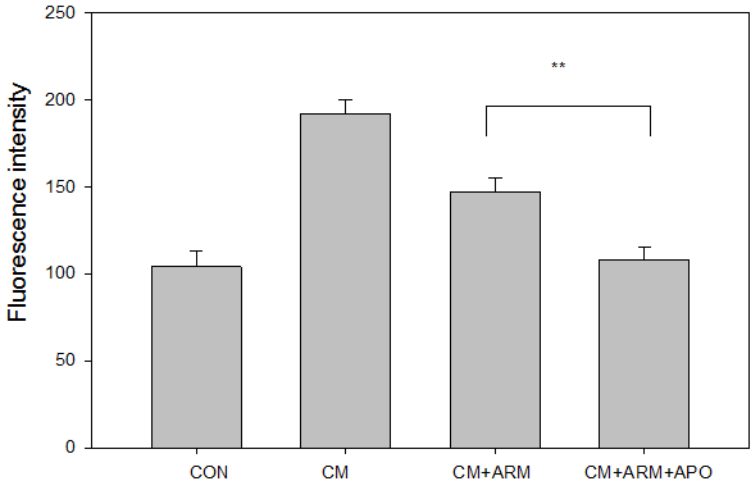

Figure 15. Graph representing the significant decrease in the ROS levels in the whole brain lysates of the CM+ARM+APO compared to the CM+ARM group. **p<0.05.

Evaluation of BBB integrity by Evan's blue staining

Our results show that mice administered with combination therapy show less leakage of the Evan's dye from the brain after incubation with 500 µl of formamide compared to monotherapy. Significant accumulation of Evan's blue dye was observed in the CM infected mouse brain shown in figure 16. Therefore, mice administered with combination therapy show restoration of BBB integrity compared to the monotherapy.

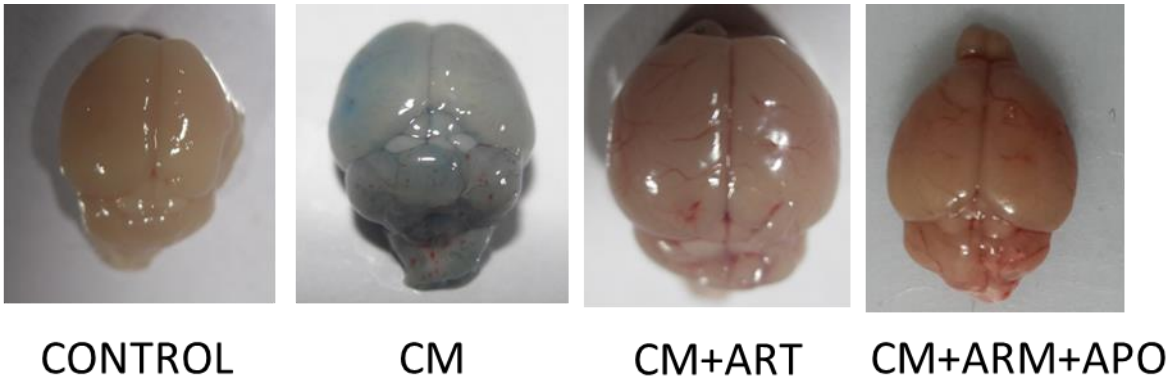

Figure 16. Representing the brains dissected from the mice administered with Evan's blue stain of all the experimental groups. Optical density of the supernatant with formamide/Evan's blue was measured at 610 nm with significant increase in the amount of Evan's blue 60 µg in CM infected brain (200mg tissue) after incubation with 500µl of formamide. Significant decrease in the amount of Evan's blue stain was observed from the mice brain administered with ARM+APO compared to ARM monotherapy.

Discussion

Cognitive decline is highly associated with the brain affected by the damage in its microvasculature. CM is categorized under the severe CNS infections with altered microvasculature of the brain.[22] Leakage of BBB, hyperactivation of microglia, aberrant activation of oxidative stress mechanisms results in neurodegeneration affecting cognitive and behavioral loss in the survived individuals of CM. The current anti-malarials are effective in curing CM but still 25% of the individuals suffer from the loss of cognition. Therefore, we studied the difference between adjunctive and monotherapy to curb the neuronal damage and restoration of the cognition in the animal models of CM by performing cognitive tests correlating to the histology studies. Despite no significance between the survival percentage between mice administered with mono and combination therapy, restoration of BBB integrity, working and reference memory, motor coordination, and neuronal ramification pattern were significantly increased in the mice with combination therapy. Apocynin may also suppress the oxidative stress induced by the artemether which is also known for its neurotoxicity. Oxidative stress plays an important role in the loss of neuronal functions by hyper-activating microglial cells secreting excess superoxides. Similarly, artemether has similar mode of action i.e heterolytic cleavage of endoperoxide bridge forming superoxides in the gut of the parasite which leads to the clearance of the parasite in the blood. Apocynin alleviates production of ROS, protect the neuronal microenvironment, possibly restoring cognition in the rescue treated mice. Our findings show significant reduction of the ROS levels in the brain lysates as well as neurodegeneration by Fluoro-Jade C staining of the brain sections of the mice treated with combination therapy compared to the monotherapy. Overall our results demonstrate that that apocynin in combination

with artemether show significant neuroprotection as well as restoration of cognition compared to artemether treated mice onset of CM.

Conclusion

Overall, the lack of studies directly relating to the signaling pathways affecting the morphology of the neurons and its repair by adjunctive therapies propelled us to carry out this study to elucidate the mechanisms behind the cognitive impairment in ECM. In chapter 1, we have demonstrated the dysregulation of actin and cofilin-1 expression resulting in the formation of actin-cofilin rods in the neurites of hippocampal and cortical regions of CM infected brain sections. In the chapter 2, our findings show altered dopaminergic signaling in ECM with altered morphology of medium spiny neuronal morphology with loss of dendritic spines. Further, hyperactivation of CaMKIIα at Thr286 is recently reported to cause the memory destabilization. In the chapter 3, we show apocynin plays a major role in the restoration of long-term and short term memories in the combination (CM+ARM+APO) rescue treated CM infected mice. Our findings demonstrate, improved neuronal ramification, reduced ROS levels and neurodegeneration in combination treated mice compared to the monotherapy. Therefore, elucidating molecular targets which could affect the cognition in ECM are necessary to define the future therapeutic strategies aiming better survivability with reduced behavioral anomalies in CM.

References

1)Renia L, Howland SW, Claser C, Charlotte Gruner A, Suwanarusk R. Cerebral malaria: mysteries at the blood-brain barrier. Virulence. 2012;3(2):193–201.

2)Storm J, Craig AG. Pathogenesis of cerebral malaria--inflammation and cytoadherence. Front Cell Infect Microbiol. 2014;29;4:100. doi: 10.3389/fcimb.2014.00100.

3)Dunst J, Kamena F, Matuschewski K. Cytokines and Chemokines in Cerebral Malaria Pathogenesis. Front Cell Infect Microbiol. 2017;7:324. doi: 10.3389/fcimb.2017.00324.

4)White NJ, Turner GD, Medana IM, Dondorp AM, Day NP. The murine cerebral malaria phenomenon. Trends Parasitol. 2010; 26(1):11-5.doi: 10.1016/j.pt.2009.10.007.

5)Li Q, Weina P. Artesunate: The Best Drug in the Treatment of Severe and Complicated Malaria. Pharmaceuticals. 2010; 3(7):2322-2332.

6)Schmuck G, Roehrdanz E, Haynes RK, Kahl R. Neurotoxic mode of action of artemisinin. Antimicrob Agents Chemother. 2002; 46(3):821-827.

7)Froestl W, Muhs A, Pfeifer A. Cognitive enhancers (Nootropics). Part 1: drugs interacting with receptors. Update 2014. J Alzheimers Dis. 2014;41(4):961-1019.

8)Simonyi A, Serfozo P, Lehmidi TM et al. The neuroprotective effects of apocynin. Front Biosci (Elite Ed). 2012; 4:2183-2193.

9)Bert A, Sjef C, Ingrid P. Apocynin, a Low Molecular Oral Treatment for Neurodegenerative Disease. Biomed Res Int. 2014; 2014: 298020.

10)Huang WY, Lin S, Chen H, Chen YP et al. NADPH oxidases as potential pharmacological targets against increased seizure susceptibility after systemic inflammation. J Neuroinflammation. 2018; 15(1):140.

11)Arandia-Romero I, Nogueira R, Mochol G, Moreno-Bote R. What can neuronal populations tell us about cognition? Curr Opin Neurobiol. 2017; 46:48-57. doi: 10.1016/j.conb.2017.07.008.

12)Frankfurt M, Luine V. The evolving role of dendritic spines and memory: Interaction(s) with estradiol. Horm Behav. 2015; 74:28-36. doi: 10.1016/j.yhbeh.2015.05.004.

13)Clemmer L, Martins YC, Zanini GM, Frangos JA, Carvalho LJ. Artemether and artesunate show the highest efficacies in rescuing mice with late-stage cerebral malaria and rapidly decrease leukocyte accumulation in the brain. Antimicrob Agents Chemother. 2011; 55(4):1383-1390.

14)Ferreira AP, Rodrigues FS, Della-Pace ID, Mota BC et al. The effect of NADPH-oxidase inhibitor apocynin on cognitive impairment induced by moderate lateral fluid percussion injury: role of inflammatory and oxidative brain damage. Neurochem Int. 2013; 63(6):583-593.

15) Deacon RM, Rawlins JN. T-maze alternation in the rodent. Nat Protoc. 2006;1(1):7-12.

16)Matthew W. P. Barnes Maze Procedure for Spatial Learning and Memory in Mice. Bio Protoc. 2018;8(5). doi:10.21769/bioprotoc.2744.

17)Lindsay M.L. Novel Object Recognition Test for the Investigation of Learning and Memory in Mice. J Vis Exp. 2017; (126): 55718.

18)Ann M.G, Scott T.G. The Striatum: Where Skills and Habits Meet. Cold Spring Harb Perspect Biol. 2015; 7(8): a021691.

19)Luong TN, Carlisle HJ, Southwell A, Patterson PH. Assessment of motor balance and coordination in mice using the balance beam. J Vis Exp. 2011; 49). pii: 2376.

20)Bayram-Weston Z, Olsen E, Harrison DJ, Dunnett SB, Brooks SP. Optimising Golgi-Cox staining for use with perfusion-fixed brain tissue validated in the zQ175 mouse model of Huntington's disease. J Neurosci Methods. 2016; 265:81-88.

21)Stankiewicz TR, Linseman DA. Rho family GTPases: key players in neuronal development, neuronal survival, and neurodegeneration. Front Cell Neurosci. 2014; 8:314. doi: 10.3389/fncel.2014.00314.

22)De Silva TM, Faraci FM. Microvascular Dysfunction and Cognitive Impairment. Cell Mol Neurobiol. 2016;36(2):241-58.

PUBLICATION

Dysregulation of LIMK-1/Cofilin-1 Pathway: A Possible Basis for Alteration of Neuronal Morphology in Experimental Cerebral Malaria

Praveen Kumar Simhadri, MSc,[1] Ruchi Malwade, MSc,[1]*
Ravisankar Vanka, MPharm,[2]* Venkata Prasuja Nakka, PhD,[1]
Gowthamarajan Kuppusamy, PhD,[2] and Phanithi Prakash Babu, PhD[1]

Objective: Loss of cognition even after survival is the salient feature of cerebral malaria (CM). Currently, the fate of neuronal morphology is not studied at the ultrastructural level in CM. Recent studies suggest that maintenance of neuronal morphology and dendritic spine density (actin dynamics in particular) are essential for proper cognitive function. LIMK-1/cofilin-1 signaling pathway is known to be involved in the maintenance of actin dynamics through regulation of cofilin-1, and in executing learning and memory functions.
Methods: Using an experimental mouse model, we analyzed the behavioral parameters of asymptomatic mice with CM by performing a rapid murine coma and behavior scale experiment. We performed Golgi–Cox staining to assess neuronal morphology, dendritic spine density, and arborization in brain cortex subjected to *Plasmodium berghei ANKA* infection compared to asymptomatic, anemic, and control groups. We studied the neural gene expression pattern of LIMK-1, cofilin-1, and β-actin in all the experimental groups by semiquantitative and quantitative polymerase chain reaction followed by immunoblotting and immunofluorescence.
Results: We observed significant loss of dendritic spine density, abnormal spine morphology, reduced dendritic arborization, and extensive dendritic varicosities in the cortical neurons of CM-infected brain. Furthermore, these observations correlated with diminished protein levels of LIMK-1, cofilin-1, phospho-cofilin-1, and β-actin in the whole brain lysates as well as formation of actin–cofilin rods in the brain sections of symptomatic mice with CM.
Interpretation: Overall, our findings suggest that the altered neuronal morphology and dysregulation of LIMK-1/cofilin-1 pathway could affect the cognitive outcome after experimental CM. Therefore, this study could help to establish newer therapeutic strategies addressing long-term cognitive impairment after CM.

ANN NEUROL 2017;82:429–443

Malaria is a life-threatening disease around the world. According to World Health Organization, >429,000 people died due to malaria worldwide in the year 2015. Malaria can be fatal in the form of cerebral malaria (CM) due to lack of proper diagnosis, improper treatment, and compromised immune system of the malaria-infected individuals. CM is a neurodegenerative disease characterized by symptoms of fever, epileptic seizures, coma, and even death caused by *Plasmodium falciparum* infection.[1] Underlying mechanisms of CM pathology include sequestration of infected red blood corpuscles (RBCs) in the brain microvasculature leading to disruption of the blood–brain barrier.[1] Cognitive deficits in children and adults are reported even after recovery from CM.[1]

View this article online at wileyonlinelibrary.com. DOI: 10.1002/ana.25028

Received Feb 6, 2017, and in revised form Aug 2, 2017. Accepted for publication Aug 18, 2017.

Address correspondence to Dr Babu, Department of Biotechnology and Bioinformatics, School of Life Sciences, University of Hyderabad, Hyderabad-500046, Telangana, India. E-mail: prakash@uohyd.ac.in

*Contributed equally for second authorship.
From the [1]Department of Biotechnology and Bioinformatics, School of life Sciences, University of Hyderabad, Hyderabad, Telangana; and [2]Department of Pharmaceutics, JSS College of Pharmacy, Udhagamandalam, Tamil Nadu, India

Additional supporting information can be found in the online version of this article.

Cognitive dysfunction in experimental cerebral malaria: Possible role of neurodegeneration and morphological alterations

by Simhadri Praveen Kumar

Submission date: 16-May-2019 12:09PM (UTC+0530)
Submission ID: 1131327496
File name: plagiarism_check_ph.D._Thesis_Praveen.pdf (4.49M)
Word count: 16653
Character count: 92014

Cognitive dysfunction in experimental cerebral malaria: Possible role of neurodegeneration and morphological alterations

ORIGINALITY REPORT

37%	4%	37%	10%
SIMILARITY INDEX	INTERNET SOURCES	PUBLICATIONS	STUDENT PAPERS

PRIMARY SOURCES

1	Praveen Kumar Simhadri, Ruchi Malwade, Ravisankar Vanka, Venkata Prasuja Nakka, Gowthamarajan Kuppusamy, Phanithi Prakash Babu. "Dysregulation of LIMK-1/cofilin-1 pathway: A possible basis for alteration of neuronal morphology in experimental cerebral malaria", Annals of Neurology, 2017 Publication	31%
2	Submitted to J S S University Student Paper	1%
3	"Encyclopedia of Signaling Molecules", Springer Nature, 2018 Publication	1%
4	www.bioscience.org Internet Source	<1%
5	Gwang Moo Cho, Seo-Yeon Lee, Jung Hwa Park, Min Jae Kim et al. "Photobiomodulation using a low-level light-emitting diode improves	<1%

exposed to chronic radiofrequency electromagnetic radiation", Metabolic Brain Disease, 2015.
Publication

34	"Arthropod Borne Diseases", Springer Nature, 2017 Publication	<1%

Exclude quotes	On	Exclude matches	< 14 words
Exclude bibliography	Off		

Cognitive dysfunction in experimental cerebral malaria: Possible role of neurodegeneration and morphological alterations

ORIGINALITY REPORT

55%	5%	54%	16%
SIMILARITY INDEX	INTERNET SOURCES	PUBLICATIONS	STUDENT PAPERS

PRIMARY SOURCES

1	Praveen Kumar Simhadri, Ruchi Malwade, Ravisankar Vanka, Venkata Prasuja Nakka, Gowthamarajan Kuppusamy, Phanithi Prakash Babu. "Dysregulation of LIMK-1/cofilin-1 pathway: A possible basis for alteration of neuronal morphology in experimental cerebral malaria", Annals of Neurology, 2017 Publication	48%
2	Submitted to J S S University Student Paper	3%
3	"Encyclopedia of Signaling Molecules", Springer Nature, 2018 Publication	1%
4	Ravisankar Vanka, Gowthamarajan Kuppusamy, Simhadri Praveen Kumar, Uday Krishna Baruah et al. " Ameliorating the antimalarial efficacy of artemether using nanostructured lipid carriers ", Journal of Microencapsulation, 2018	<1%

	Publication	
5	www.nature.com Internet Source	<1%
6	apiindia.org Internet Source	<1%
7	Submitted to University of Brighton Student Paper	<1%
8	Submitted to University of Melbourne Student Paper	<1%
9	Submitted to Massey University Student Paper	<1%
10	"Arthropod Borne Diseases", Springer Nature, 2017 Publication	<1%

Exclude quotes	On	Exclude matches	< 14 words
Exclude bibliography	On		

University of Hyderabad
Hyderabad- 500 046, India

PLAGIARISM FREE CERTIFICATE

This is to certify that the similarity index of this thesis as checked by the Library of University of Hyderabad excluding bibliographic content 37%. Out of this 31% similarity has been found to be identified from the candidate's own publication (Simhadri Praveen Kumar) which forms the adequate part of the thesis. The details of student's publication are as follows:

a. Simhadri PK, Malwade R, Vanka R, Nakka VP, Kuppusamy G, Babu PP. Dysregulation of LIMK-1/cofilin-1 pathway: A possible basis for alteration of neuronal morphology in experimental cerebral malaria. Ann Neurol. 2017; 82(3):429-443. doi: 10.1002/ana.25028. **Similarity index – 31%**

About 6% similarity was identified from external sources in the present thesis which is according to prescribed regulations of the University. All the publications related to this thesis have been appended at the end of the thesis. Hence the present thesis may be considered to be plagiarism free.

Prof.P.Prakash Babu
Supervisor